

Aus dem Bereich
Klinische Medizin
der Medizinischen Fakultät
der Universität des Saarlandes, Homburg/Saar

Keeping Living Therapeutic Materials under the Radar of Neutrophils

Dissertation zur Erlangung des Grades eines
Doktors der Naturwissenschaften
der Medizinischen Fakultät der
UNIVERSITÄT DES SAARLANDES

2025

vorgelegt von
Islam Mohamed Hassan Mohamed
Geb. am 10.03.1987 in Bani Souwaif, Ägypten

Die experimentellen Arbeiten im Rahmen der vorliegenden Dissertation wurden in der Arbeitsgruppe von Frau Prof. Dr. Sigrun Smola am Institut für Virologie am Universitätsklinikum des Saarlandes in Homburg/Saar durchgeführt.

Tag der Promotion 17.07.2025
Dekan: Prof. Dr. M. Hannig
Erstberichterstatte:r: Prof. U. Römer
 Prof. S. Smola

Contents:

List of figures.....	IV
List of Tables.....	V
Summary.....	I
1 Introduction:	1
1.1 Microorganisms as a tool of therapy	1
1.1.1 Advantages and disadvantages of microbial therapy.	2
1.2 Biomaterial history and definition.....	4
1.2.1 Biomaterial classification and application.	5
1.2.2 Living therapeutic materials (LTMs).	7
1.3 Biosafety of therapeutic materials.....	8
1.3.1 <i>In vitro</i> biocompatibility (cell culture safety).	9
1.4 Immune system and fighting enemies.....	10
1.5 Neutrophils.....	11
1.5.1 Granulopoiesis to the circulation in the blood vasculature.	11
1.5.2 Recruitment during inflammation.	14
1.5.2.1 Activation process of neutrophils.....	14
1.5.2.2 Neutrophil extravasation.	15
1.5.3 Killing mechanisms involved in neutrophil response.	18
1.5.4 Neutrophil proteins.....	20
1.5.4.1 Matrix-Metalloproteinases (MMPs).....	21
1.5.4.1.1 Forms of MMP-9 (gelatinase B).	22
1.5.4.2 Cytokine secretion.....	23
1.5.4.2.1 CXCL-8 (IL-8).	24
1.5.4.2.2 VEGF.	25
1.6 Immune system response to tissue biocompatibility.....	25
1.7 Study objectives.	29
2 Material and Methods	30
2.1 Materials.....	30
2.1.1 Cell lines.....	30
2.1.2 Basal Media.....	30
2.1.3 Reagents and Antibiotics for cell culture	30

2.1.4 Complete Media.	31
2.1.5 Bacterial Media.	32
2.1.6 Bacteria and biomaterials provided by INM, Saar. University	33
2.1.7 Reagents and Chemicals.....	33
2.1.8 Methodological Reagents/ Kits.	34
2.1.9 Buffers and Solutions.	35
2.1.10 Software.	38
2.1.11 Laboratory Equipment/Systems.	38
2.2 Methods.	41
2.2.1 Cell culture.	41
2.2.1.1 Eukaryotic cells.	41
2.2.1.1.1 Storage and thawing of eukaryotic cells.	41
2.2.1.1.2 Test of mycoplasma existence.....	41
2.2.1.2 Prokaryotic cells (bacteria).....	43
2.2.1.2.1 Culture of <i>E. coli</i> and <i>ClearColi</i>	43
2.2.1.2.2 <i>Lactobacillus plantarum</i> (5 candidates).	43
2.2.2.2.1 Killing the bacterial candidates by heat.	43
2.2.2 Storage of bacteria.....	43
2.2.3 Growth test of inactivated (heat-killed) bacteria.....	43
2.2.2 Cell Transient and Transfections.....	44
2.2.3 Granulocytes (neutrophils) isolation.	44
2.2.4 Transwell-Control Experiment.....	45
2.2.5 Construction of PluDA Hydrogel.....	46
2.2.5.1 Coating of coverslips.....	46
2.2.5.2 Preparation of Pluronic Diacrylate (PluDA).	47
2.2.5.3 Structure of Hydrogel.....	47
2.2.6 Direct stimulation assay (DSA).....	49
2.2.7 Enzyme-linked immunosorbent assay (ELISA).....	49
2.2.8 Zymography.	51
2.2.9 Calcium Imaging.	52
2.2.10 Antibody-dependent cellular cytotoxicity (ADCC).	52
2.2.11 Organotypic 3-dimensional (3D) culture.	54
2.2.11.1 Generation of 3D cultures.	55
2.2.11.2 Staining of 3D cell culture.	56
2.2.11.2.1 Hematoxylin-Eosin (HE) staining.	56
2.2.11.2.2. Immunohistochemistry (IHC) stain.....	57

2.2.12 Endotoxin Detection.....	58
2.2.13 General schema summarises the experimental workflow.	59
3 Results.	61
3.1 Investigation of direct and indirect contact of neutrophils with live bacteria.	61
3.2 Preliminary results of pre-stimulated neutrophils by drug-producing LTMs.	63
3.3 Bacteria-conditioned supernatants trigger the release of neutrophil proteins.	66
3.4 Bacteria-conditioned supernatants enhance neutrophil-mediated ADCC.....	69
3.5 Bacteria-conditioned supernatants have similar activation levels of neutrophil FPR1 and similar LPS concentration.	71
3.6 LPS increases neutrophil degranulation and activity for tumor cell-killing.	73
3.7 LPS enhances the neutrophil-activating capacity of <i>ClearColi</i>	75
3.8 Endotoxin LPS is the essential effector in neutrophil activation by TLR.....	77
3.9 LPS secreted-trans hydrogel is the main effector of neutrophil activity.....	83
3.10 Neutrophils respond to LPS-secreted <i>E. coli</i> strongly through migration.	84
3.11 <i>L. plantarum</i> -conditioned supernatants trigger neutrophil degranulation and enhance ADCC.....	88
3.12 Supernatant and heat-killed <i>L. plantarum</i> increase neutrophil migration.	92
3.13 Capabilities of <i>L. plantarum</i> to enhance neutrophil degranulation.	93
3.14 Under various conditions, the status of <i>L. plantarum</i> increases the capacity of neutrophils in ADCC.....	94
4 Discussion.	99
4.1 Interaction of neutrophils with <i>E. coli</i> and <i>ClearColi</i> strain.....	99
4.2 Bacterial LPS and other PAMPs are mediators of neutrophil activation.	100
4.3 Immune response to <i>E. coli</i> and <i>ClearColi</i> in case of the encapsulation (gel).	102
4.4 Impact of <i>L. plantarum</i> strain on the immune cell response.	104
4.5 Factors may affect immunogenic response and thus influence the outcomes.....	106
4.5.1 Cell subsets (neutrophils).	107
4.5.2 Sex differences.	107
4.5.3 Geographical environment.	109
5 Conclusion.	110
6 Abbreviations.	108
7 Literatures.	115
8 Publication/ Conference.	140
9 Acknowledgement.	141
10 Curriculum vitae.	141

List of Figures:

A-Introduction figures:

Figure 1 Graphical abstract.....	II
Figure 2 Historical evolution of human potential therapeutic microorganisms.....	2
Figure 3 Illustration of used biomaterials during history.....	4
Figure 4 Application of biomaterials in medicine.....	6
Figure 5 Stages of drug discovery and development process.....	8
Figure 6 Development of neutrophils from bone marrow to circulation and homing back...12	
Figure 7 Illustration of neutrophil recruitment from the blood vasculature to infected tissues.....	17
Figure 8 Main killing mechanisms by neutrophils.....	19
Figure 9 Activation of TLR4 and FPR pathways.....	20
Figure 10 Potentially cytokines and chemokines of human neutrophils.....	24
Figure 11 Immunogenic response to implantable biomaterials.....	27
Figure 12 LTMs project in LIFMAT.....	29

B-Methodological figures:

Figure 13 Isolation of neutrophils (Granulocytes) from human peripheral blood.....	45
Figure 14 Monitor of neutrophils and bacteria interactions.....	46
Figure 15 Stages of bacterial incorporation in PluDA hydrogel fabrication.....	47
Figure 16 Main details of PluDA constructions and their final morphology.....	48
Figure 17 Stimulation of neutrophils with different components.....	49
Figure 18 Stages of cytokine detection by ELISA.....	50
Figure 19 Zymography procedure for MMP detection.....	51
Figure 20 Procedure of ADCC assay.....	53
Figure 21 Phases of ADCC procedure affect the electrical impedance (EI) readout.....	54
Figure 22 Stages of 3-D culture production.....	56
Figure 23 HE stain of the micro-hydrogel (μ Gel) incorporation trial in 3D culture.....	57
Figure 24 LAL assay measurement of Endotoxin concentrations.....	58
Figure 25 Diagram of neutrophil stimulation procedure in vitro.....	59

C-Result figures:

Figure 26 Neutrophil response exposed directly and indirectly to different bacteria.....,.....	62
Figure 27 Release of MP9 molecules marks neutrophil degranulation, leading to a decrease in tumour-killing efficacy by ADCC.....	64
Figure 28 Delta Cell Index calculation.....	65
Figure 29 MMPs and cytokines release marks activation and degranulation of neutrophils stimulated by bacterial supernatant.....	67
Figure 30 Release of MMP9 is at an earlier stage of CXCL-8 in ADCC.....	68
Figure 31 Both <i>E. coli</i> and <i>ClearColi</i> supernatants enhanced neutrophil activation for tumour-killing b ADCC.....	69
Figure 32 Potential activation in neutrophils is independent of Formyl peptides.....	72
Figure 33 Purified LPS showed neutrophil activation and enhanced ADCC compared to unpurified LPS (<i>ClearColi</i> supernatant).....	74
Figure 34 Adding LPS to <i>ClearColi</i> supernatant increases MMPs release and efficacy of IgA2.0 to engage neutrophils for ADCC.....	77
Figure 35 Potential activation in neutrophils possibly relies on TLRs stimulated by LPS....	78
Figure 36 Delta cell index and cytotoxic effect of neutrophils.....	79
Figure 37 Prolonged incubation of <i>ClearColi</i> supernatant may increase neutrophil MMP release.....	82

Figure 38 Different doses of LPS enhance neutrophil response to <i>ClearColi</i>	83
Figure 39 PluDA hydrogel (gel) may reduce neutrophil activation by monitoring soluble protein secretion.....	84
Figure 40 Bacterial supernatants and gel with/without bacteria attracted neutrophil transmigration in organotypic 3D culture.....	86
Figure 41 Supernatant/ heat-killed of <i>L. plantarum</i> may enhance neutrophil degranulation and activation for tumor-killing by ADCC.....	90
Figure 42 Delta cell index calculation.....	91
Figure 43 Strong chemoattraction of neutrophils towards supernatant and heat-killed <i>L. plantarum</i> (vector).....	92
Figure 44 Various levels of protein secretion can be triggered by bacterial phases.....	94
Figure 45 Elevation in neutrophil capacity to kill the tumour in impedance-based ADCC assay.....	95
Figure 46 Cytotoxic effect of bacterial status with neutrophils with and without nonspecific antibodies.....	97

D-Discussion figures:

Figure 47 Comparison of LPS in <i>E. coli</i> and Engineered <i>E. coli</i> strain (<i>ClearColi</i>).....	101
Figure 48 Sex-related hormones may lead to differences in human life stages.....	108

List of Tables:

Table 1: DAMP and PAMP of the neutrophil receptor.....	15
Table 2: Human (a: specific) and mice (b: specific) neutrophil granules.....	21
Table 3: MasterMix preparation.....	42
Table 4: PCR process by PTC-200 Thermal Cycler.....	42
Table 5: Comparison of 2D and 3D cultures.....	55
Table 6: P-values (Fig. 36A, B).....	80
Table 7: P-values (Fig. 36C, B).....	80
Table 8: P-values (Fig. 36E).....	81
Table 9: P- value of Vector and nuclease candidates (Fig. 45C, D).....	96

Summary:

Living therapeutic materials (LTM) is a promising approach for long-term drug delivery *in vivo*. The basic principle is a bacteria encapsulated in hydrogel, engineered to produce the drug of interest. Bacterial components, such as formyl peptides and lipopolysaccharides (LPS), are potent mediators of neutrophil chemotaxis. Therefore, neutrophils sense bacteria by formyl peptide (FPR) and Toll-like receptors (TLR) that activate neutrophil chemotaxis, degranulation, the release of matrix metalloproteinases (MMPs), cytokines, reactive oxygen species (ROS), and NETs. The strong response of neutrophils can result in severe tissue damage and systemic side effects. To circumvent this, *ClearColi*, an *E. coli* strain genetically modified to produce mutated LPS, with a potentially lower capacity to activate neutrophils. Furthermore, *L. plantarum* was used to develop a commensal bacteria-based drug-delivery system to target inflammatory disease conditions.

The study aimed to investigate the response of neutrophils, relevant immune cell population *in vivo*, to living therapeutic materials (LTMs). This is the first evaluation of the potential activation of neutrophils. The LTM includes hydrogel, hydrogel-encapsulated bacteria and only bacteria like *E. coli* and candidates derived from *L. plantarum* WCFS1. The investigation was performed on various assay types classified into simple and short term, intermediate complex, and more complex assays allowing long term evaluations. This includes, respectively, direct stimulation assays (DSA) which are utilized to check cytokine production resulting from direct short-term interaction of neutrophils exposed to a single condition. Antibody-dependent cell cytotoxicity (ADCC) is used to evaluate the cytotoxic effects of neutrophil interaction with various conditions influencing target cells as intermediate term technique. More complex (organotypic 3D-cultures) provide the dynamics of neutrophil migration through tissue-like culture (in vivo-like culture). We found that all hydrogel constructs could activate neutrophils strongly. Then, both *E. coli* and *ClearColi* supernatants could trigger neutrophil activation, which was higher in the case of *E. coli* than *ClearColi*, translated to the release of MMPs and cytokines, and enhancing neutrophils' ability to kill tumor cell line (A431) in ADCC.

To determine the difference in activation level between both strains, LPS was applied in the same concentration (conc.) and measured in both candidates' supernatants. As expected, LPS could activate neutrophils higher than *ClearColi* supernatants. Then by comparing *ClearColi* (modified LPS), *E. coli* (unmodified LPS), and commercial LPS, we could prove that the higher activation level of *E. coli* supernatant originated from LPS, which can activate neutrophil TLR-signaling. *L. planetarium* is a lactic acid bacteria characterized by health-promoting and disease-curing effects. *L. planetarium* candidates displayed significant activation and attraction

marked by neutrophil degranulation and migration. Moreover, the response of neutrophils varied at different bacterial statuses, showing there might be different signaling pathways. However, more studies are needed including neutrophil function assays in addition more modifications are required for *ClearColi* so as not to trigger a neutrophil response.

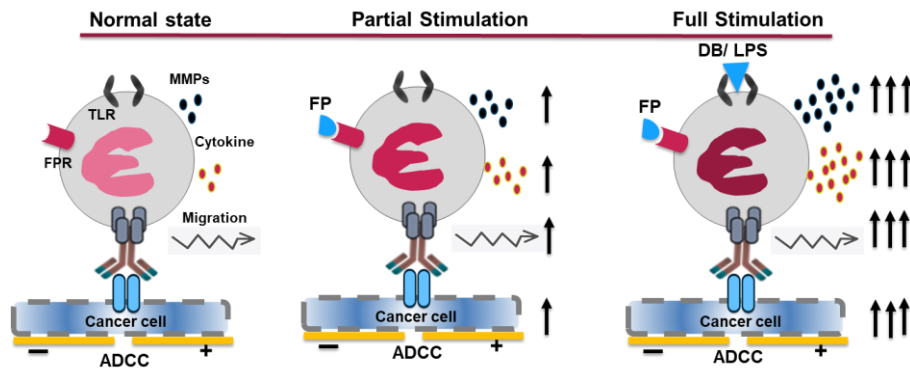


Figure 11 Graphical abstract: neutrophil response depends on the cue type of bacterial product. FP: Formyl Peptides, LPS: Lipopolysaccharides, DB: Dead bacteria (vaccine, recognized as DAPM), FPR: formyl peptide receptor, TLR: Toll-like receptor, ADCC: antibody-dependent cell cytotoxicity, MMPs: Matrix-metalloproteinases, Cytokine: CXCL-8, Activation level: ↑↑, Gold electrical electrodes: -/+

1 Introduction:

1.1 Microorganisms as a tool of therapy

Human body health relies on microbiota (so-called microbiome). Therefore, microbiomes are an important field of research because of their significant role in human health and disease [1]. Microorganisms represent about 38×10^{12} microbes in humans, which include bacteria, fungi, and viruses [2]. Microorganisms can live in humans as non-pathogens, facultative and obligate pathogens [3]. The ecosystem of microbiomes can be healthy or harmful depending on species diversity, balance, functionality, and resistance to diseases or treatment. For example, dysbiosis originates from an imbalance in the gut microbiota ecosystem. So, the rebalance of the microbial system may form a novel therapeutic approach [1]. Microbiota may also aid tumor tissue colonization by destroying mucus, hematogenic invasion, and changing the tumor microenvironment affecting the tumor-promoting mechanisms [2]. On the other hand, the interaction between the microbe and the host leads to commensalism, in which the host can get physiological aid from microbes. Thus, microbiota can assist in metabolism, and trigger mucosal immunity, vitamin production, food nutrient digestion, and pathogen resistance or tolerance [4]. Furthermore, oncolytic viruses or bacteria are in development as a novel therapeutic approach to treat cancer [5].

Immunotherapy targets healthy cells too, for instance, cetuximab, chemo- radio- and immunotherapy hit healthy cells causing side effects, one of the reasons is the systemic application, where LTM would provide a local solution. Therefore, scientists have paid attention to the role of bacteria in disease treatment [6]. In the past, microorganisms had an essential role in various approaches including food fermentation. Microbes have been used throughout history from eight thousand years Before the Common Era (B.C.E) to recent times [4] (Fig.2). One hundred years ago, William B. Coley found that streptococcus pyogenes injection into sarcomas patients can function as cancer immunotherapy. Thus, natural antigens of bacteria work as stimulators for immune cell activation [7]. Further, *Escherichia coli* Nissle (EcN) isolated in 1917 has been used as a probiotic for a century [8]. The market size of therapeutic microbiota was evaluated in 2019 by 34.1 U. S \$. However, this number may increase to 838.2 U. S \$ by 2026 [9]. Natural compounds can be derived from primary and secondary metabolism from plants, animals, or microorganisms, where progress and development of science led to the discovery of about 1×10^6 natural compounds. They range between 50–60% for plants, such as alkaloids, and flavonoids, and 5% for microbes. Biological active compounds represent about 20–25%, while microbes-derived compounds represent

approximately 10%. Microbial active compounds count about 22,500 derived from actinomycetes, fungi, and unicellular bacteria with 45%, 38%, and 17%, respectively. This reflects the central role of microorganisms in antibiotics and drug production that treat serious diseases [10].

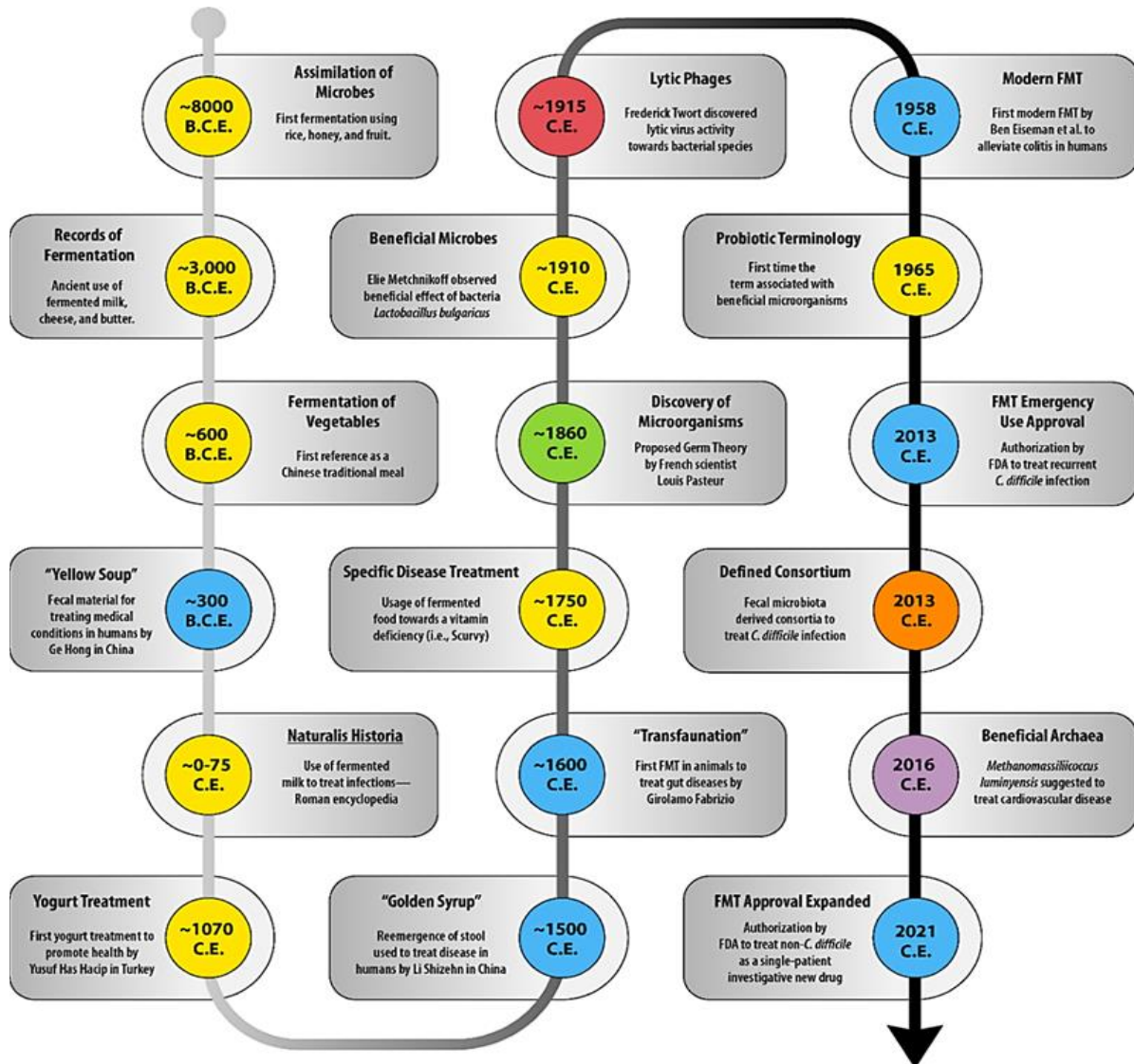


Figure 21 Historical evolution of human potential therapeutic microorganisms. Development of therapeutic stages is colored as follows: Probiotics (Amber), Fecal transplants (blue), Lytic phase (Red), Anchors (Green), Consortia (Orange), and Archea treatments (Violet) [4].

1.1.1 Advantages and disadvantages of microbial therapy:

Therapy by microbiota is a field of engineering microbiomes to use them or their metabolites as native or designed forms to treat diseases. In this way, it provides treatment characterized by harmonization and reliability in the sustainable system, avoiding the disadvantages of traditional therapy [9]. Therapeutic microbiota may have some advantages which do not exist

in common therapy. This includes i) multiple mechanisms for invasion. There are some difficulties when using a mixture of treatments, encountered by multi-branched resistance or barriers. For instance, some pathogens can resist antibiotics and promote the resistance of cancers against specific drugs. Further, microorganisms use different mechanisms for survival to overcome microenvironmental barriers such as skin and defensins [11]. One of those mechanisms is that bacteria can express adhesins, motile and attached factors, to avoid host mechanical removal. They can also secrete toxins, which lead to fluctuation of the host microenvironment, thus facilitating bacterial colonization. Furthermore, bacteria release proteolytic factors that degrade host immunoglobulin, opsonizing their membrane [12]. Other bacteria form biofilms to adapt to the new environment by reducing their metabolism and cell division as a survival strategy. They have also become dominant in escaping from immune cells, which may cause tissue damage and acute infection lately [13]. ii) In the age of synthetic biology, microbes' capability of passing mucosal barriers can be genetically modified to drug delivery systems or vaccines, to overcome microbe-related treatment resistance. iii) Microbes used in therapy can multiply at the disease location inside the host. Therefore, multiple doses of microbes are not mandatory for disease treatment. Thus, it leads to a decrease in the prevention of side effects compared to traditional cures [11]. iv) Enhancing treatment by immunity-engineered microbes can stimulate the response of innate and adaptive immune systems to fight the disease jointly. This results in the efficacy of treatment in addition to extending immunity. v) The safety of therapeutic microbes can be modified and engineered to aim at multiple diseases with specificity and not to trigger the strong response of immunity leading to enhancement biosafety [11, 14]. Microbial metabolites, for instance, are widely used in clinical and drug research for their unique chemical structure and interaction with the host [5]. However, there are also obstacles, which encounter microbial therapy when using bacteria in tumor treatment. One of the main problems with using bacterial agents against cancer is that the effective dose required for cancer treatment is toxic, and any reduction in the dose leads to a wider decrease in efficacy. Furthermore, systemic bacterial infection may contain a high risk of toxicity. In addition, bacterial therapy also does not lead to destroying the whole malignant tissues. Therefore, it was required to accompany chemo with bacterial treatments [15].

The cellular microbiology field focuses on studying mechanisms and development of infection at cellular levels, in which infectious microbes and infected cells interact. One of those mechanisms, such as bacterial toxicity, is used to generate enzymes, immunotherapeutic factors, and bacteriocins, which can interfere with RNA in addition to degrading prodrugs [6]. Therefore, genetically modified bacteria are used as living therapeutic tools to treat disease

conditions [3, 14]. However, they have potential toxicity [14]. Under uncontrolled conditions, neutrophil activity may cause damage to the host tissues due to their cytotoxic compounds. This also results in self-imposed diseases such as autoimmune diseases [16,17]. Also, in patients with rheumatoid arthritis (RA) as well as systemic lupus erythematosus (SLE), neutrophils could produce increased levels of ROS and NETs supporting disease progression [16]. Therefore, it is essential to have a system encapsulating the therapeutic microbes to avoid or eliminate severe conditions that can be integrated into the biosystem.

1.2 Biomaterial history and definition:

Natural biomaterials have been used for ages because they have unique characteristics, such as low toxicity and allergenicity, tissue biocompatibility, and biodegradability [18]. In ancient times, biomaterials were applied and discovered in the last two thousand years. Egyptians, Romaan, Etruscans, and Greeks used prostheses and implants in their bodies, such as skulls and skeletons [19]. For example, ancient Egyptians applied biomaterials, such as suture materials, about 3000 years B.C.E. Materials, such as plant fibers, hair, tendons, and wool threads, were also discovered in mummified remains [20]. Furthermore, the suture was described in forty-eight cases in papyrus bearing Smith's name, found out by Edwin Smith, and codified in 1600 B.C.E. [20]. Egyptians also used Linen threads for wound healing, four thousand years ago [21].

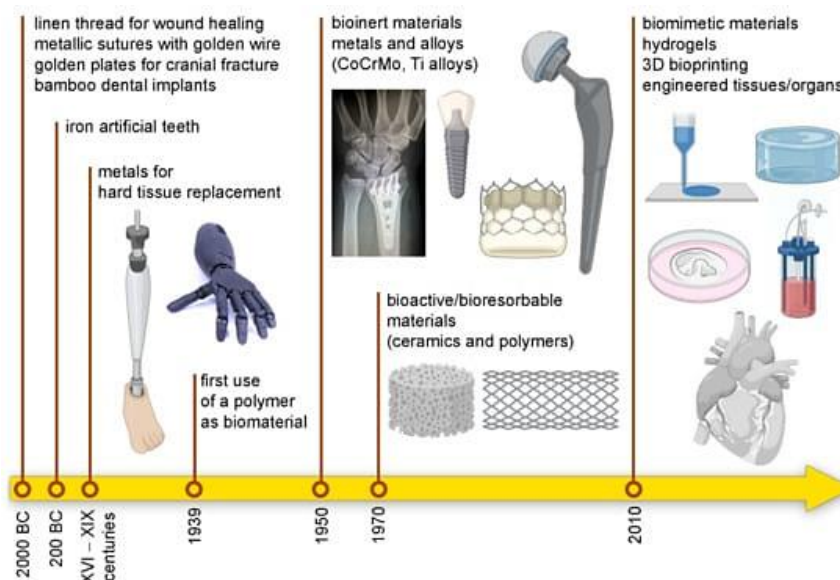


Figure 3| Illustration of used biomaterials during history: Different biomaterials were used in old ages from 2000 BC to recent years [21].

According to the Cambridge Dictionary, materials are physical substances, that things can be made, including stone (building materials) and crude oil (raw material) used for making plastics [22]. Materials are classified according to the International Organization of Standardization norms (ISO) and the German Institute for Standardization norms. It includes materials-derived glass production such as ceramic, leather, metal, paint and color, paper, plastic, stone, textile, and wood [23]. Additionally, composite materials, a combination of two or more materials on a macroscopic scale, and raw materials, are further classified as primary and secondary [23, 24].

Biomaterials refer to a specific category of materials engineered to interact with human beings for medical targets [25]. Biomaterials play a role in therapy (disease treatment, augment, repair), replacing the function of tissues, or for diagnosis courses such as sensors, cancer models, and animal test substitution [26, 27]. Many definitions of biomaterials have been presented in the last decades. However, the most acceptable one is *“Any substance or combination of substances, other than drugs, synthetic or natural in origin, which can be used for any period of time, which augments or replaces partially or totally any tissue, organ or function of the body, to maintain or improve the quality of life of the individual”* [28]. These materials can be used as a partially complex or entire system to monitor the interaction with living system components [26, 29]. Biomaterials are biologically active and instructive. They can cause signals to the living system, for instance, cells and tissues [30]. Biomaterials were also designed to trigger specific immune responses, including wound healing without causing severe responses that lead to damage to tissues [31]. The discipline of biomaterials indicates the science of using materials in medicine to replace or fix damaged organs and tissue to improve life [32].

1.2.1 Biomaterial classification and application:

Biomaterials are classified variously but, in general, are divided into three groups. (i) Organic materials are used for therapy, delivery systems, and tissue engineering, like Food and Drug Administration (FDA)-approved polyethylene glycol (PEG), and poly lactic-co-glycolic acid (PLGA), respectively. (ii) Inorganic materials are characterized by controllable synthesis and rigid structure. (iii) Bio-based materials originate from cells (like bacteria) such as protein-based nano-systems [18]. Biomaterial classification can also rely on either the chemical structure, for example, metal, ceramic, polymer, and composites, or the interaction level with the biological environment, such as inert, bioactive, and bioresorbable [28]. Moreover, biomaterials are categorized according to the origin, but less common, to (a) natural, such as living cells, tissue, collagen, and starch, (b) synthetic, such as polymers (hydrogel), and (c)

semi-synthetic (hybrid), which combines natural and synthetic sources. Another classification distinguishes if these materials are living or non-living [18, 19, 26-28, 33]. Some factors affect biocompatibility. This includes i) interaction with the environment including toxicology and allergy inflammation. ii) The period of the applicable implant includes long and short-term applications. iii) Structure influences the adaptation of implants with host tissue. vi) Biomaterial surfaces affect biocompatibility, which involves biological, chemical, and morphological adaptation. In addition to that, v) the function and the size of the implant are considered [34].

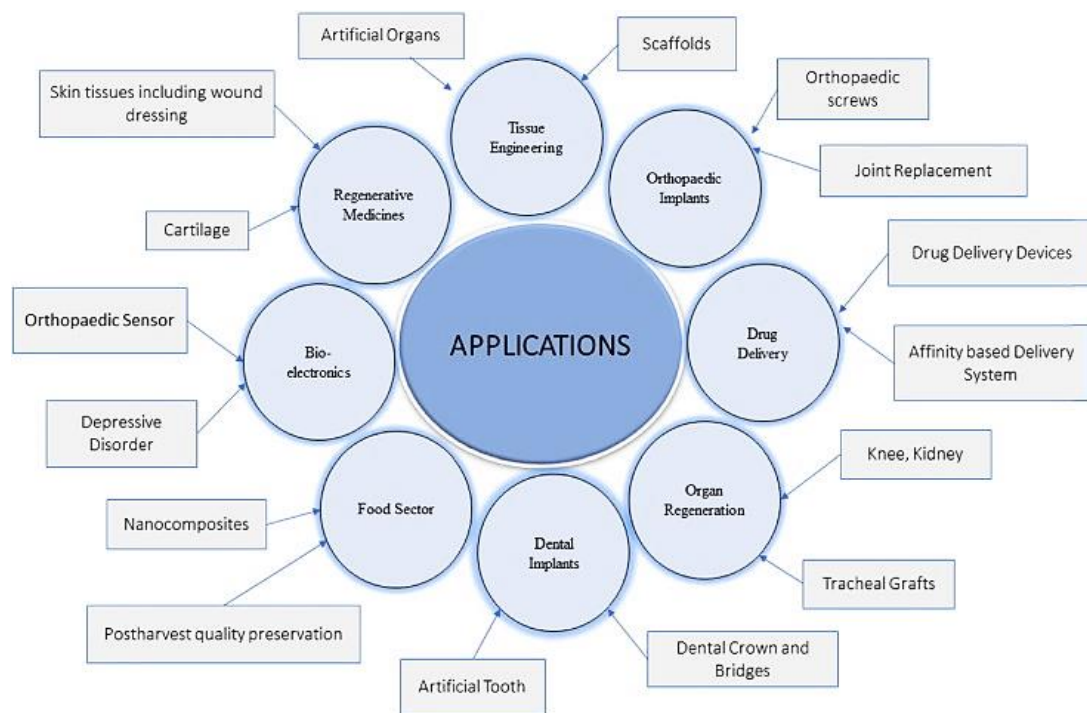


Figure 4I Application of biomaterials in medicine. Biomaterials are involved in many fields such as Drug delivery and tissue engineering.... etc. The scheme summarizes most of the medical applications with some examples [34].

The science of biomaterials plays a critical role in medicine, where biomaterials are used in medical applications such as healing wounds, implanting human organs, and drug delivery systems [35]. The reason is that they have biological, chemical, physical, and mechanical characteristics, affecting their functions and applications in humans [19]. Natural biomaterials may be considered the best materials for having unique characteristics such as nontoxic, biodegradable, and biocompatible [35]. Scientists could use biomaterials in various applications, summarized as the following (Figure 4): i) implants involve artificial joints, ligaments, and heart valves. ii) Human tissue healing includes sutures and clips. iii) Human tissue regeneration includes a mix of biomaterial supports and bioactive molecules. iv) Molecular probes and nanoparticles help in cancer imaging and therapy. v) Biosensors aid in

the detection of specific molecules. vi) System of drug delivery carries drugs for disease treatment [19, 27, 33].

1.2.2 Living therapeutic materials (LTMs):

Systemic administration of drugs may result in inaccurate drug delivery because increased doses of the drug must be administered to achieve effective doses at the targeted site in the body, which may ultimately result in side effects due to off-target effects. One of the main goals of current pharmaceutical research is to develop systems for improving the delivery of drug molecules to specific targets and to avoid delivery to nonspecific targets [36]. Although development in biotechnology could apply microbes, biofilms, nanoparticles, and biopolymers to reach the target site and monitor activation, there were also some challenges, such as stability, biosafety, accuracy, autonomous repairing, and cost [36, 37]. For that reason, biomaterials can be applied in medicine, as indicated previously, in diverse ways for tissue regeneration, wound healing, and drug delivery [32]. In this regard, the term LTMs is defined as monitored stimulus-responsive drug-producing microorganisms, as long-term implantable treatment solutions for local disease settings. These composite materials, consisting of two or more of various materials, are classified as the fifth class of biomaterials [35]. This system should have specific conditions for application, which include four characteristics: (i) a delivery vector, (ii) stability until a specific site, (iii) stability inside the target site, and (vi) release of the drug on time for a specific function [36].

Engineered living materials (ELMs) are living entities, such as *Escherichia coli*, engineered by synthetic biology, such as the CRISPRi tool and synthetic gene circuits, which can modify their characteristics [37]. Synthetic biology can change main characteristics by inserting promoters, inducers, or nucleic acid-modifying enzymes [38]. Therefore, the ELMs can function and respond to detectable micro-environmental stimuli [37, 39]. Furthermore, recent studies have concentrated on synthetic cell fabrication for having similar features to natural cells [38]. Engineered microorganisms can be encapsulated in biofilms by viscoelastic hydrogel [40]. Thus, this encapsulation can protect and react with the living entities inside. It acquires living characteristics like biosensing and self-regeneration [37]. Utilizing encapsulation and engineered cells emerges as a promising method to avoid activating immune cells [41]. Drug delivery systems, fabricated from biomaterials, are characterized by a good capacity for packing and their variable functions, which lead to drug release at the target location and continually [18]. Designing such delivery systems enables bacteria to sense the change in the environment and then inhibit or regulate protein expression [36]. Therefore, therapeutic microbes refer to genetically engineered microorganisms designed to be sensitive and respond to the signals in

their environment by releasing specific target molecules. These materials have advantages, such as self-renewal, non-resistance inducible, various inhibitory mechanisms for pathogens, specific pathogen targeting, and lower toxicity [4].

1.3 Biosafety of therapeutic materials:

Biosafety indicates prevention and monitoring of risks of biological danger factors caused by pathogens or biotechnological factors. It concentrates on ecology and human health to stop the loss of biological coherence on a large scale [25]. To discover and develop a drug or a therapeutic agent until it is validated, many steps proceed using various skills and technologies [42]. Regarding biosafety, to inhibit the escaping of engineered bacteria into the environment, biocontainment systems should be applied. This includes the use of kill switch variants, and non-natural amino acids, making the bacteria depending on factors only available in the human system. *E. coli*, for instance, can sense cues of the microenvironment after engineering by circuit-based kill control, a synthetic circuit (essentializer and cryodeath) [37, 43]. Although one advantage of hydrogel is its ability to integrate into safe by-products, allowing controlled decomposition to serve as a carrier for drug delivery, biocompatibility, or drug release, this aspect has not yet been fully investigated [32]. Stages of therapy or drug discovery are summarized as follows: (i) Pre-drug discovery includes medical conditions such as disease without treatment, then the research to answer basic questions like disease mechanism and possible treatment targets which, for example, inhibit or activate protein or pathway [42, 44].

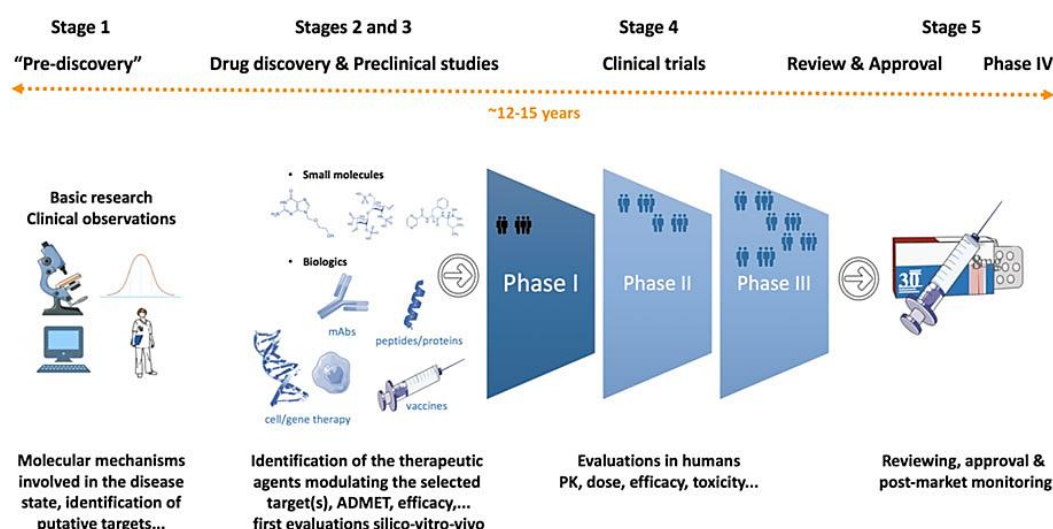


Figure 5I Stages of drug discovery and development process. The figure divides the drug progress process into five stages. It starts with pre-discovery, drug discovery, and preclinical stages. The final two steps are the clinical trials, which are applied in humans and followed by FDA approval. The time required for all phases of therapy finding is about 12 to 15 years. The cost is approximately 2.8 billion dollars [42, 44].

(ii) Drug discovery involves searching for molecules or strategies for a therapy leading to interaction or treating the disease, which results, at least, in symptom restrictions. (iii) Preclinical development includes knowing the drug candidate mechanism, cytotoxicity, and validation *in vitro* and *in vivo*. Afterward, (iv) the investigation stage of the drug candidate inside humans is called the clinical stage. The last step is (v) approving or non-approving drug candidates, where the FDA performs this process [42]. During the preclinical stage and after a potent drug or therapy selection, the drug must be safe through testing *in vitro* (cells) and *in vivo* (mouse). If not, it fails in the clinic as it does not meet the requirements [42, 44]. Although drug numbers increased by approximately 62%, 1 of 10 drugs was only approved by the FDA. Furthermore, 3.5% of approved drugs were withdrawn from the American market between 1980-2009 because of safety issues [75].

1.3.1 *In vitro* biocompatibility (cell culture safety):

Cytotoxicity evaluation by *in vitro* models aims to predict the toxicity risk in humans and displays a standard procedure with rising relevance in view of implementing animal replacement techniques [45]. Thus, *in vitro* biocompatibility investigation of biomaterials can determine their compatibility with biological systems and the potential biological response to materials in or on human tissues [46, 47]. Any novel material is considered a medical device only after being proven *in vitro*. It is, explained earlier, followed by preclinical and clinical investigations to ensure biosafety [48]. However, three essential biocompatibility assessments are required, including cytotoxicity, irritation, and sensitization. Further cytotoxic risk assessments are proceeded depending on the material nature and targets. These include genotoxicity, systemic toxicity, hemocompatibility, and implantation research [47].

Cytotoxic tests aim to determine if the devices or their extract are safe to be used in contact with biological systems like cells, tissues, or animals. The exposure time is about 24 h and incubated with known cell lines used commonly, such as Balb 3T3 (fibroblasts), L929 (fibroblasts), and Vero (kidney-derived epithelial cells). The test evaluates different endpoints, including cell viability, detachment, lysis, and morphological changes. Irritation test evaluates the potential irritation of the skin with medical devices during incubation time. The exposure time ranges from 18-24 hours with a 3D skin model (RhE model), potentially replacing animal testing. The irritation test is followed by an assessment of cell damage and inflammation, such as the MTT test and profile of cytokine release. The sensitization test aims to evaluate allergic or hypersensitivity reactions to devices or their materials by the immune system [47]. The

immunogenic response is investigated *in vitro* and evaluated using primary cell types such as PMBCs, macrophages, NK, and dendritic cells. The evaluation of immunogenicity concentrates on three directions: i) cell viability, ii) maturation, and iii) activation. After the interaction of the immune cells with biomaterials, cell viability can be determined for cytotoxic evaluation, and maturation of immune cells with respective cell surface markers, indicative of pro- and anti-inflammatory conditions. The immune cell activation measurement relies on detecting release cytokines via functional assays such as phagocytosis, nitric oxide, and ROS production. Thus, these short-term assays can provide information on cell activation levels after contact with biomaterials [49].

1.4 Immune system and fighting enemies:

The immune system prevents and protects the body from external factors such as infection and internal factors such as cancer or sterile inflammation. It involves two main categories, innate and adaptive immunity [50, 51, 53]. Microbes are either obligatory pathogenic, facultative pathogenic, or commensal [51]. Microbial invasion into the human body stimulates the response of the immune system, demonstrated by the increase in the number and recruitment of immune cells involved in the innate immune response [54].

The innate immune system, antigen-dependent but nonspecific, includes physical and chemical barriers (skin and soluble protein) followed by effector cells like granulocytes (neutrophils, eosinophils and basophils) [51]. These cells can be distinguished by morphological, histological, and immunological characteristics [53]. When microbes overwhelm the barriers, neutrophils are the first migrants to the infection site, which respond rapidly and typically in minutes or hours [50]. Further, they may have immunogenic memory. Trained immunity, for example, can increase the resistance to reinfection in adaptive immunity-lacking organisms, as demonstrated in plants, invertebrates, and mammals [50, 55]. Moreover, neutrophils can also activate adaptive immunity (T and B cells) leading to a cascade of proinflammatory cytokines [54]. Neutrophils have membranous and intracellular receptors like toll-like receptors (TLRs), which recognize and bind pathogen-associated molecular patterns (PAMP) either released in the microenvironment or expressed on microbes [51]. Further, N-formylated peptides marking the bacterial mitochondria are recognized by FPR-1 and -2 expressed on neutrophils [52]. More about neutrophils, their activation and sensing to biomaterials are discussed in the following text.

1.5 Neutrophils:

Neutrophils are polymorphonuclear cells (PMNs) and function as the first line of defense in the human body. They form about 50-70% of white blood cells (WBCs) circulating in body vasculature [53, 56]. Thus, they represent the most migrated leukocytes. However, they have a short life span [56]. Neutrophils can live for hours in circulation while tissue immigration and factors such as growth factors can extend the life span of neutrophils up to several days [57]. Bone marrow is the place of origin and maturation of neutrophils, in which they leave it to blood circulation [58]. Under normal conditions, they are produced in approximately 10^9 (1 billion) cells/ kg and circulate in peripheral blood as resting cells. Under infection conditions, the neutrophils rise in number up to 10-fold and become activated [16, 56, 59]. The total number of neutrophils was approximated by one hundred billion (100×10^{12}) between entering and leaving the blood vasculature each day, forming the initial response of innate immunity and the neutrophil role in the resolution of microbes [58]. Neutrophils are the dominant leukocyte population in circulation and tissue, with tissue residing neutrophils acting as potent first responders to microbial infections [60].

1.5.1 Granulopoiesis to the circulation in the blood vasculature:

Hematopoietic stem cells (HSC) are the main center of most immune cells including innate and adaptive immune systems such as granulocytes, dendritic cells and monocytes. Further, tissue macrophages are produced from precursors in the yolk embryo [251, 252]. Hematopoiesis is a process of hematopoietic stem cell (HSC) production [253]. Thus, HSC might be a heterogeneous pool of multipotent cells [251]. The HSC differentiation process relies on internal and external cellular factors affecting mature immune cell function and generation [253]. It can be divided into three categories. The stem cell pool involves undifferentiated HSCs. The mitotic pool includes granulocytic progenitor cells. Further, the postmitotic pool contains fully mature and differentiated neutrophils [61]. In bone marrow, HSC differentiates into multipotent progenitor (MPP) cells that cannot produce themselves again. Then, MMPs convert to lymphoid-primed multipotent progenitors (LMPPs), resulting in granulocyte–monocyte progenitors (GMPs). Then, granulocyte colony-stimulating factor (G-CSF) can convert GMPs to neutrophil generation. This includes myeloblasts, myelocytes, metamyelocytes, band cells, and mature neutrophils at the final stage [60, 61, 252]. At the myeloid progenitor line, immune cells can be divided into seven subsets of precursors including granulocytes (neutrophils, basophils, eosinophils), monocytes, DCs, erythrocytes, and megakaryocytes, based on scRNA-seq (MARS-seq) analysis [251]. Neutrophil production

relies on host cues instead of monocyte generation and vice versa. Some arguments are related to the production of neutrophils and monocytes. MPPs are generated by having the capability to differentiate into neutrophils and monocytes. In another way, cell type-generated progenitors are expanded to differentiate later into both cell types [62]. The whole differentiation process till the production of mature neutrophils takes over 10 days [240].

Multiple factors can regulate neutrophil development. This includes proteins (S100A8, S100A9, neutrophil elastase), transcription factors (Egr1, HoxB7, STAT3, PU1, C/EBP α - ζ), and receptors (*N*-formyl-methionyl-leucyl-phenylalanine receptor and GM-CSF receptor) [61]. During neutrophil development, they change their nucleus, receptor expression, and granule formation. Neutrophils, for instance, upregulate the expression of CXCR2 and Toll-like receptor 4 (TLR4) and downregulate CXC chemokine receptor 4 (CXCR4) and integrin $\alpha 4\beta 1$ (VLA4) expression. Those receptors play a crucial role in retaining progenitor cells in bone marrow, where ligands such as chemokine stromal-derived factor-1/SDF-1 (CXCL12) and vascular cell adhesion molecule 1 (VCAM1) bind to CXCR4 and VLA4, respectively [60]. Based on activation and recruitment, neutrophils change their expression of the surface markers [66].

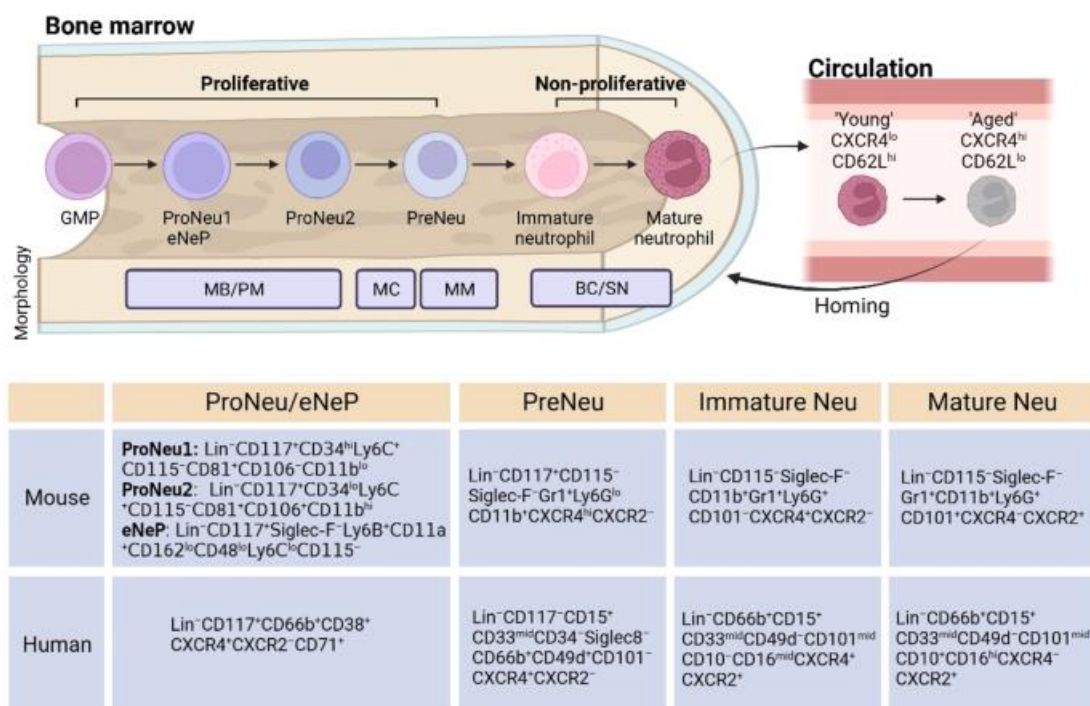


Figure 6l Development of neutrophils from bone marrow to circulation and homing back. Circadian rhythms recruit neutrophils back to bone marrow. Abbreviations [MB, myeloblast; PM, promyelocyte; MC, myelocyte; MM, metamyelocyte; BC, banded cell; SN, segmented neutrophils [63].

Neutrophils leave the bone marrow by induction of G-CSF which interferes with CXCL12 and CXCR4 expression, where neutrophils downregulate CXCR4 expression, and stroma cells downregulate their ligand, CXCL12. Furthermore, endothelial cells release ligands such as CXCL1, CXCL2, CXCL5, and CXCL8 binding with CXCR2 to attract neutrophils into the vasculature [60]. Neutrophils' functional processes can be involved in physiology, such as wound healing, angiogenesis, and hematopoiesis, and pathology, such as inflammatory response and autoimmune diseases [64]. Neutrophil homeostasis can quickly change. Therefore, subsets of circulating mature neutrophils can maintain their size via a balance between granulopoiesis, release into the vasculature, and homing back to bone marrow. Moreover, these subsets vary in blood circulation during their lifespan [65]. Neutrophil lifespan increases in the presence of stimuli like LPS, whereas they have relatively short longevity without it [252]. Circulating (freshly released) neutrophils have a short half-life in the bloodstream ranging from 8 to less than 24 hours, where they become aged and home back to the bone marrow [236, 237-239]. Circulating neutrophils (45–65%) of healthy individuals can be CD177⁺, which promotes endothelial cell-neutrophil interaction and extravasculature. Another proportion of circulating mature neutrophils (~20–25%) have glycoprotein olfactomedin 4 (OLFM4⁺) which showed a distinctive production of NETs *in vitro* [63, 65]. In healthy individuals, there are also TCR $\alpha\beta$ ⁺ or proangiogenic circulating neutrophils (CD49d⁺CXCR4⁺VEGFR1⁺) [66]. Neutrophils reside in organs such as the liver, BM, lung, kidney, lymph node, and spleen to perform specific functions with context-specific phenotypes. Neutrophils in the splenic marginal zone (MZ), for instance, support B cells in multiplication and antibody production where they are called B cell helper neutrophils' (NBH cells) [65-67]. Additionally, they support endothelial cell proliferation to maintain endothelial intact as a barrier [66].

Further, neutrophils were well studied during infections with bacteria and fungi. Regardless, they also exist in organs, like lungs and bronchoalveolar lavage, in humans, mice and rats, after viral infection by HMPV, HRSV, and IAV [66]. During infection, neutrophils can quickly sense and attack microbes after invasion via munition including antimicrobial agents [62]. Neutrophils can work as antigen-presenting cells (APCs) to stimulate tissue T cells. It was shown that, for instance, they activate tissue CD4⁺ and CD8⁺ T cells during viral infection [65, 66]. Furthermore, many studies have also reported the pro- and anti-tumorigenesis of neutrophils in cancer, which reflects their significant role in infectious and cancer diseases with highly context-specific functions [67]. During inflammation, neutrophils can phagocytose virus-infected cells. They can be engulfed by macrophage (efferocytosis), converting macrophage to

a more effective anti-inflammatory phenotype [66]. Immature neutrophils ($CD66b^{+}CD10^{-}$) enter blood circulation as a response to LPS and G-CSF adding or a disease such as cancer, and infection. These cells can perform chemotaxis and antimicrobial defense as a part of innate immunity. During inflammation, mature activated neutrophils have suppressive characteristics such as normal-density neutrophils (NDN) and low-density neutrophils (LDN). However, LDNs/PMN-MDSCs subpopulations are immunosuppressive while other LDNs contain immature and non-suppressive neutrophils that are proinflammatory or have undefined functions [65, 67].

1.5.2 Recruitment during inflammation:

1.5.2.1 Activation process of neutrophils:

Most microorganisms invading tissues are either commensal or pathogenic microbes and are recognized and attacked by neutrophils. The microbial recognition process may have two forms. Neutrophils can express pattern recognition receptors (PRRs), which bind to specific structures. Also, soluble proteins such as complement proteins and antibodies can opsonize microbes to facilitate recognition [68]. Generally, the activation process has two stages. The priming process is a pre-activation that enables neutrophils to respond to activating stimuli. This leads to the second stage, in which neutrophils become fully activated. During migration, neutrophils are primed by factors activating their receptors such as chemokines and adhesion molecules. Neutrophils express PRRs, a receptor group that recognizes specific molecular structures of apoptotic or damaged cells and pathogens [69]. These molecules include pathogen-associated molecular patterns (PAMPs) and damage-associate patterns (DAMPs) that complete neutrophil activation based on binding with PRRs [16]. Pattern recognition receptors (PRRs) expressed on neutrophils include TLRs (TLR1/2, TLR2/6, TLR4, 5, 7, and 9), RIG-I-like receptors (RIG-I, MDA-5), C-type lectin receptors, and NOD-like receptors binding directly with PAMPs [66]. Furthermore, DAMPs are derived from damaged and necrotic cells and can cause the initial cues in most inflammatory cases. DAMPs include DNA, proteins, N-formyl peptides (derived from mitochondria of tissue damage), components of extracellular matrix, ATP, and uric acid, recognized by neutrophilic surface toll-like receptors (TLRs) or/and NOD-like receptors (NLRs) [59]. Pathogenic microorganisms produce exogenic products, including formyl peptides, lipoproteins, or peptidoglycan, released during microbial invasion and multiplication. Furthermore, pathogenic invasion causes damage to the host, leading to the release of chemo-attractants and cytokines and causes inflammatory cues [58]. Neutrophils can be recruited to the infection site by mast cells indirectly, which produce TNF or a tryptase.

These molecules aid tissues in chemokine production [70]. There are other various triggers, which can activate neutrophils. This includes: i) mediators of complement activation such as C3a and C5a via G-protein coupled receptors [56]. ii) Lipid mediators derived from arachidonic acid such as eicosanoid leukotriene B4 (LTB₄, LTC₄) through the BLT1 receptor. LTB₄ is produced by mast cells and activates neutrophils directly [56, 70]. iii) Growth factors and cytokines as well as chemokines through cognate receptors; v) danger-associated molecules such as extracellular ATP through purinergic receptors; vi) Extracellular cold-inducible RNA-binding protein (CIRP) through triggering receptor expressed on myeloid cell [TREM]–1; vii) microbial proteins like LPS and lipoproteins by Toll-like receptors, viii) N-formylated mitochondrial peptides via the formyl-peptide receptor 1 (FPR1) [56]. Moreover, microenvironmental proteins derived from tissues such as TNF- α , IL-1 β , IFN- γ , and GM-CSF activate and multiply neutrophil recruitment to migrate to the infection site [66].

Table 1: DAMP and PAMP of the neutrophil receptor [71].

PAMPs:	Receptors:	DAMPs:	Receptors:
Viral ssRNA	TLR7/8	RNA	TLR3, TLR7, TLR8, RIG-I, MDA5
dsRNA	RIG-I, MDA5, PKR	DNA	TLR9, AIM2
LPS	TLR4	Histones	TLR2, TLR4
Lipoarabinomannan	TLR2	HMGB1	TLR2, TLR4, RAGE
Zymosan		S100 proteins	TLR2, TLR4, RAGE
Lipoteichoic acid		Biglycan	TLR2, TLR4, NLRP3
CpG motifs of bacteria and viruses	TLR9	N-formyl peptides	FPR1
Bacterial flagellin	TLR5	ATP	P2X7, P2Y2
Triacyl lipoproteins	TLR1/TLR2		
Fungal mannose	Mannose receptor, dectin-2, DC-SIGN	Interleukin 1 α	IL-1R
Parasitic hemozoin	TLR9	Interleukin 33	ST2
		Heat shock proteins (HSPs)	TLR2, TLR4, CD91
		Amyloid- β	TLR2, NLRP1, NLRP3, CD36, RAGE

1.5.2.2 Neutrophil extravasation:

Neutrophil extravasation is a complex process that involves various stages and relies on interactions with other cells such as endothelial cells, perivascular cells (monocytes and macrophages), and stromal cells. Chemoattractants such as CXCL-1, -2, -12, and LTB₄ are produced by perivascular leukocytes after activation and play a key role in attracting neutrophils

captured by endothelium. CXCL8, interferon-gamma (IFN- γ), tumor necrosis factor-alpha (TNF- α), platelet-activating factor (PAF), complement factors C3a and C5a, and bacterial peptides can prime neutrophils that firm the endothelial adhesion [67]. Then, upon stimulation, neutrophils migrate through the blood vasculature and reach the endothelium of the site of microbial infection. Then, neutrophils can extravasate the tissues in four stages by the interaction of the leukocytes with endothelial cells: rolling and capture, adhesion, crawling, and transmigration [68, 72]. Moreover, other studies divided the extravasation process into capturing' (tethering'), rolling, slow rolling, arrest, post-adhesion strengthening, crawling, and paracellular or transcellular transmigration [59, 73]. Blood cells, including neutrophils, monocytes, NK, B, and T, express E-selectin ligand (ESL-1). As a response to inflammatory proteins including LPS, IL-1, and TNF- α , ESL-1 is represented in the endothelial cells [74]. On the other side, the L-selectin (CD62L) expressed by neutrophils binds weakly with E-selectin (CD62E) or P-selectin (CD62P) on the endothelium [74, 75]. Such binding is not hard enough to be constant against the strong blood flow [53]. Therefore, upon neutrophil-endothelium contact, chemokine ligands (ex. CXCL-8) of inflamed endothelium bind with special neutrophilic chemokine receptors. This process leads to a conformational change in neutrophils, L-selectin shedding, and activates the expression of β 2 integrin expression such as lymphocyte function-associated antigen (LFA)-1 and macrophage antigen (MAC)-1/ so-called also: complement receptor (CR)-3/ CD11b/CD18, α M β 2) [53, 72]. The lack of β 2 integrins (CD11/CD18) on leukocytes, in particular neutrophils, leads to immunodeficiency syndrome called Leukocyte Adhesion Deficiency Type 1 (LAD-1)/Variant [233]. Furthermore, the deficiency in LAD leads to infection or tissue damage [73]. The adhesion process is firmed and ensured by adhesion molecules such as ICAM-1 and -2, VCAM-1, and a ligand of LFA-1 induced by TNF- α ↑ expressed in the endothelium [53, 72]. The strong interaction of ICAMs with integrin arrests neutrophils (stop rolling) and lets them transmigrate between endothelial cells. Then, neutrophils release matrix-metalloproteinase, such as MMP9, to cross the basement membrane. Afterwards, Chemokines secreted from cells directly extravasated neutrophils to the site of infection [53]. Extracellular matrix (ECM) exists in all organs and tissues to connect cells jointly. It is formed from collagen fibers like collagen I and II, fibronectin, elastin, and proteoglycans. ECM is also involved in the basement membrane components, containing type IV collagen, laminin, and heparan sulfate proteoglycans [76]. Collagen is the best-known protein in ECM and forms one-third of all proteins totally. Collagen maintains tissue characteristics, shape, and structure [77]. Neutrophils release a bunch of proteases that digest the ECM allowing neutrophils to migrate inside tissues [76]. Neutrophil

migration through ECM includes cell identification and protein destruction. For that reason, neutrophils undergo oxidative and nonoxidative processes inside ECM to degrade proteins, microbes, and other objects [79]. Thus, neutrophils have a group of protease enzymes such as serine, including elastase, proteinase 3, and cathepsin G stored in primary granules and can degrade materials like elastin, fibronectin, laminin, and collagen IV. Moreover, Matrix metalloproteinases (MMPs) exist in the secondary and the tertiary granules and can degrade matrix proteins, including all collagen types [76].

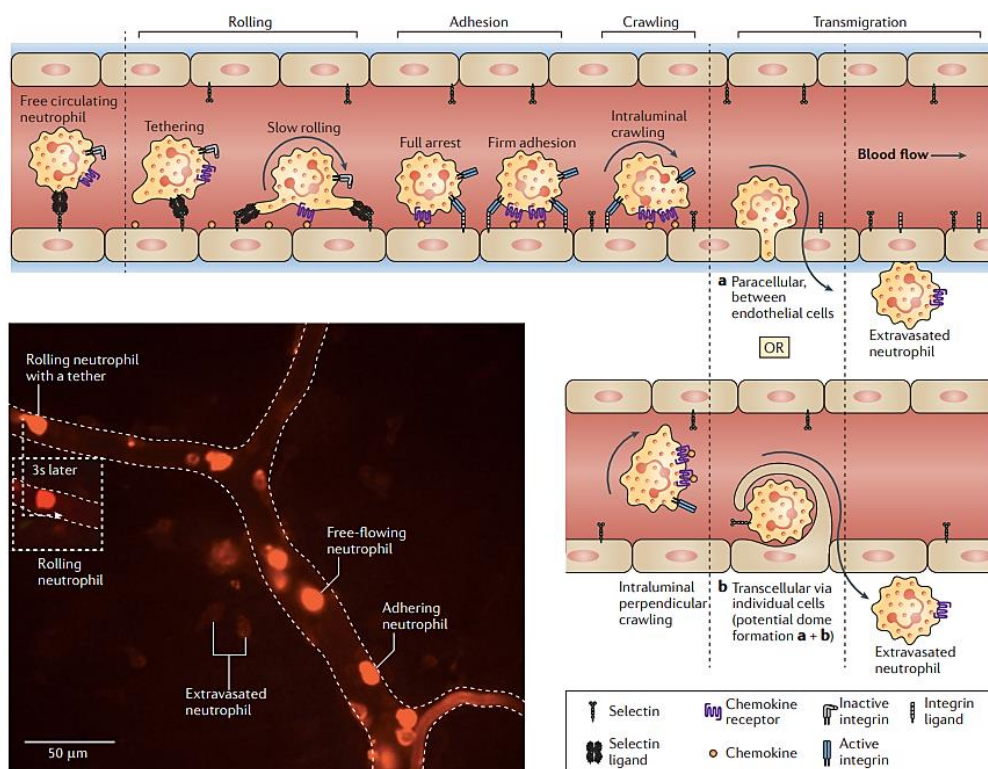


Figure 71 Illustration of neutrophil recruitment from the blood vasculature to infected tissues: Schema (upper) shows stages of neutrophil recruitment in detail. *Staphylococcus aureus* was used to infect mouse skin for 2 h. Image (lower left) of neutrophils (LY6G+ cell, red) was taken by intravital microscopy in skin postcapillary venule [78].

Neutrophils can prolong their life inside ECM by interaction with fibrinogen. However, neutrophils select transmigration through ECM with low proteins [79]. Neutrophils can remodel ECM by producing MMPs and elastases leading to the release of NETs and exosomes. Sequentially, ECM renovates the microenvironment of inflammation by adjusting neutrophil functions [77]. Tissue-immigrated neutrophils can survive from one to several days. The increase in neutrophil lifespan is related to a downregulation of proapoptotic proteins after transmigration [236, 238-241]. Furthermore, neutrophil phenotype changes by expressing a double amount of CD11b interacting with ECM. This affects neutrophil adhesion, motility, and

rapidness after transmigration [79]. After surveying the infected tissues, neutrophils may come back to blood vasculature in a mechanism called reverse migration, to bone marrow [68, 80]. Some reverse-migrated neutrophils move to the lung to die in a process called programmed cell death (apoptosis) [80].

1.5.3 Killing mechanisms involved in neutrophil response:

During activation and upon reaching the infection site, neutrophils can kill or cause harm to pathogenic microorganisms in diverse ways. These processes include: i) degranulation, in which neutrophils secrete a cascade of pre-stored effective and proteolytic proteins. These proteins contain matrix metalloproteinases (MMPs), myeloperoxidase (MPO), and neutrophil elastase (NE) [16, 81]. Degranulation can be intercellular after phagocytosis or extracellular to kill microbes [59]. The principal three granules of neutrophils have various functions and contents. They have granules such as azurophilic (primary) enriched in MPO, specific (secondary) containing lactoferrin, and tertiary containing gelatinase, MMP9, and other proteins [76]. ii) Phagocytosis, where neutrophils produce oxidative burst after engulfing the microbe. Based on the catalyzation of NADPH oxidase, ROS can be generated, such as superoxide anion (O_2^-), hydrogen peroxide (H_2O_2), and hydroxyl radicals ($HO\cdot$) [16, 58]. Moreover, they can secrete antimicrobial proteins such as cathepsins, defensins, lactoferrin, and lysozyme [59]. Neutrophils are professional terminally differentiated cells whose function is to eliminate microbes, dead cells, and cellular debris. [66]. iii) ROS are produced by mediated NADPH, leading to an oxidative burst [16]. ROS can be released intracellular inside the phagosome to kill smaller microbes or extracellular to fight bigger pathogens. It may kill a pathogen directly and indirectly by autophagy through NETosis induced by inhibition of mTOR kinase or to promote the death of pathogen-infected cells. Scientists could prove that the location of ROS functions as a mechanism to measure the microbe size affecting neutrophil response. Intracellular ROS production was induced *in vitro* by *small C. albicans* (spore) as a neutrophil response. This resulted in decreased IL-1 β production and restricted neutrophil recruitment to the site of infection. In contrast, using large *C. albicans* (hyphae) led to the production of extracellular ROS and caused an increase in IL-1 β and neutrophil recruitment [66]. vi) NETosis is the release of a net containing DNA loaded with histones, proteins, and enzymes. The net can immobilize pathogens, thus facilitating microbial engulfing or killing microbes directly by antimicrobial proteins [16, 59]. Microorganisms, including bacteria, fungi, parasites, and viruses, are considered inducing factors of NETosis [66]. Furthermore, NET release forms in two ways, either suicidal or vital NETosis [82]. The non-lytic form of NETosis does not kill microbes. However, NETs are thought to be secreted for the larger microbe, which

cannot be phagocytosed [66]. v) Antibody-dependent cellular cytotoxicity (ADCC) is a mechanism, where immune cells, such as neutrophils, kill cancer cells using supplemented antibodies (explained in detail in the method section). Effector cells have Fc receptors like Fc γ - and Fc α , expressed on neutrophil surfaces. Those receptors can bind IgG or IgA antibodies, respectively, to opsonize tumors for killing [57].

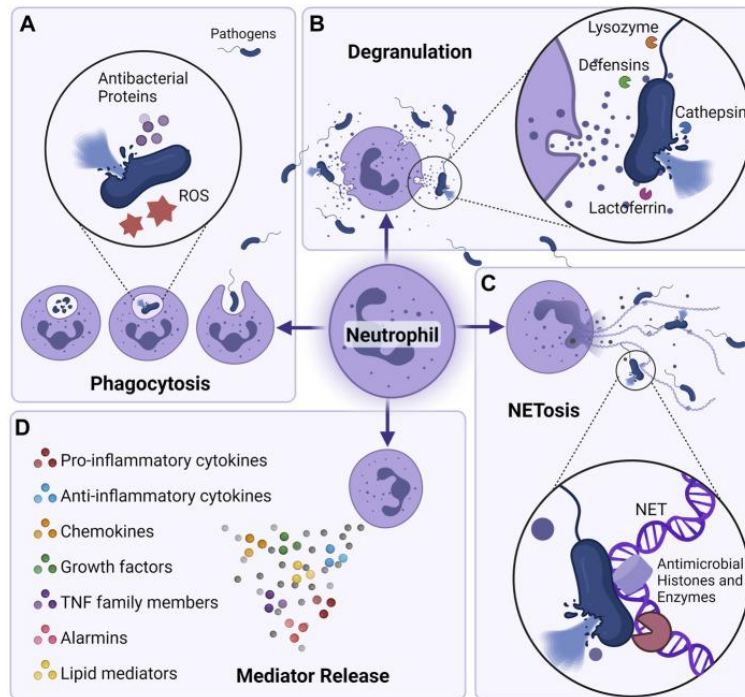


Figure 8I Main killing mechanisms by neutrophils. **A)** The pathogen is engulfed and killed by the release of antimicrobial protein or ROS. **B)** Release of extracellular antimicrobial proteins to kill pathogens. **C)** NETosis is a process of releasing nets of DNA, Histones, and enzymes to fix and kill microbes. **D)** Neutrophilic release of some mediators can reshape the immune response and change the function of neutrophils themselves [59].

However, neutrophils can attack and kill microbes using different strategies, pathogens can escape from killing by various mechanisms. This involves avoiding chemotaxis and extravasation, inhibition of opsonization and phagocytosis, and escape from NETosis as well as survival inside neutrophils, even dead cells [58]. Other functions include the release of v) soluble mediators and iv) extracellular vehicles (EVs) that may modulate the microenvironment, leading to various responses of other immune cells [16]. Extracellular vesicles, so-called micro-vesicles or ectosomes, are released as a response to microenvironmental cues such as DAMP and enable neutrophils to react with other cells [82]. Neutrophils can secrete various products, including pro-inflammatory proteins (IL-1 β , IL-6, IL-17, TNF- α) and anti-inflammatory proteins (IL-1RA, IL-10). Furthermore, they release chemokines (CXCL-1, -2, -8, -10), growth factors (BAFF, G-CSF, M-CSF), and lipid mediators

(resolvin, lipoxin) as well as alarmins (S100A8/A9, S100A12) [59]. iv) it is possible that neutrophils participate in tumor apoptosis through cell-cell interaction by the Fas-Fas-ligand (FasL of neutrophil) signaling pathway [57].

1.5.4 Neutrophil proteins:

Neutrophils can produce more than 1200 specific proteins [83]. However, blood neutrophils can increase their protein contents during systemic infection. Proteomic proteins were estimated by the average number of 4950 in humans and 5384 in mice with total protein mass of 60 and 40 pg/cell, respectively [84]. Moreover, neutrophils can secrete cytokines and chemokines to perform a specific function [67]. LPS and N-formyl peptides can activate TLR4 and FPRs of neutrophils, respectively, and produce proinflammatory cytokines, degranulation, and others [85-87]. Activation of TLR4 has two specific signaling pathways. The first pathway is Toll/interleukin-1-receptor (TIR)-domain-containing adaptor protein (TIRAP) followed by Myeloid differentiation primary response (MyD)88 resulting in the release of proinflammatory cytokines. The second pathway is TIR-domain-containing adaptor protein inducing interferon- β (TRIF) followed by TRIF-related adaptor molecule (TRAM) resulting in type I interferon production [88]. Activation by LPS leads to ROS generation, cell migration, phagocytosis, and NETosis [85]. The FPR family consists of FPR1, FPR2, and FPR3, which are known by different names in the literature: FPR, lipoxin A4 (LXA4) receptor (ALX)/FPR-like receptor (FPRL)-1, and FPRL-2, respectively [85, 86]. Bacterial peptides like fMLF are FPR ligands that activate neutrophils [89, 90].

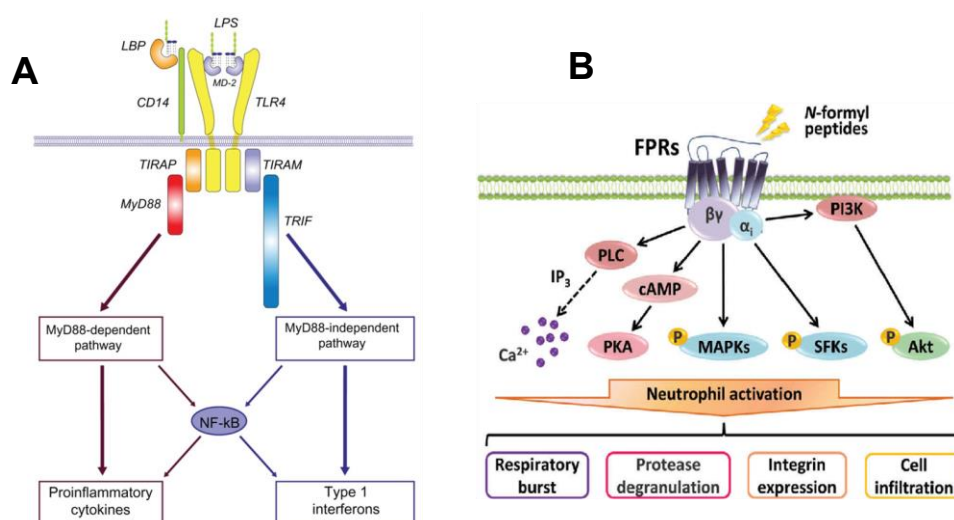


Figure 9I Activation of TLR4 and FPR pathways. (A) LPS activates two pathways shown in the schema including TIRAP-MyD88 and TIRAM-MyD88 signaling. (B) N-formyl peptide signaling leads to Calcium mobilization. LBP: ligand-binding protein; CD: cluster of differentiation [86, 87].

Additionally, cells can produce N-formyl peptides (N-FP) from endogenous mitochondrial proteins during damage or injury. These mitochondrial peptides are identified as DAMPs and can initiate sterile inflammation by activating FPRs in monocytes and neutrophils. FPR activation triggers calcium mobilization and MAPK phosphorylation, resulting in ROS production, neutrophil migration and degranulation including MMP release [85, 86].

1.5.4.1 Matrix-Metalloproteinases (MMPs):

MMPs are extracellular macromolecule groups found in multicellular organisms and can degrade the extracellular matrix (ECM) [91-93]. MMPs are Zn^{2+} -containing endopeptidases. They are released in an inactivated state and activated by the Ca^{2+} -binding domain. They can break down peptide bonds in the connective tissue proteins [92-94]. MMPs are divided into six groups according to structure and type of target substrate. These groups include i) Gelatinases, ii) Collagenases, iii) Membrane type [MT-MMP], iv) Stromelysins, v) Matrilysins, and vi) other MMPs [92, 94]. 28 MMP members have been discovered in vertebrates, including 24 MMPs in humans and 14 in blood vessels, controlled or regulated by four inhibitors of MMPs (TIMPs) [91, 92]. They not only participate in natural cell processes, such as tissue remodeling, invasion, cartilage degradation, and wound healing, but also in cell pathology, where gene dysregulation may cause diseases such as chronic kidney, chronic obstructive pulmonary, and cancer [91, 94].

Table 2: Human (a: specific) and mice (b: specific) neutrophil granules. The table summarises most of the proteins secreted by neutrophils in three secretory granules and one secretory vesicle [96].

Azurophilic granules		Specific granules		Tertiary granules		Secretory vesicles	
Membrane	Matrix	Membrane	Matrix	Membrane	Matrix	Membrane	Matrix
CD63	Elastase	CD11b/CD18	Collagenase	CD11b/CD18	Gelatinase	CD11b/CD18	Plasma proteins
CD68	Cathepsin G	CD66	Gelatinase	CD67 ^a	Lysozyme	CD67 ^a	
Presenilin	Proteinase 3	CD67 ^a	uPA	Ly-6G ^b	Arginase 1	Ly-6G ^b	
	Defensins ^a	Ly-6G ^b	Cystatin C	Cytochrome _{b558}	B2-microglobulin	CD10, CD13, CD14, CD16, CD35, CD45	
	BPI	CD15	Cystatin F	fMLPR	CRISP3	MMP25	
	MPO	TNFR	hCAP18	MMP25	fMLPR	Gp91phox/p22phox	
	Lysozyme	uPAR	NGAL	TNFR		LIR1-4,-6,-7,-9	
	Sialidase	Cytochrome _{b558}	B12BP	Gp91phox/p22phox		C1q-R	
	Azurocidin ^a	SNAP-23	Lysozyme	SNAP-23		IFN- α R1, R2	
	B-glucuronidase	VAMP-2	Lactoferrin	VAMP-2		IFN- γ R1, R2	
	Azurocidin	Stomatin	Haptoglobin	Nramp1		TNFR1, TNFR2	
		PGLYRP	Pentravin 3			IL-(1,-4,-6,-10,-13,-17,-18)R	
		fMLPR	Prodefensin ^a			TGF- β R2	
		Fibronectin-R	A-1-anti-trypsin			CXCR-1,-2,-4	
		Laminin-R	SLPI			CCR-1,-2,-3	
		Vitronectin-R	Orosomucoid			Ig(G,A,E)FcR	
			Heparase			TLR-1,-2,-4,-6,-8	
			B2-microglobulin			MyD88	
			CRISP3			MD-2	
						fMLPR	
						TREM1	
						SNAP-25	
						Nramp1	
						Alkaline	
						Phosphatase	
						DAF	

MMP enzymes take their names and classification from extracellular matrix proteins, which they degrade such as collagenases (MMP-1, -8, -13, and -18), gelatinases (MMP-2 and -9),

stromelysins (MMP-3,-10,-11, and-19), matrilysins (MMP-7 and-26), membrane-type (MT)-MMPs (MMP-14,-15,-16,-17,-24, and -25) [108]. Neutrophils can produce MMP-8 and -9 during migration in addition to MMP-2 [89, 109]. MMP-2 (gelatinase A) and MMP-9 (gelatinase B) can degrade gelatine and elastin in addition to several types of collagens [93]. The genes of the MMP family, such as MMP-9, -2, -12, and -16, may be used as therapy targets and in prognosis for Kidney clear cell renal carcinoma (KIRC) [95]. MMPs can cut precursor variants of cytokines and release the active form. Thus, they can regulate cytokine release and activity. MMP-9 and 2, for instance, cleave latency-associated peptide (LAP) bound to TGF- β 1 to release pro-fibrotic TGF- β 1 in the active state [93].

1.5.4.1.1 Forms of MMP-9 (gelatinase B):

There are three forms of MMP9: monomer, homodimer, and heterodimer (complex with NGAL). These three forms of MMP9 actively proteolyze both gelatin and naïve collagen substrates [97]. There are two essential forms of pro-MM9 (inactive form): monomer of ~92 kDa and homodimer of ~220 kDa [98, 99]. These forms of pro-MMP9 enzyme catalyze the proteins at a similar level [97]. The zymogen of pro-MMP9 and pro-MMP2 can bind with tissue inhibitors of metalloproteinases (TIMPs) known as endogenous inhibitors of MMP activity [98]. Pro-MMP9 (homodimer and monomer) are inhibited by binding with TIMP-1 and catalyzed by MMP-3[97, 98]. MMP9 can be activated through prodomain removal by serine protease to be 83 kDa. It plays a crucial role in active VEGF release [100]. Also, pro-MMP-2 binds to TIMP-2 and-4 [98]. MMP2, inactive form, is expressed at 72 kDa. It degrades the basement membrane thus assisting in the migration of neutrophils and lymphocytes or stimulating them for chemoattractant production. MMP2 plays a key role in inflammation by inhibition or activation through the production of inflammatory proteins such as interleukin-1 β [100]. During inflammation, MMP-9 participates in the catalysis of ECM, trophoblast implantation, wound healing, and angiogenesis [98]. Inflammation of joints (arthritis) induced by antibodies showed raised and reduced degrees of arthritis in mice with MMP2 (gelatinase A) deficiency and MMP9 deficiency, respectively. These findings indicate the essential role of MMP2 against joint inflammation and the severe role of MMP9 [101]. During inflammation and in TIMP-1 absence, neutrophils release MMP9 in massive quantities. Regarding its essential role, neutrophils cannot migrate in MMP9-lacking mice towards a granulocyte chemotactic protein-2 (GCP-2/CXCL6) gradient [102]. MMP9, in active form, can cleave human chemokines at the initiation stage of inflammation [99, 102]. Thus, it modulates the function of cytokines, influencing the process of inflammation [103]. For example, active MMP9 can degrade human chemokines leading to inhibition of growth-regulated proteins such

as CXCL1 (GRO α), CXCL2 (GRO β), CXCL-4 (PF-4), CXCL-7 (NAP-2) stimulated by CXCL-9 (MIG), CXCL-10 (IP-10), CXCL-12 (SDF-1 α), CXCL-8 (IL-8) [102].

Neutrophil Gelatinase-associated lipocalin (NGAL) is a lipocalin family member [104]. NGAL has different names, lipocalin-2 siderocalin and 24p3, and many forms, including monomer (25 kDa), homodimer (46 kDa with disulfide-linkage), and heterodimer (135 kDa with disulfide-linkage) [105]. Based on activation, neutrophils produce NGAL associated with MMP9 (gelatinase 92kDa) [105]. NGAL functions as a protector for MMP9 against autolysis. Thus, NGAL assists in promoting MMP9 activity by creating a complex of MMP9/NGAL [104]. During infection and inflammation, neutrophils secrete NGAL, which withdraws the ferric siderophore of bacteria, and thus NGAL works as an antibacterial in the process of iron depletion [105]. Reflecting on its critical role, NGAL might be a novel indicator based on the samples of brain tumors (gliomas) and cancer patient urine, which showed a high level of MMP9 complex [104]. The study of MMP9-lacking mice showed presence of MMP9, during an influenza infection, is necessary for neutrophil migration. Also, the release of neutrophil MMP9 depends on the signaling of TLR. However, CCL3 (chemoattractant) mediated by MyD88 signaling in non-hematopoietic cells is necessary to recruit neutrophils. [106]. Other studies proved TLR4 activation in macrophages and SMCs led to MMP9 release. However, the absence of functional TLR4 resulted in a reduction of MMP9 expression [107].

1.5.4.2 Cytokine secretion:

Cytokines are small proteins belonging to a large family of pro- and anti-inflammatory proteins. Their division relies on function, structure, and receptor similarities [67]. They are produced by immune or non-immune cells to regulate substantial immunological interactions such as inflammation and angiogenesis [64]. Further, chemokines are a specific subgroup of cytokines. In addition to the human neutrophil cytokines (Fig. 12), there are further cytokines and chemokines produced by neutrophils and other immune cells that potentially affect neutrophils. In addition to cytokines and chemokines shown in Figure 12, others can be added as follows: Pro-inflammatory cytokines (IL-12, IL-17, CSF2, and CSF3) [67], (IL-7, -9, -16, -17, -18?) [64], Immunoregulatory (INF- β and INF-Y) [67], (INF α , IL-27, TSLP) [64], Anti-inflammatory (IL-10, TGF β -1 and -2) [67], (IL-4) [64], Colony stimulating factors (CSF2/GM-CSF and CSF3/ G-CSF), CXC chemokines (CXCL-16) [67], (-4,-12 and -13) [64], C-C chemokines (CCL-8 and -12), neutrophil mobilization factors (C3a, C5a, PDGF, CXCL-7 and -17) and Lipids (LTB4 and PAF) [67] as well as TNF family (LIGHT) and (NGF, BDNF, NT4) [64].

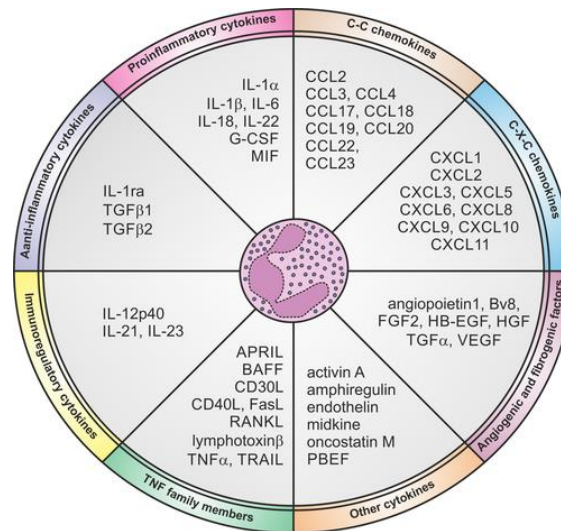


Figure 10| Potentially cytokines and chemokines of human neutrophils. The graph shows various groups of cytokines reflecting their functions by the name of some cytokines [110].

1.5.4.2.1 CXCL-8 (IL-8):

Neutrophils release CXCL8, a well-known chemokine attracting neutrophils [67]. It is also known as IL-8, NAF, GCP1, LECT, LUC, and other abbreviations [111]. IL-8 has two isoforms derived from ninety-nine amino acids (aa) by translation. An isoform of seventy-two amino acids is processed in immune cells like monocytes and macrophages, and an isoform of seventy-seven amino acids in non-immune cells. Based on the ELR motif (tripeptide Glu-Leu-Arg), CXC chemokines have two groups, either positive or negative ELR motif. Thus, CXCL-8 is a positive ELR motif (ELR+) [112]. In addition to neutrophils, CXCL-8 is secreted by other cells such as mononuclear macrophages, eosinophils, T lymphocytes, epithelial cells, and fibroblasts, as well as in tumor microenvironment (TME) cells such as stromal cells, and tumor cells [111, 112]. CXCL-8 is a chemoattractant (chemotactic factor) that guides neutrophils to the site of infection, inflammation, and injury [111-113]. During the inflammation, CXCL-8 can cause an additional influx of neutrophils to the infected tissue [67]. CXCR 1 and 2 are G protein-coupled receptors (GPCR) activating intercellular signaling pathways based on binding with CXCL-8 [112]. For instance, the binding of CXCL-8 with its receptor (IL-8RB/CXCR2) can elevate vessel permeability. However, the increased level of CXCL-8 may indicate some diseases like sepsis [111]. Also, CXCL-8 plays a vital role in facilitating the indirect progression of tumorigenesis by changing TME components and directly promoting their survival [112]. However, CXCL-8 on endothelium is secreted first, followed by neutrophil binding and transmigration through MMP during inflammation [53]. Thus, it may demonstrate the difference in CXCL-8 between immune and non-immune cells, which have 72 and 77 amino acids, respectively [111, 112].

1.5.4.2.2 VEGF:

Vascular endothelial growth factor (VEGF) is one of the growth factors used in regenerative medicine, supporting the formation of vascular endothelial cells, which improve the local oxygen supply [114]. In mammals, there are VEGF-A, B, C, and D and placenta growth factor (PlGF), which play an essential role in physiological functions [115]. VEGF engages with two principal receptors, VEGFR1 (Flt-1) binding to ligands such as VEGF-A, B, and PlGF, in addition to VEGFR2 (KDR/Flk-1) binding to VEGF-A, C, D, and E [116]. A recent study showed that VEGFR1 can be expressed on neutrophils in mice and humans and engage with VEGF to activate neutrophils [116,117]. It was noted that mice exposed to high levels of VEGF-A could attract neutrophils, resulting in a 10-fold production of MMP-9 more than ones attracted to the inflammation site [118]. In general, growth factors are used widely in medicine because of their coefficient. However, they can cause serious problems such as tumorigenesis if they are not controlled [114]. Further, recombinant VEGF is sensitive to high levels of pH and temperature, and degradation by enzymes [149]. Due to the unstable protein, costly production, and the fact that the inhibition mechanism of the side effects of VEGF cannot be controlled, there is an alternative strategy to address these challenges [114]. Therefore, peptidomimetic (QK) is produced by fermentation in *E. coli BL21* in large quantities [148]. It is a vigorous alternative to VEGF in addition to that it is shorter and cheaper [114]. *In vitro*-engineered VEGF mimicking peptides (QK) showed the same characteristics as full VEGF, such as stimulating capillary formation. Besides, an *in vivo* study demonstrated that QK is like VEGF in pro-angiogenesis [114, 151]. Moreover, *ClearColi* bacteria could be designed genetically to secrete QK-bearing fusion protein (YCQ), a 15 kDa fusion peptide-protein shortened as a YebF signal peptide-collagen binding domain-QK peptide, stimulated by light. YCQ contains a carrier protein (YebF), collagen-binding domain (CBD, sequence–WREPSFMVLS), a Strep-TagII peptide (WSHPQFEK), and QK (KLTWQELYQLKYKGI) peptide [114]. Furthermore, bacteria, integrated into PluDA hydrogel, can grow and secrete metabolites such as VEGF peptide for at least 7 days, where they are controlled [150].

1.6 Immune system response to tissue biocompatibility:

Investigation of drug candidates *in vitro* is a procedure used only to confirm safety. However, it does not anticipate accurately the *in vivo* toxicity [45]. After biomaterials implanting, the response of immune cells is a critical challenge, facing scientists [35]. Additionally, the engineered bacterial strains can produce therapeutic protein continually or by induction, which may lead to protein overexpression. Therefore, the increased protein level may pose a potential

risk to the surrounding environment if the concentration is not monitored [36]. Engineering microorganisms can be encapsulated in biofilms such as hydrogel [40]. After their investigation *in vitro*, and *in vivo* followed by FDA approval, they can be applied in humans [89]. Therefore, this chapter will discuss biomaterial implantation and foreign body recognition (FBR).

Host defense recognizes enemies and subsequently recruits immune cells to fight, for instance, microorganisms at the site of infection [89]. Further, during human biomaterial implantation, the immune reactions in the body can lead to inflammation with the healing of damaged tissues and impact graft survival [119, 120]. Two stimuli are generated from implantation, recognized as danger and stranger molecules. First, tissue damage leads to cell death or stress, generating damage-associated molecular patterns (DAMPs, danger molecules). Second, host immune cells recognize the presence of graft as ‘non-self’ antigens (stranger molecules), thus increasing immune activation [119]. Furthermore, biomaterials can cause inflammation based on activation of the complement system [121]. The immune system response to implantation is known as foreign body response (FBR). It initiates with the attachment to biomaterials by host blood proteins (albumin, fibrinogen, fibronectin, vitronectin) and the complement family, especially C3a and C5a [122, 123]. These factors opsonize the biomaterial surface, creating surrounding gradients that recruit immune cells. Thus, the response of the host immune system enables tissue regeneration and healing. However, the uncontrolled response may cause biomaterial failure [122]. Protein adsorption and desorption on the implant surface which leads to triggering immune cells is known as the Vroman effect [124]. Therefore, neutrophils and neutrophil-like cells (HL-60) are the first lines of hosts that conflict with organisms from slim molds to mammals [125]. Further, they respond to damaged tissue [123]. The circulating PMNs, particularly neutrophils, can infiltrate the tissues within hours and strive for weeks around biomaterials. Neutrophils play an essential role in preventing foreign materials by three mechanisms including degranulation, phagocytosis, and NETosis. Neutrophils participate in FBR by their excessive recruitment and the release of neutrophil extracellular traps (NETs). Moreover, neutrophils can regulate the neighboring immune responses by producing cytokines and chemokines, including interleukin 8 (IL-8), monocyte chemoattractant protein (MCP)-1, and macrophage inflammatory protein (MIP-1 β) and others like IFN γ and IL-10. Thus, they activate immune cells like monocytes, macrophages, dendritic cells (DCs), and lymphocytes [49, 120, 122, 126]. Neutrophils become more active as a response to rough material where they produce elevated levels of ROS [123].

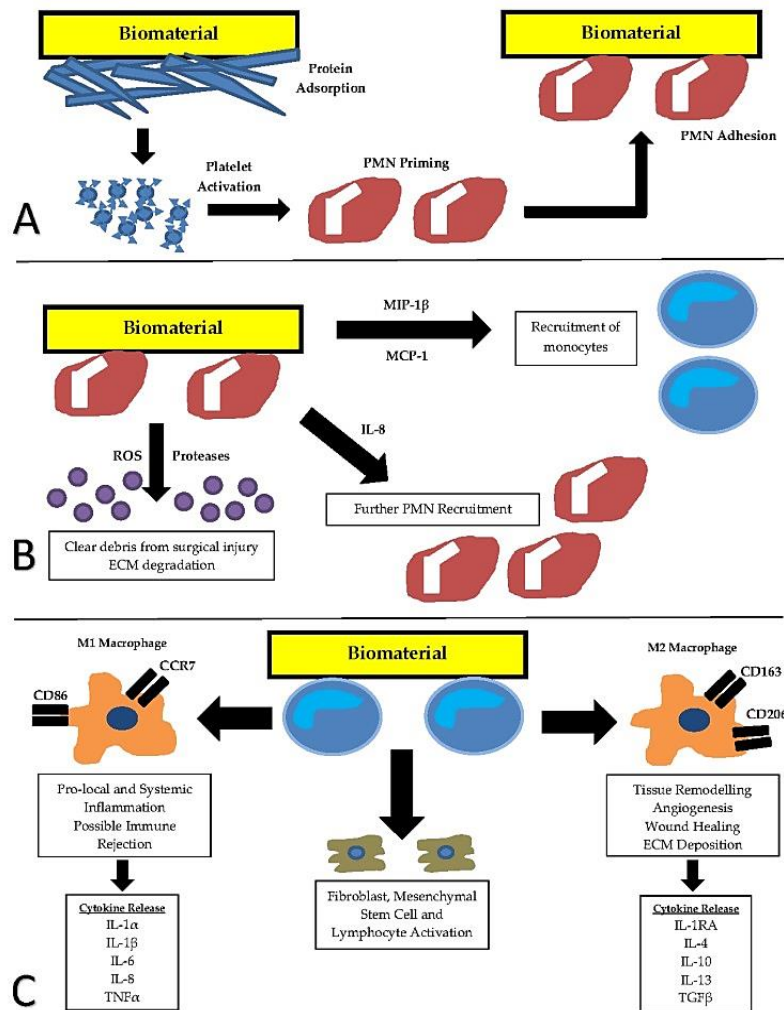


Figure 11I Immunogenic response to implantable biomaterials. **A)** Biomaterial implants lead to protein adsorption triggering an immunogenic response by recruiting neutrophils. **B)** Neutrophil proteins, IL-8, MCP-1, and MIP-1 β , attract more neutrophils and **C)** monocytes which differentiate into Macrophages. Then, they can polarize into M1 and M2. This process proceeds after the complement family protein adsorbs the foreign bodies, which are the potent effector for immune cell recruitment [49].

The presence of PMNs (neutrophil, eosinophil, and basophil) at the site of injury indicates acute inflammation, which takes place within minutes to days. At this stage, neutrophils can activate the host mechanisms and remove surgical injury-derived debris [49]. However, neutrophils can respond to biomaterial implantation by secreting cytokines and enzymes facilitating the recruitment of further neutrophils and other immune cells [234]. Importantly, the recruitment of mononuclear leukocytes (monocytes and macrophages), chronic inflammation markers, transforms acute inflammation into a chronic state. They play an essential role in wound healing by producing proteins for tissue regeneration [49].

At the implantation site, monocytes can differentiate into two activated phenotypes. First, pro-inflammatory macrophages (M1/classical) are stimulated by LPS, IFN- γ , and TNF α . They

function as phagocytic cells aiming at degrading the implant by release of ROS and proteolytic enzymes at an early stage. However, as a response to bigger biomaterials, M1 turns into a mechanism known as frustrated phagocytosis, in which M1 fuses with foreign body giant cells (FBGCs) to elevate the phagocytic capacity. Consequently, the fusion process converts M1 to M2 (alternative) as an anti-inflammatory macrophage stimulated by IL-3 and -4. FBGCs at the interface of tissue materials release elements attracting fibroblasts producing collagen [123]. Then, the continued triggering of innate immune cells resulting in macrophage fusion into FBGCs leads to fibrous capsule formation, a collagenous capsule, isolating implanted biomaterials from tissues via a process known as FBR [49, 123, 126]. The organism's response varies depending on numerous factors, which include material composition, surface, and decomposition mechanism. So, the response from organisms can be local or systemic, including immune cells, foreign body reactions, and potential infection. Implants are, in most cases, well integrated into environmental tissues [120]. However, the level of intensive reactions can determine whether biomaterials are safe or unsafe, meaning biocompatible or incompatible [122, 127]. Therefore, there are common cytokines known to assess the safety of biomaterials. Pro-inflammatory proteins used for rejection are IL-1 α , IL-1 β , IL-6, IL-8, IL-17A, CXCL10, and TNF α and anti-inflammatory cytokines of acceptance are IL-1RA, IL-4, IL-10, IL-13 and TGF β . Further, other factors such as ROS, nitric oxide, and monocyte phagocytosis can be investigated for safety evaluation [49].

1.7 Study objectives:

Neutrophils are critical and effective in microbe sensing and FBR making it imperative to investigate if current LTM concepts based on encapsulated bacteria are capable of activating these immune cells. The aim is to perform the first evaluation of the potential activation of neutrophils, the relevant immune cell population *in vivo*, by LTM. Further, to develop an understanding of how LTMs may activate neutrophils and how they could be improved to stay under the radar of neutrophils.

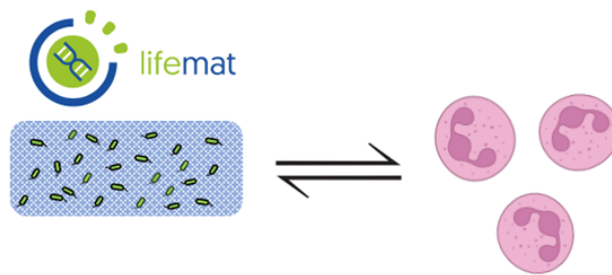


Figure 12| Neutrophil response against LTMs *in vitro*. Engineered therapeutic microorganisms are encapsulated in biomaterials, such as PluDA hydrogel. The pre-clinical stage is performed *in vitro* to investigate neutrophil activation after contact with LTMs or their components.

Briefly, the aims of the project are:

1. Identification of immunogenic response of neutrophils interacting with bacteria directly and indirectly.
2. The risk assessment for LTMs used in LIFEMAT.

To do so, the following questions were targeted for our purpose:

- a) Which LTM components trigger neutrophils?
- b) Which receptors are activated by LTMs/their components?
- c) Which pro-inflammatory proteins are released during activation?
- d) Which encapsulation procedure ensures an acceptable safety profile?
- e) How do LTMs and their components modulate the functional properties of neutrophils?

Therefore, neutrophil responses were investigated and monitored against LTM and their components using state-of-the-art methods.

2 Material and Methods:

2.1 Materials:

2.1.1 Cell lines:

A-431	Human vulvar squamous epithelial carcinoma cell line (HPV negative) (DSMZ, ACC-91, obtained 2018, RRID: CVCL_0037)
Ki-PeCa	Human penile cancer cell line (P2)
Ki-PeCa	Human penile cancer cell line (L2)
HPK1A	HPV16-immortalized human foreskin keratinocyte cell line (Durst et al. ,1987) (HPV-16 transformed, non-malignant)
NFF	Primary human fibroblasts, isolated from foreskin tissue of anonymized. patients (normal foreskin fibroblasts)
U-87	Human glioblastoma cell line
HEK293	Human embryonic kidney cells (<i>in vitro</i> transfected cell)
HL-60	Human leukemia cell line

2.1.2 Basal Media:

Dulbecco's Modified Eagle Medium (DMEM) (High Glucose (4,5 g/L) with L-Glutamine)	PAN Biotech, Aidenbach
Roswell Park Memorial Institute Medium (RPMI-1640) (With L-glutamine and sodium bicarbonate)	PAN Biotech, Aidenbach
DMEM Nutrient Mixture F-12 Ham	PAN Biotech, Aidenbach
Keratinocyte Growth Medium 2	PromoCell, Heidelberg
M9 Minimal Salts, 5x	Sigma-Aldrich, Steinheim

2.1.3 Reagents and Antibiotics for cell culture

Penicillin/Streptomycin (10000 U/ml, 10 mg/ml)	Sigma-Aldrich, Steinheim
Sodium Pyruvate (100 mM), sterile filtered	Sigma-Aldrich, Steinheim

Fetal Calf Serum (FCS), (inactivated for 30 min at 56 °C)	Gibco™, Karlsruhe
Dulbecco's Phosphate Buffered Saline (DPBS)	PAN Biotech, Aidenbach
Dimethyl sulfoxide (DMSO)	Sigma-Aldrich, Steinheim
TrypLE™ Express	Gibco™, Karlsruhe
Cholera Toxin (0,01 mg/ml)	Sigma-Aldrich, Steinheim
Hydrocortison (0,4 mg/ml)	Lonza, Basel, Schweiz
Epidermal Growth Factor (0, 1 mg/ml)	Invitrogen, Karlsruhe
Keramix (5 mg/ml)	Sigma-Aldrich, Steinheim
Kyratinocyte supplementMix	Promocell c-39016
CaCl ₂ solution	Promocell c-34005
Pancoll human, density: 1,077 g/ml	PAN-Biotech™, Aidenbach
MEM Non-essential amino acids solution (NEAA)	Thermo Fisher, USA
Rogosa and Sharpe (MRS) agar	Merk KGaA; Darmstadt
Erythromycin	

2.1.4 Complete Media:

-RPMI 1640 (R10⁺⁺) Medium

500 ml RPMI 1640: plus

10% FCS

1% Penicillin/Streptomycin

1 mM Sodium pyruvate

-Keratinocyte Growth Medium 2 (PeCa medium)

500 ml Keratinocyte Growth Medium 2: plus

12,3 ml supplement mix

60 µl CaCl₂ solution

1% Penicillin/Streptomycin

Mix complete Keratinocyte Growth Medium 2 and complete RPMI 1640 medium (1:1)

-DMEM (D10⁺⁺) Medium

500 mL DMEM High Glucose with L-Glutamine: plus

10% FBS

1% Penicillin/Streptomycin

1 mM Sodium pyruvate

-DMEM & DMEM/Nutrient Mixture F-12 Ham (FAD-) Medium

500 ml mixture 1:1 medium plus

1% Penicillin/Streptomycin

10% Fetal Calf Serum (FCS)

55 µl Cholera Toxin (0,01 mg/ml)

550 µl Hydrocortisone (0,4 mg/ml)

550 µl Epidermal Growth Factor (0,1 mg/ml)

2,2 ml Keramix (5 mg/ml)

-Storage Medium (eukaryotic cells)

Dimethyl sulfoxide (DMSO)	100 µl
---------------------------	--------

FCS	900 µl
-----	--------

2.1.5 Bacterial Media:

-M9 Minimal Salts (*E. / ClearColi*) Medium

1x M9 Minimal Salts	1 L
---------------------	-----

20% glucose	20 ml
-------------	-------

1M magnesium sulphate	2 ml
-----------------------	------

0.2% MEM amino acids (50x) solution	2 ml
-------------------------------------	------

-Rogosa and Sharpe (MRS) Medium

MRS agar	52.2 g
dH ₂ O	1 L
Autoclaved 15 min for 121 °C, PH: 5.7 to 5.9	
10 µg/ml Erythromycin	5 µl/5 ml (1/1000)

-Storage Medium (prokaryotic cells)

Dimethyl sulfoxide (DMSO)	200 µl
Bacterial culture medium	800 µl

2.1.6 Bacteria and biomaterials provided by INM, Saar. University

E. coli BL21 and Engineered *E. coli* (LPS free-*ClearColi*)

Lactobacillus plantarum candidates include: mCherry, I6P7, KFC18, NGF, and Nnuclase.

Pluronic Hydrogels

2.1.7 Reagents and Chemicals:

Name	Source
Acetic acid (100%)	AnalaR NORMAPUR®
Albumin Fraction V (pH 7.0)	AppliChem
Ampuwa® Spüllösung 1000 ml Plastipur	Frisenius Kabi AG
Aqua	Braun
β-mercaptoethanol	Merck
Bromphenol blue	Sigma-Aldrich
BSA, 5 mg, 20 mg/ml (bovine serum albumin)	Thermo Scientific
Dimethyl sulfoxide (DMSO)	Sigma-Aldrich
Eosin G, Certistain®	Merck
Ethanol > 99% (C ₂ H ₅ OH)	Thermo Fisher
Ficolite-H, sterile filtered density 1.0770 g/ml+ 0.001	Linaris Manfred Decker
Glycerol	Serva
Hematoxylin	Vector Laboratories
Hydrogen peroxide (H ₂ O ₂)	Merck
Methanol (CH ₃ OH)	Thermo Fisher

Non-fat milk powder	Heirler Cenovis GmbH
Octoxinol 9 Triton®X-100	AppliChem
PCR grade H ₂ O	Ampuwa
Polybren Hexadimethrinebromide	Sigma 9268-10 g
Potassium chloride (KCl)	Grüssing GmbH
Potassium dihydrogen Phosphate (KH ₂ PO ₄)	Merck
Sodium azide (NaN ₃)	VWR
Sodium chloride (NaCl)	VWR
Sodium dihydrogen phosphate (NaH ₂ PO ₄)	J.T. Baker Chemicals B.V
Sulfuric acid (2 N)	Merck
Tetramethylbenzidine (TMB)	Sigma-Aldrich
Tetramethylethyldiamine (TEMED)	AppliChem, Darmstadt
Tris-EDTA buffer pH 8.0	Sigma-Aldrich
Tris-hydroxymethyl-aminomethane (Tris)	Roth
Trisodium citrate dihydrate	Roth
Trizma base	Sigma-Aldrich
Triton-X	Sigma-Aldrich
Trypan blue	Sigma-Aldrich
Tween®20 pure	Serva
WesternBrightTMECL sensitive HRP substrate	Biozym
WesternBright	asvansta
Sirius HRP substrate Xylene (C ₈ H ₁₀)	Otto Fischar GmbH & Co. KG
SimplyBlue™ SafeStain	Thermo Fisher Scientific, USA
Nucleotides	Peqlab VWR (Darmstadt)

2.1.8 Methodological Reagents/ Kits:

-DNA extraction

QIAamp® DNA Mini Kit

QIAGEN GmbH, Hilden

-ELISA

ELISA MAX Deluxe Set-Human IL-8

Biolegend Cat#431504

ELISA MAX Deluxe Set-Human VEGF

Biolegend Cat#446504

-E-Gel

E-Gel 0.8-2% with SYBR Safe™	Thermo Fisher Scientific
Loading Buffer	Thermo Fisher Scientific
E-Gel™ 1 Kb Plus DNA-Leiter	Thermo Fisher Scientific

-Immunohistochemistry

2.5% Normal Horse serum blocking solution	Vector Laboratories, Burlingame, USA
Monoclonal Mouse Anti-Human CD15	ak agilent/Dako M3631
ImmPRESS™ HRP Anti-Mouse IgG (Peroxidase)	Vector Laboratories,
Polymer Detection Kit	Burlingame, USA
Impact DAB Peroxidase (HRP) Substrate	Vector Laboratories, Burlingame, USA
VectaMount™ Permanent Mounting Medium	Vector Laboratories, Burlingame, USA
Hematoxylin Gill's Formula	Vector Laboratories, Burlingame, USA
Färbekästen mit Falzdeckel	VWR, Darmstadt
SuperFrost®PlusObjektträger	R.Langenbrinck GmbH

-Zymogram

Novex™ 10% Zymogram Plus (Gelatin) Gel	Thermo Fisher Scientific
Zymogram Developing Buffer	Thermo Fisher Scientific
Zymogram Renaturing Buffer	Thermo Fisher Scientific

2.1.9 Buffers and Solutions:

10x buffer (Mycoplasma Test):

Tris HCl pH 8.88	37.5 ml
(NH ₄) ₂ SO ₄	1.32 g
MgCl ₂	0.203 g
Tween 20	0.5 ml

Buffer was sterile filtrated after mixing and stored at -20 °C.

dNTP mix:

Nucleotides (10 µM)	10 µl
---------------------	-------

dH ₂ O	60 µl
-------------------	-------

10x Tris-buffered saline (10x TBS):

Tris	24.2 g
------	--------

NaCl	80 g
------	------

dH ₂ O	ad 1 L
-------------------	--------

pH	7.6
----	-----

1x TBS:

10x TBS	100 ml
---------	--------

dH ₂ O	900 ml
-------------------	--------

TBS-T:

10x TBS	100 ml
---------	--------

Tween20	1 ml (0.1%)
---------	-------------

dH ₂ O	ad 1 L
-------------------	--------

10x Phosphate buffered saline (10x PBS):

NaCl	80 g
------	------

KCL	2 g
-----	-----

Na ₂ HPO ₄	2 g
----------------------------------	-----

dH ₂ O	ad. 1 L
-------------------	---------

1x PBS:

10x PBS	100 µl
---------	--------

dH ₂ O	ad 1 L
-------------------	--------

Buffer was adjusted to pH: 7.2 and sterile filtered.

TE buffer (pH 9.0):

10 mM Tris

1 mM EDTA ($\text{C}_{10}\text{H}_{14}\text{N}_2\text{O}_8\text{Na}_2 \cdot 2 \text{H}_2\text{O}$)

5x Laemmli buffer:

Tris (1M, pH 6.8)	1650 μl
-------------------	--------------------

SDS (10%)	3438 μl
-----------	--------------------

Glycerol	2500 μl
----------	--------------------

Bromphenol blue	0.62 mg
-----------------	---------

dH ₂ O	10 ml
-------------------	-------

20% glucose:

Glucose monohydrate	110 g
---------------------	-------

dH ₂ O	500 ml
-------------------	--------

The solution was sterile filtrated.

1M magnesium sulfate:

MgSO ₄ -7H ₂ O	24.65 g
--------------------------------------	---------

dH ₂ O	87 ml
-------------------	-------

The solution was sterile filtrated.

Trypan blue solution (0.25%):

Trypan blue	0.25 g
-------------	--------

1x PBS	100 ml
--------	--------

The solution was sterile filtrated after mixing.

2.1.10 Software:

Name	Source/ Company
Azure Imaging Systems 1.5.0.0518	Azure biosystems
Bio-Plex Manager	Bio-Rad, California, USA
CellDrop (Trypan Blue) 1.6.7.482	DeNovix, Wilmington USA
Diva Software	BD Biosciences, Heidelberg
GraphPad Prism 8.0	Software, San Diego, USA
ImageJ 1.52e	software, Maryland, USA
Leica V3	Leica Microsystems, Wetzlar
LightCycler® 480 II Software 1.5	Roche, Mannheim
Microsoft Office 2016	Microsoft, Redmond, USA
NewCast V7.2	Visiopharm
QuantityOne Software	BioRad, München
Universal ProbeLibrary Assay Design	Roche, Mannheim
Workout 2.5 Software	Dazdaq, Brighton, GB
XCELLigence Software	ACEA Bioscience, San Diego, USA
Calculatorsoup.com	Online

2.1.11 Laboratory Equipment/Systems:

Name	Source/ Company
Trans-well with 0.4 µm pore size (3401)	RENNER GmbH
6 Well Cell Culture Plate	Greiner bio-one GmbH
12 Well Cell Culture Plate	Greiner bio-one GmbH
24 Well Cell Culture Plate	Greiner bio-one GmbH
96-well cell culture microplate, µclear®	Greiner bio-one GmbH
96-well cell culture microplate, U-bottom	Greiner bio-one GmbH
96-well cell culture microplate, V-bottom	Greiner bio-one GmbH
96-well cell culture microplate, K, C-bottom	Sarstedt AG & Co. KG
Azure Q500	Azure Biosystems
Bio-Plex® 200 System	Bio-Rad
CellCamper Mini-12	neoLab Cat# 2-3702
Cell counting chamber DHC-N01	iNCYTO
Cell Culture Dishes CELLSTAR® 60 x 15 mm	Greiner bio-one GmbH

Cell scraper 25 cm	Sarstedt AG & Co. KG
Cell Drop BF	DeNovix
Corning Costar Stripette serological pipettes	Merck
Coverslips 24 x 60 mm	R. Langenbrinck GmbH
Dry Block Heater	Thermo Fisher
E-Gel™ Power Snap Electrophoresis Device	Thermo Fisher Scientific Cat#G8100
FACS tube 5 ml, 75 x 12 mm	Sarstedt AG & Co. KG
Hood MaxiSafe 2020	Thermo Scientific
Incubator Heracell 240i	Heraeus
PowerEase™ Touch 120 W Power Supply	ThermoFischer™
Leica DMI 6000 B	Leica Microsystems
Leica DMi1 inverted microscope	Leica Microsystems
Magnetic mixer	IKA® -Werke GmbH & Co. KG
Megafuge 1.0R	Hereaus,
Megafuge 16R	Thermo Scientific™
Microcentrifuge 1-15PK	Heraeus™
Microcentrifuge Pico 17	Sigma Laborzentrifugen GmbH
MicroWell™ 96-well-plates, Nunc-Immuno™	Thermo Scientific™
Mikrotome RM2235	Heraeus™
Mini-blot-Module	ThermoFischer™
Mini Gel Tank	Thermo Scientific Cat#A25977
Multi-channel pipette (50 µl-200 µl)	Thermo Fisher
Nunc MaxiSorp™, U bottom	ThermoFischer Cat#44-2404-21
Olympus BX51	Olympus
OneTouch Tips One Touch™ (10/1000 µl)	Brand
pH-meter	INTEGRA Biosciences GmbH
Pipettes	Gilson, Middleton
Poly-Prep® Chromatography Columns	BioRad Cat#731-1550
PTC-200 Thermal Cycler	MJ Research
PVDF membrane Amersham™ Hybond™	GE Healthcare Life Sciences
P0.45 PVDF 0.45 µm, 300 mm x 4 m	Peqlab VWR
Safeguard filter tips 1-200 µl	Denver Instruments
Scales SI-2002	B. Braun
Scalpel (Surgical disposable scalpel)	Sarstedt AG & Co. KG

Serological pipettes	GFL
Shaker	Sarstedt AG & Co. KG
S-Monovette® 10 mL 9NC	BANDELIN GmbH & Co. KG
Sonifier Sonorex Super RK103H	R. Langenbrinck GmbH,
TC Flask T75, Stand. Vent. Cap (75 cm ²)	Techno Plastic Products TPP®
Tissue culture flask 150 (150 cm ²)	Sarstedt AG & Co. KG
Tubes (50/25/2/1.5 ml)	PerkinElmer
Victor™ X4 Multilabel Plate Reader	neoLab® Migge GmbH
VIVASPIN6 50,000 MWCO PES (sartorius)	SigmaAldrich REF#VS0631
Vortex Mixer	GE Healthcare Life Sciences
xCELLigence plates E-plates 16	Agilent
xCELLigence RTCA, SP system, Model W 380	Agilen

2.2 Methods:

2.2.1 Cell culture:

2.2.1.1 Eukaryotic cells:

All cell lines were cultured under the same conditions, including incubation of the cells at 37 °C with 5% CO₂ and 80% humidity. After reaching about 80% confluence, the medium was removed and the cells, in the culture flask, were washed twice with 10 ml of 1x PBS. To detach cells, TrypLE™ Express (Trypsin) solution was added and incubated for 3 to 5 min at previous conditions. Then cells were neutralized with growth medium to stop Trypsin enzyme activity and then cell suspension was centrifuged at 1500 rpm for 5 min. After discarding the cell supernatant, the cell pellet was re-suspended in an adequate amount of culture medium and counted using trypan blue solution with a Neubauer chamber. To subculture the cells, an appropriate volume of the cell suspension was taken, depending on the flask size, and mixed with an adequate volume of the growth medium. Finally, they were incubated at the incubator. Cells were monthly tested negatively for mycoplasma during usage and before freezing.

2.2.1.1.1 Storage and thawing of eukaryotic cells:

Cells with a concentration of 1×10^6 were resuspended in a mixture of DMSO-FCS 1:10, respectively. Then, they were stored in cryovials, firstly at -08 °C for 24 h and later at -150 °C for long-term storage or in a liquid nitrogen tank. To thaw the cells, the cryovial was transferred to a water bath adjusted to 37 °C with handy rotating until it dissolved. Then de-frozen cells were resuspended in a growth medium and centrifuged at 1500 rpm for 5 min. After discarding the cell supernatant, the cell pellet was resuspended in an appropriate volume of culture medium and incubated at the indicated conditions. The growth medium was changed every two days.

2.2.1.1.2 Test of mycoplasma existence:

Mycoplasma is a prokaryotic cell that can cause cell contamination [128]. It can be found in other cell lines and cross between cells as well as in products of animal-derived media and individuals working in the laboratory [129]. Mycoplasma has an impact on cell physiology and thus experimental results. Therefore, thawing new cells or before cell storage, mycoplasma should be tested [128]. 1 ml supernatant of cells cultured for 24 h was taken and centrifuged for 5 min at 1500 rpm to remove dead cells. DNA was isolated according to the QIAamp® DNA Mini Kit protocol. The Master-Mix was prepared as described in Table (1) and mixed with 2 µl of isolated DNA for the PCR process. Two controls were used in that test, a positive one

containing mycoplasma DNA isolated from contaminated cells as well as negative control containing dH₂O instead of DNA. Samples were then incubated in a Thermo-cycler adjusted to the conditions indicated in table (2). After getting samples from PCR, they were loaded in E-Gel 0.8-2% with SYBR Safe™ and mixed with 1:1 with the loading buffer. Running was performed for 12 min and then visualized by UV light.

Table 3| MasterMix preparation:

Materials	Quantity (μl)
10x buffer	2.5
dNTP mix	2
Primer mix (100 μl of each primer)	10
Taq polymerase	1
dH ₂ O	9.3
DNA template	2

Table 4| PCR process by PTC-200 Thermal Cycler:

Condition	Temperature (°C)	Time	Cycles
Denaturation	94	1 min	1
Denaturation	94	30 s	35
Annealing	62	30 s	
Amplification	72	30 s	
Elongation	72	3 min	1
Cooling	4	∞	-

2.2.1.2 Prokaryotic cells (bacteria):

2.2.1.2.1 Culture of *E. coli* and *ClearColi*:

Three independent colonies, *E. coli* or *ClearColi*, were inoculated into a flask containing 10 ml medium. After incubation at 37 °C in a rotary incubator at 150 rpm for 24 h, the OD_{600 nm} value of a 1:10 dilution was determined spectrophotometrically. For larger volumes, bacteria were taken from preculture, prepared in the appropriate volume (50-100 ml) to an OD_{600 nm} = 0.1, and incubated overnight at 37 °C in a rotary incubator at 150 rpm. Eventually, bacterial suspension was adjusted to an OD_{600 nm} = 1 for normalization purposes.

2.2.1.2.2 *Lactobacillus plantarum* (5 candidates):

One to three colonies of each candidate were added to 5 ml MRS + Erythromycin (stored at 4 °C) in 50 ml falcon. Then they were incubated at 37 °C while shaking at 100-300 rpm. Measurement of OD_{600 nm} and sub-culturing were done in an equivalent way to the earlier section.

2.2.2.2.1 Killing the bacterial candidates by heat:

This section was adjusted using the publication of Junhua Jin [130]. *L. plantarum* (5 candidates) were adjusted to OD₆₀₀ = 1, CFU = 6 x 10⁸/ml measured by INM. Bacterial suspensions were centrifuged at 6000 rpm for 10 min at 4 °C. The supernatants were then filtered by a 0.22 µm pore-size sterile filter and stored at -20 °C for further experiments. After washing three times with 1x PBS, bacterial pellets were resuspended in 1 ml of 1x PBS and incubated at 121 °C for 15 min.

2.2.2 Storage of bacteria:

DMSO was mixed with bacterial culture medium in a concentration of 20%, and 80%, respectively (200 µl: 800 µl). The cryovial containing the bacteria was frozen directly at -80 °C for a day and then transferred to -150 °C.

2.2.3 Growth test of inactivated (heat-killed) bacteria:

10 µl of heat-killed bacteria was added to the culture medium, such as *L. plantarum* with the MRS medium. The optical density of bacteria was measured at OD₆₀₀ before and after incubation for at least three days. Observation of any bacterial growth indicates incomplete killing by heating. However, no bacterial change was recorded.

2.2.2 Cell Transient and Transfections:

(Performed by AG Bernd Bufe, Kaiserslautern University of Applied Sciences, Zweibrücken). HEK293T cells (ATCC) were cultured in Dulbecco's Modified Eagle Medium (DMEM, Biowest) supplemented with 10% (v/v) heat-inactivated fetal calf serum (FCS, Pan Biotech), 1 unit/ml penicillin-streptomycin (Biowest) and 2 mM L-glutamine (Biowest) to 80% confluence. For transfection, approximately 2×10^3 cells were seeded in each well of poly-D-lysine-coated (PDL) (10 µg/ml in PBS, Sigma) black optical 96-well µCLEAR-plates (Greiner Bio-One). Cells were transfected after 24 h using jetPEI (Polyplus-transfection SA) with 0.125 µg of DNA plasmids encoding the respective receptors and equal amounts of a plasmid encoding the G protein subunit Gα1670. The medium of transfected cells was changed 24 h after transfection.

2.2.3 Granulocytes (neutrophils) isolation:

Although neutrophils have a central role in many diseases, including inflammation, immunologists encounter a challenge during neutrophil research due to their short life span. Furthermore, neutrophils cannot be either multiplied in *ex vivo* or cryopreserved. Therefore, scientists use either freshly isolated neutrophils from human peripheral blood or proper neutrophil-like cell models such as HL-60 [131]. Different procedures are employed to isolate neutrophils, such as density-gradient, fluorescence-activated cell sorting (FACS), and immunomagnetic beads, which differentiate between time-consuming and costly. Also, they may influence the quantity and the quality of neutrophil purification, leading to various artificial stimulation between methods [132]. Neutrophil purification performed by the density-gradient method is old and traditional. Human blood is set on the Pancoll/Ficoll (separating solution). After centrifugation, the Pancoll solution leads to the sedimentation of PMNs and red blood cells/ erythrocytes (RBCs) layer [132]. Pancoll (1.077 g/ml) contains polysaccharide (MW= 4×10^5 Da), a hydrophilic polymer, inducing the production of aqua solution separating cells with a density of up to 1.2 g/ml (PAN-Biotech). During PMN isolation, anticoagulants, including Citrate, EDTA, and Heparin, can be used. Citrate and EDTA anticoagulants chelate the calcium ions in a similar mechanism, and the difference between them is less compared to Heparin, which interferes with apoptosis. EDTA solution can stimulate PMN clotting, leading to pseudo-neutropenia samples. Further, Citrate was noted to prevent the activity of formyl-methionyl-leucyl-phenylalanine (FMLP) and ROS of PMNs. Therefore, these anticoagulants have a potential effect on PMNs [133]. Thus, neutrophils were rested in RPMI medium for 1 to 2 h to reach the quiescence state after purification.

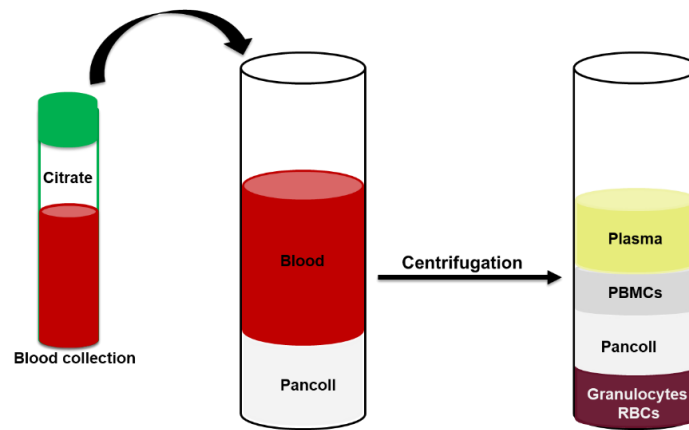


Figure 13| Isolation of neutrophils (granulocytes) from human peripheral blood. Blood is layered on the Pancoll solution and centrifuged. Blood solution is separated into four layers: plasma, peripheral blood mononuclear cells (PBMCs = lymphocytes, monocytes, natural killer cells, dendritic cells), pancoll, and granulocytes with red blood cells (RBCs). After aspiration of the first three layers, RBCs were lysed, using cold water to get granulocytes (neutrophils represent 50-70%). Then neutrophils were resuspended in complete RPMI and rested for 1-2 h at 37 °C.

Shortly, granulocytes were obtained from the peripheral blood of healthy adult volunteers and collected into 10 ml citrate tubes (Sarstedt-Monovette®10ml 9NC). Then, 20 ml of blood was diluted and mixed with 10 ml Dulbecco's PBS (1:1) and carefully layered, without mixing, on 12.5 ml human Pancoll solution (1.077 g/ml), which allowed sedimentation of all cells with higher density (PMNs, RBCs). The gradient was centrifuged at 800x g for 30 min at room temperature (RT). Afterwards, plasma, peripheral blood mononuclear cells (PBMCs)/ (PMNC), and pancoll layers were aspirated carefully and serially. The layer of granulocytes-erythrocytes (5 ml) was transferred to a 50 ml tube, and followed by adding 40 ml cold hypotonic dH₂O to induce lysis of erythrocytes for 30 s. To block the lysis of erythrocytes, 10x PBS (5 ml) was added and mixed. The tube was then centrifuged for 5 min at 1600 rpm and by repeating the lysis step for more one or two times. The pellet of PMNs was resuspended in complete RPMI-1640 medium and deactivated by incubation at 37 °C with 80% humidity and 5% CO₂. PMNs were centrifuged and washed at least 2x in RPMI medium, then counted in a 1:10 dilution with 0.25% trypan blue before subjecting them to assays.

2.2.4 Transwell-Control Experiment:

Neutrophils were stimulated with live bacteria by either direct (physically) contact or indirect (separated by transwell) contact. A 12-transwell plate with a pore size of 0.4-μm was utilized for this experiment. After neutrophil isolation and resting for 60 to 120 min, cells were washed at least 2x with a complete RPMI medium. Then, cells were mixed in 800 μl of RPMI medium and added to 12 well plates as well as 12 transwell plates in a final concentration of 4×10^6

cells/well. The plates were incubated for 15 min at RT to let the cells settle down. *E. coli* and *ClearColi* strains were measured and adjusted at $OD_{600} = 1$. Afterward, they were centrifuged at 4000 rcf (rpm), washed 2 times, and resuspended, in the end, in a complete RPMI medium. 10 μ l of bacterial suspension was mixed with 190 μ l RPMI medium and transferred to the well plate (Fig. 16B) and the insert of the transwell plate to separate bacterial contact physically (Fig. 16C). The plate was incubated at 37 °C with CO₂ for 60 min. The supernatants were collected, centrifuged, and stored at -20 °C.

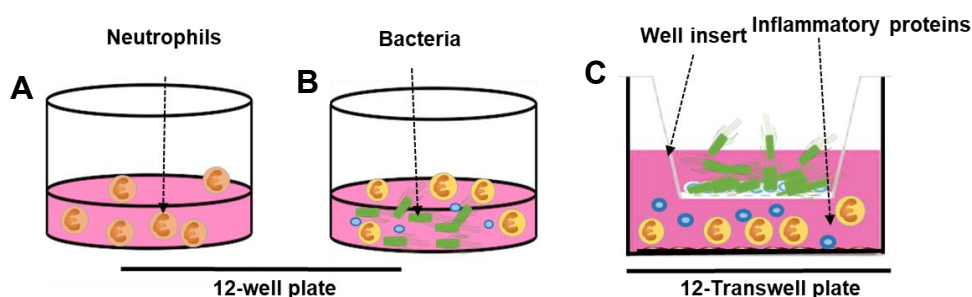


Figure 14 Monitor of neutrophils and bacteria interactions. (A) Neutrophils without bacteria. (B) Direct contact of bacteria and neutrophils. (C) Indirect contact of bacteria and neutrophils using Trans-well with 0.4- μ m pore size. Neutrophils were cocultured with/without physical separation with bacteria for specific time points in dilution factor 1/100 of $OD_{600} = 1$. After incubation for 60 min, the supernatants were collected to investigate MMP release and cytokine secretion.

2.2.5 Construction of PluDA Hydrogel:

The constructs, described in this protocol, were made in INM, Saarland University, Campus D2.2, Saarbrücken by groups of Dr. Sankaran (Bioprogrammable materials) and Dr. Trujillo Muñoz (Materials -host interactions).

2.2.5.1 Coating of coverslips:

Coverslips, 16 x 13 mm, were arranged in Teflon and immersed in the following steps: 99% ethanol, milli Q water (MQ H₂O), and again in 99 % ethanol. Mold with intact coverslips (was suspended in a beaker with 99% ethanol, sonicated for 10 min, and washed in water and 99% ethanol. That structure was immersed in 20 ml solution (95% ethanol, 4% MQ H₂O, and 1% of 3- (trimethoxy silyl) propyl acrylate) and kept on a shaker at 50 rpm overnight. Coverslips were transferred into MQ H₂O and stored for further use to prevent the oxidation of silyl groups presenting on the coverslip.

2.2.5.2 Preparation of Pluronic Diacrylate (PluDA):

Pluronic diacrylate (PluDA, 30%) with IRGACURE solution (0.02%) was prepared for the constructs. For preparation of PluDA solution (30%), 3 grams of PluDA and 20 mg of IRGACURE 2959 (2-Hydroxy-4'-(2-hydroxyethyl)-2-methylpropiophenone) photo-initiator were added and mixed in an amber glass bottle to which 10 ml of MQ H₂O was added. The contents were kept on a rotary shaker at 4 °C overnight and stopped only after ensuring the completion of dissolution.

2.2.5.3 Structure of Hydrogel:

Bacterial culture (1 to 5 ml), incubated overnight in LB-NaCl medium, was centrifuged at 3×10^3 rpm for 6 min at room temperature (RT). After measurement by the Nanodrop-One device, the cell pellet was resuspended in m199 culture medium and adjusted to an OD₆₀₀ = 1. Pluronic diacrylate–bacterial suspension was prepared by mixing 90% volume of PluDA/gel and 10% volume of bacterial culture (OD₆₀₀ = 1), such that the final OD of bacteria in the Pluronic mixture was 0.1. The solutions of PluDA were always on ice during their use. 3-APS-coated coverslips were arranged on a petri dish covered with paraffin paper. PDMS mold, selected 6 mm in the following experiments, was placed on a coverslip such that the surfaces were bound/attached firmly. 22 ul of PluDA–bacterial mixture was pipetted onto the coverslip surface, presenting in the PDMS cavity to make a thin core section of radius 3 mm and a height of 0.7 mm.

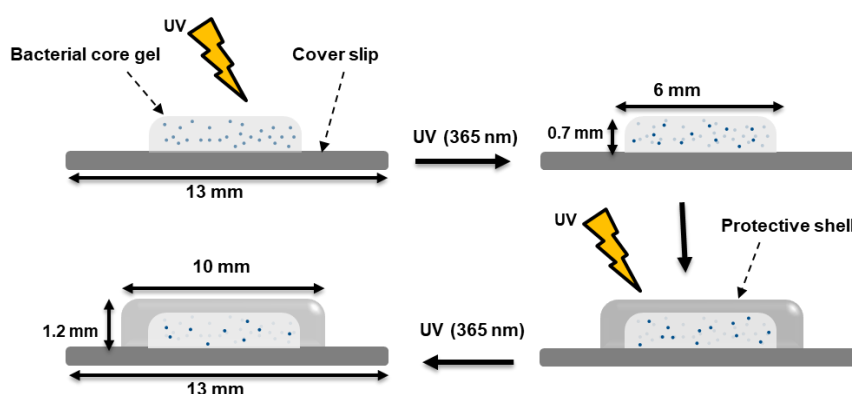


Figure 15I Stages of bacterial incorporation in PluDA hydrogel fabrication. After producing PluDA hydrogel and loading the target bacteria on the core gel, the construct was placed and firmly fixed on a coverslip and exposed to UV for some seconds. For protection, the protective shell was placed and again exposed to UV [Schema was designed by INM, Saar. Uni. with some modifications].

It was incubated undisturbedly for 2 min at RT. PDMS-coverslip setup was transferred to Gel-Doc, and the PluDA-bacterial mixture was cross-linked by irradiating it with low UV transillumination for 60 s. The whole setup was transferred back to the sterile hood, and then the PDMS mold was removed from the coverslip after confirming the solidification of the Pluronic mixture. The bigger PDMS mold, in diameter, was placed on the same coverslip to produce a protective PluDA cap, preventing bacterial leakage into the external environment. 55 μ l of PluDA was pipetted onto the PluDA-Bacterial core, forming a layer on the entire surface of the core ranging from a diameter of 10 mm and height of 1 mm for the complete construct. The setup of PDMS with coverslip was transferred to Gel-Doc, and the construct was cross-linked by UV transillumination for 90 s. The whole setup was transferred back to the sterile hood, and the PDMS mold was removed from the coverslip after ensuring the solidification of the PluDA cover. The hydrogel (gel) construct was transferred into a 24-well plate containing 300 μ l of m199 cell culture media and 21 μ l of 15% Glycine. The 24-well plate was incubated under the light source in the incubator. After 5 h, the light source was switched to irradiated blue light at 1 pulse/min frequency. The media were pipetted out at regular intervals (3rd day, 5th day, 7th day...) and added the same volume of new media. Quantitative ELISA was performed with the medium pipetted from the constructs on the same day.

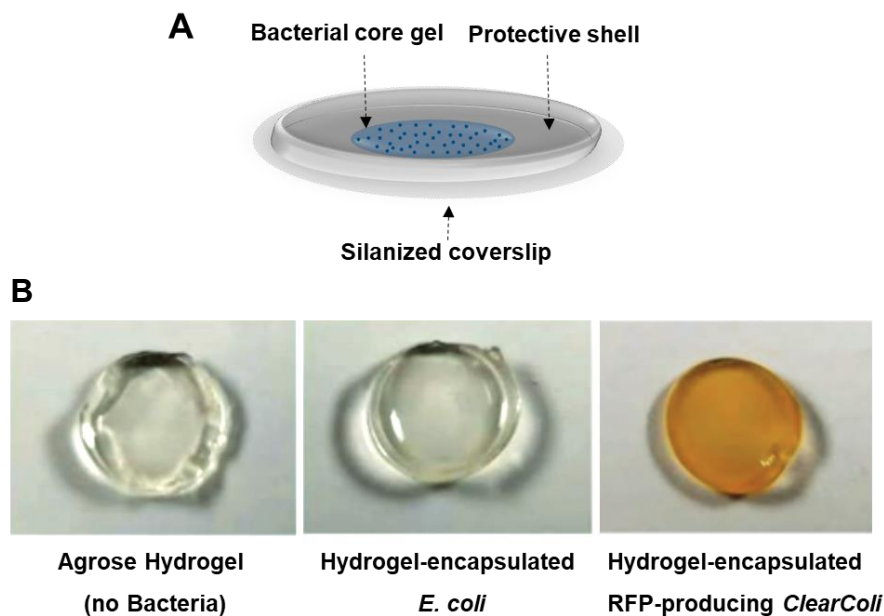


Figure 16| Main details of PluDA constructions and their final morphology. (A) Schema of bacteria-contained hydrogel has three main parts: core gel for loading bacteria, protective shell to prevent bacterial leakage, and coverslip to have a stable base. (B) The hydrogel shapes, *in vitro*, are, from left to right, no bacteria, *E. coli*, and red fluorescent protein (RFP)-producing-*ClearColi* [Shrikrishnan Sankaran *et al.* 2019, 134].

2.2.6 Direct stimulation assay (DSA):

The experiment name comes from the direct reaction between neutrophils and components, such as bacterial supernatant, without further steps or overlapping other conditions. This technique can provide us with natural and obvious results after evaluating the activation level. Also, it is characterized by simplicity by allowing variable time points and conditions. Neutrophils (4×10^6 cells/ml) were cultured with gel (PluDA hydrogel) with/without (w/o) bacteria or different concentrations of bacterial supernatants in a 24-well plate. Then, they were incubated for specific time points at 37 °C in an incubator with 80% humidity and 5% CO₂. After supernatant centrifugation, neutrophils were collected for further experiments. Then supernatants were stored at -20 °C or directly used to check protein secretion by ELISA or Zymography.

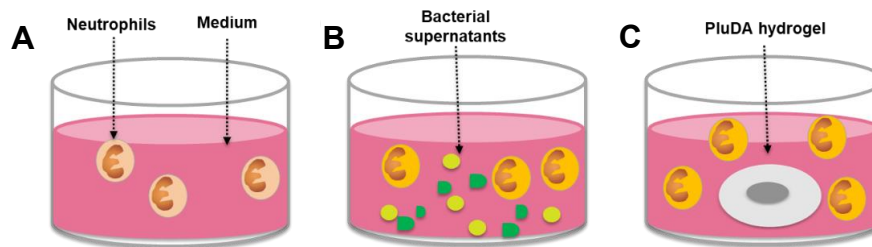


Figure 17I Stimulation of neutrophils with LTM components. Neutrophils were maintained in physical contact with the targets. (A) medium as control, (B) bacterial supernatants, *E. coli* or *ClearColi*, (C) PluDA hydrogel (gel) w/out bacteria, all were incubated with neutrophils at 37 °C for proper time points. Supernatants or neutrophils were collected and used in various experiments.

2.2.7 Enzyme-linked immunosorbent assay (ELISA):

ELISA is a traditional method used in immunology, based on the interaction of antigen with antibody, in which the binding of the target antigen is confirmed by an enzyme-linked (conjugated) antibody that catalyzes the substrate like avidin-HRP. Then, the antigen is detected either qualitatively by visual investigation or quantitatively by readouts from a luminometer or a spectrophotometer [135]. ELISA immunoassay involves four basic steps. a) coating by antigen or antibody, b) blocking by BSA, c) detection, and d) final read. ELISA is divided into four types: direct, indirect, sandwich, and competitive [135, 136]. Direct ELISA is an antigen-coated plate, detected directly by a primary antibody (enzyme-linked). Indirect ELISA can detect primary antibodies (binding directly to antigen) by secondary antibodies (enzyme-linked) [135]. Further, competitive ELISA is a test for antibody presence, being specific for the serum antigen. It utilizes two antibodies specific for serum antigen detection, where both

compete to bind it [136]. Also, the competition can be between antigen coated-plate and sample antigen to bind the primary antibody, which binds to the secondary antibody (enzyme-linked) [135].

The sandwich ELISA is the fourth type performed in this project (Fig. 20). This type includes a sample antigen introduced to the capture antibody-precoated plate. Then, the antigen can be caught by secondary antibodies (enzyme-linked) to the recognition sites [135]. This technique has disadvantages, such as time consumption and expense because of using two antibodies [136]. However, using pair antibodies to recognize the antigen makes the method more specific [Cell signaling technology]. The ELISA Kit includes materials, such as wash buffer, stop solution, TMB substrate, standard diluent, and detection antibodies. The kit materials were combined, and the experiment was achieved according to the manufacturer's protocol of Biolegend.

Briefly, 100 μ l of diluted Capture Antibody in 1x Coating Buffer A was added to a 96-well plate and incubated overnight between 2 and 8 °C. After washing 4x with wash buffer (300 μ l/well), 200 μ l 1x Assay Diluent was added for blocking non-specific binding and incubated at RT for 1 h with shaking at 500 rpm. After washing, 50 μ l of 1x Assay Diluent A was transferred to the plate, followed by adding 100 μ l/well of standards and the supernatants (target samples). It was incubated at RT for 2 h with light shaking, followed by washing. The diluted Detection antibody solution was then applied and followed by adding diluted Avidin-HRP solution, 100 μ l/well for each, and then incubated for 60, then for 30 min, respectively, at RT with shaking.

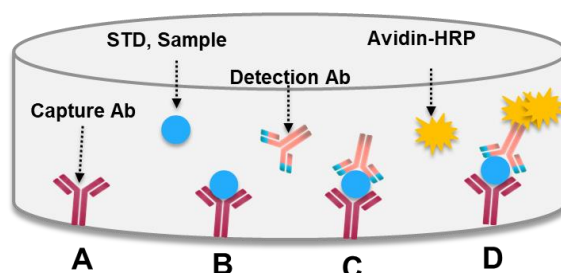


Figure 18| Stages of cytokine detection by ELISA. (A) Overnight incubation of capture antibody in 96-well plate at 4 °C. **(B)** Arresting proteins (cytokines) from standard and samples by capture Antibody. **(C)** Binding of detection antibody with proteins. **(D)** Joining Avidin-HRP (substrate) with a detection antibody yielded a colorimetric reaction.

For each step, incubation was done at RT with shaking at 500 rpm, and after each incubation time, a 96-well plate was washed 4x. The last step was to add 100 μ l of substrate solution C

and incubate in the dark for 15 min. The reaction was stopped by adding 100 μ l of Stop Solution. The plate was measured by absorbance at 450 nm and 570 nm subtracted from 450 nm.

2.2.8 Zymography:

Zymography is a method for detecting the activity of proteolytic enzymes [94]. It marks protease enzymes such as metalloproteinases, which degrade substrates such as gelatin using Novex zymogram gel [ThermoFischer, 94]. Proteases, involved in loading samples, are renatured by renaturing buffer containing non-ionic detergent. Afterward, the developing buffer can equilibrate gel by adding divalent metal cations required for enzymatic activity. Then, staining and destaining can show protease activity sites as bands [ThermoFischer]. The Novex®Zymogram Gel protocol was conducted in most cases according to the manufacturer's protocol followed by the Coomassie assay. 2 μ l of the samples were used with 8 μ l of Laemmli buffer, resulting in a total volume of 10 μ l mixture. After loading the samples, the system voltage was adjusted to 15 mA for 45 min, followed by 25 mA for about 2 h. Then, the gel was separated and washed in dH₂O.

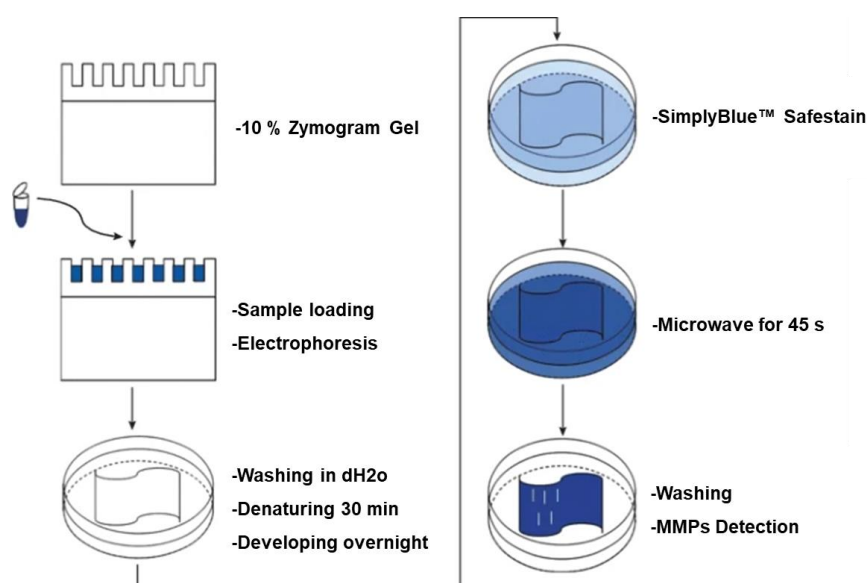


Figure 19| Zymography procedure for MMP detection. 10% Zymogram (gelatin) gel is used for MMP detection, where sample loading in the gel leads to a separation range of 10–220 kDa. After electrophoresis, the pre-casting gel is separated and washed in H₂O to remove the rest of the running buffer. The gel is surrounded by simplyBlue Safestain and microwaved for about 45 s followed by shaking for 5 min. The washing was done 2x for about 60 min for each using H₂O. [119, with modification].

Subsequently, the gel was incubated with 1x denaturing buffer at RT for 30 min and equilibrated with developing buffer at the same conditions with light agitation. 1x Developing buffer was

added and incubated overnight at 37 °C with light agitation. The coomassie assay was performed in the following steps. The gel was set in 100 ml of dH₂O, microwaved for 1 min (or until it started boiling), and then agitated on the shaker for 2 min. The step washing was repeated three times for each step. Afterward, 20 ml of SimplyBlue SafeStain solution was added to the gel and microwaved for 45 s (or until it started boiling). Then, it was agitated on the shaker for 10 min. To enhance the MMP band visualization, the gel was washed in 100 ml dH₂O for 10 min and 20 ml dH₂O with 20% NaCl for 10 min. The gel was stored in the salt solution until acquisition using the Azure Q500.

2.2.9 Calcium Imaging:

(Protocol was derived from Busch et al., 2022 and performed by AG Bernd Bufe, Kaiserslautern University of Applied Sciences, Zweibrücken). Cell population responses of transfected HEK293T cells were recorded using a FLIPRtetra (Molecular Devices). Cell populations were used in specific numbers, such as $\sim 50 \times 10^3$ cells/well for HEK293T, HL-60, and U-87, besides 100×10^3 cells/well for human neutrophils (granulocytes). All cells were incubated with the indicated dilution factors of bacterial supernatant for 30 min at room temperature (RT), followed by washing. Briefly, cells were incubated with 2 μ M Calbryte™ 520 AM (AAC Bioquest) at RT for 2 h in C1 assay buffer with 5 mM glucose (Carl Roth). Before each experiment, cells were rinsed 3x with C1 (remaining C1 solution at the end 100 μ l), while the human neutrophils were loaded in a complete RPMI medium for 45 min. Experiments with HEK293T cells were conducted 48 h after transfection. Acquisition of baseline fluorescence was performed for 25 s before ligand application, and cell population response was measured for 125 s after application. Responsiveness of cells was controlled by the appropriate buffer and solvent controls and with 10 μ M WKWMVm-NH₂ or WKWMVm-CHO as those ligands are potent activators of all three human and mouse FPRs50.

2.2.10 Antibody-dependent cellular cytotoxicity (ADCC):

It is an impedance-based cell analysis (IBCA) designed to monitor cell culture's cellular presence, morphology, and behavior. It is a non-invasive and label-free technique. Thus, the dynamic of changes can be monitored in real-time for long-term observations, to avoid disturbing the cell culture biology [OLS Biosystem]. This assay was established firstly for T-cells [137] and later for granulocytes, particularly neutrophils [138]. xCELLigence® Real-Time Cell Analyzer (RTCA) was used for ADCC and provided with E-Plate®, a gold electrode-covered bottom plate. The E-plate can measure any change in electrical impedance caused by cell attachment, growth, or de-attachment when they die. Then, a change in impedance (altering

current flow) is measured by delivering a small electrical current to embedded electrodes in a cell culture medium and reported as a Cell Index (CI).

Tumour cells, target cells (A-431), were trypsinized and harvested, then adjusted to a concentration of 0.2×10^6 cells/ml. After adding 50 μ l complete RPMI medium to 96-well E-plate for background measurement (blank wells) by RTCA system, 100 μ l of cell suspension in the medium was added into each well with a final concentration of 20×10^3 cells/well. Afterward, cells were kept directly at room temperature for half an hour to let them attach to the bottom of the E-plate before putting them into the RTCA unit. The cells were left to grow for 24 h. Then, they were treated with antibodies such as functional IgA2.0 (Engineered IgA) and non-specific IgA standard (STD) as isotype control. Neutrophils (50-70% of granulocytes) were added by mixing them in a complete RPMI (R10++) medium with a ratio of 40:1 of tumor cells and a final concentration of 4×10^6 neutrophils /ml. 5 μ l of 0.2% Triton was added as a positive control to monitor the experiment resulting to the highest lysis level. The last step was to add our target conditions, such as bacteria or bacterial supernatants, to the antibody-engaged neutrophils. Real-time ADCC monitoring was performed for at least 48 h and documented using RTCA software 2.0, where impedance levels were measured as Cell Index (CI). The data were normalized to the treatment time point and indicated as normalized Cell Index (nCI). All experiments were run in duplicates or triplicates, depending on the conditions needed for the 96-well E-plate.

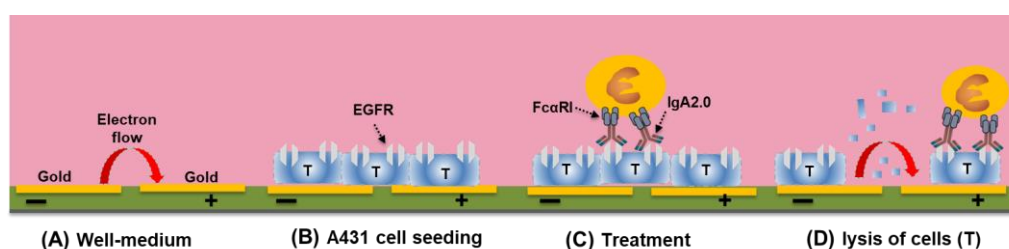


Figure 20I Procedure of ADCC assay. The graphical shape represents a 96-well plate with gold +/- electrodes bottom. **(A)** Well contains only culture medium as electrical conduct. **(B)** Seeding target cells (A431), expressing Epidermal growth factor receptor (EGFR), render the increase of the electrical flow as they attach well bottom. **(C)** Adding antibody (IgA2.0), connecting with EGFR, and binding with IgA2.0 leads to cell lysis. **(D)** Electrical flow comes back increasingly after killing cells based on ADCC-related lysis of tumor cells.

Data can be shown in different ways. Cell Index (CI) measures cell adhesion/ each well. However, we choose to show the data as a Normalized Cell Index (nCI) is a quantitative measurement of data manipulation at a specific time point and values represented as a proportion of 1 (100/%) [139]. Furthermore, data can be displayed as Delta Cell Index (Δ CI)

which is the selection of delta (a given) time point from normalized cell index (nCI) [140]. The notion used in this procedure is that Fc α RI expressed on myeloid cells, including neutrophils, is the responsible Fc receptor for mediating ADCC. Therefore, the 225-IgA2.0 antibody was engineered to mediate Fc α RI-neutrophils directed to EGFR-expressing tumor cells (A431). Thus, it is called granulocyte-mediated cytotoxicity, which can kill adherent and growing tumor cells [141].

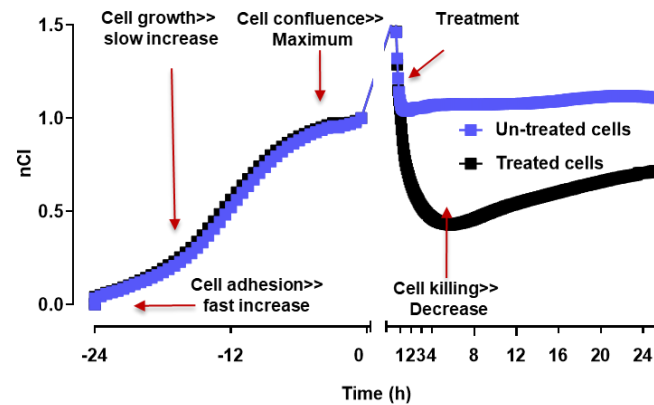


Figure 21I Phases of ADCC procedure affect the electrical impedance (EI) read out. Steps of ADCC analysis were documented by RTCA software, representing different stages of cell growth or death translated to the electrical impedance (EI). When wells contain only culture medium, EI counts zero. After seeding tumor cells (A431), EI increases fast at the beginning due to rapid cell adhesion and slowly, later, as the cells grow, leading to rendering the electron flow. After 24 h, EI reaches the maximum level due to cell conjunction, referred to as the plateau, taking a horizontal shape. Cell treatment by neutrophils with IgA2.0 causes cell killing, leading to cell death. Thus, cells initiate the de-attachment from the bottom. This causes a decrease in EI (**Black**) compared to untreated cells, which have no change (**Blue**) in EI level because cells were not killed.

2.2.11 Organotypic 3-dimensional (O3D) culture:

Culturing the cells in 3D is more physiologically related to the microenvironment than traditional two-dimensional (2D) monolayer cultures. The microenvironment in 3D can behave similarly to the *in vivo* natural extracellular matrix (ECM), which consists of collagen, elastin, fibrin, proteoglycan, cytokines and gelatin, laminin, and vitronectin [75, 142]. It provides information about cell growth and response to the immunological, chemical, and physical stimuli [141]. Because 3D culture is closer to the complex *in vivo* environment, it is more realistic for translating research data for application *in vivo* than traditional 2D monolayer cultures. More differences between 2D and 3D models are shown in table 5. This 3D model is used in various research areas, such as drug discovery, cell differentiation, apoptosis, survival, and gene as well as protein expression [142]. Therefore, this model is beneficial for use as an

in vitro pharmaceutical method in the preclinical stage. Thus, the potential therapeutic drug can be specified, avoiding non-success at an earlier stage [75].

Table 5: Comparison of 2D and 3D cultures [143].

Feature/function	In 2D	In 3D
Tissue-specific architecture	Poor	Rich
Cell morphology	Flat, extended	Round, contracted
Interactions	Limited	Multiple
Cell motility	Fast, free	Slow, restricted
Cell adhesion	Weak	Strong
Cell growth	Directional	In all directions
Cell proliferation	High	Low
Apoptosis	Induced	Tissue-like
Intracellular stiffness	An order-of-magnitude higher in 3D	
Cell polarization	Partly	Full
extracellular matrix remodeling	Absent or poor	Present
Fluid perfusion	1D	3D
Signaling and diffusion	Asymmetric	Nearly symmetric
Metabolic rate	High	Low
Cell survival when exposed to cytotoxic agents	Low	High

2.2.11.1 Generation of 3D cultures:

Organotypic 3-dimensional cultures (OC/ 3D culture) were established by Marthaler AM *et al.*, 2017 and the protocol was performed as described by Bernhard *et al.*, 2020 with minor modifications. Collagen type I was isolated from Rat tails and dissolved in 0.1% (v/v) acetic acid to a concentration of 4 mg/ml. Volumes are given per well of 24-well plate. Firstly, dermal equivalents were prepared by mixing 800 µl of ice-cold Rat tail collagen with 100 µl of 10x DMEM on ice. Then, the mixture was neutralized with 1N NaOH, using phenol red as a pH indicator. Finally, 100 µl of FCS containing 0.5×10^6 primary human foreskin/ectocervical fibroblasts (up to passage 6) were added, and the mixture was placed in a 24-well plate and solidified in a cell culture incubator. After 1 h, the collagen matrix was covered with 1 ml of supplemented DMEM.

The next day, the culture medium was removed, and the cells ($0.5\text{-}0.7 \times 10^6$ of HPKIA, PeCa L2) were added to 1 ml of keratinocyte growth medium. 24 h later, 3D cultures were lifted onto the autoclaved metal grids at the air-medium interphase and grown for 7 or 14 days, depending

on cell type. Before 24 h of the 3D culture collection, the medium was changed to 1 h before adding the treatments. Bacterial supernatants or hydrogel constructs were added under the metal grid. Then, neutrophils in a concentration of $5 \times 10^6/50 \mu\text{l}$ were added to the top of the culture. After 24 h, the supernatants were collected and stored at -20°C . 3D cultures were then fixed at 4°C with 4% buffered paraformaldehyde (4% PFA) solution until attaching the lower surface of the metal grid. After 1 h, 3D cultures were overloaded by 4% PFA overnight and later embedded in paraffin and sectioned. To maintain the normal growth of 3-D culture, the growth culture medium was changed every 2 days.

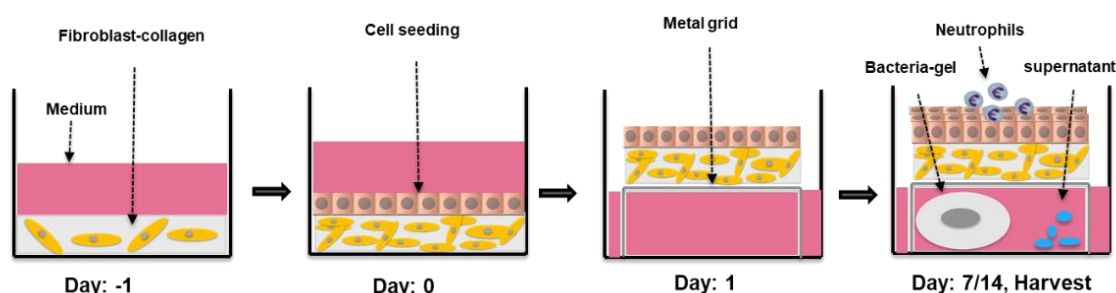


Figure 22| Stages of 3-D culture production. On day 1, fibroblasts were mixed with collagen and incubated for 24 h with an appropriate medium. On day 0, keratinocytes were added and left to grow for another 24 h. On day 1, constructs of 3-D culture were transferred onto a metal grid in air-phase conditions and incubated for 7 or 14 days in total for HPK1A and PeCa cells (L2), respectively. The medium was added to attach the lower surface of the metal grid and changed every 2 days. 24 h before 3D cultures collection and after medium change 1 h before, target materials, gel (PluDA hydrogel) with/out bacteria or bacterial supernatant, were added under the metal grid. Further, 1-2 h rested- neutrophils were transferred onto the surface of 3D cultures and left for 24 h.

2.2.11.2 Staining of 3D cell culture:

2.2.11.2.1 Hematoxylin-Eosin (HE) staining:

Hematoxylin and Eosin (HE) are two different stains, used to investigate the morphology and structure of the 3-D cultures. Hematoxylin stain is used to stain the cell nucleus, but Eosin can stain alkaline structures, such as cytoplasmic proteins and mitochondria. Before staining, slides were de-paraffinized in xylol (3x, 10 min each) and rehydrated in a descended ethanol series (99, 90, 80, 70, 50%; 2 min each) ending with putting them in dH_2O for 5 min. Afterward, the slides were stained in Hematoxylin (vector) for 1-2 min and developed under running water for 5 min. Counterstaining was done in 1% Eosin for 10 min before the slides were dehydrated

again in an ascending ethanol series (50-99%). The slides were washed in xylol (3x, 3 min each) and closed with 20 μ l VectaMount™ Permanent Mounting Medium (vector) and adequate coverslips.

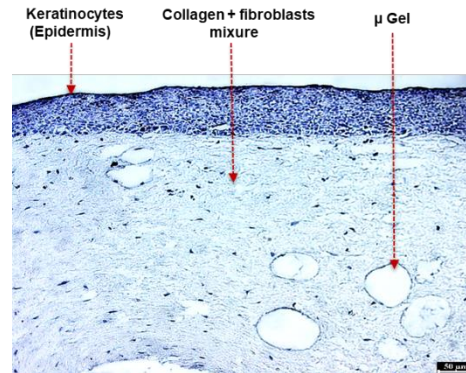


Figure 23| HE stain of the micro-hydrogel (μ Gel) incorporation trial in 3D culture. μ Gels were mixed, on the first day, with collagen and fibroblasts to produce 3D cultures according to the previous protocol. A hematoxylin-Eosin stain was applied to check the structure of μ gel.

2.2.11.2.2. Immunohistochemistry (IHC) stain:

To investigate the response or migration of neutrophils towards specific conditions, CD15 expression, as a marker, was stained on treated and untreated 3D cell culture sections. First, de-paraffinization (3x, 10 min in xylol) and rehydration were performed as described in the previous section. Afterward, the slides were incubated in TE buffer for 7 to 10 min in a water-path system (at 95 °C) and then incubated for 15 min at room temperature (RT). After washing with 1x TBS and drying, endogenous peroxidase was blocked with 3% H_2O_2 in 1x TBS (pH 7: 6) for 5 min (in the dark) before the slides were washed similarly. The sections of 3D culture slides were then incubated with 2.5 % normal horse serum at RT for 1 h to prevent unspecific results. The primary antibodies, mouse anti-human CD15 (Dako Agilent), were diluted 1:500 in 0.5% BSA in 1x TPBS, added to the slides, and incubated overnight at 4 °C. Slides were washed with 1x TPBS for 5 min. Impress™ HRP anti-human CD15 Detection Kit was used as a secondary antibody for 30 min at RT and washed with 2x TBS before and after substrate (1 ml Impact DAB Diluent + 1 drop of DAB Chromogen ImmPACT DAB SK-4105 Vektor BioZol) application for 5 min. Counterstaining was done with hematoxylin, and the slides were dehydrated in 50 to 99% ethanol. Finally, the stained slides were covered with 20 μ l of VectaMount Permanent Mounting Medium and evaluated at the DMI6000 Fluorescence microscope from Leica.

2.2.12 Endotoxin Detection:

(Performed by AG. Markus Bischoff, institute of medical microbiology and Hygiene, Homburg). Limulus amoebocyte lysate (LAL) assay is a technique used to detect endotoxin's existence. The experiment was carried out according to the Pierce™ Chromogenic Endotoxin Quant Kit protocol of thermoscientific (Cat. No. A39552S). LAL is a quantitative endpoint assay, which uses amoebocyte lysate taken from the horseshoe crab (*T. Tridentatus*/ Limulus) hemocytes/amoebocytes to determine endotoxin in samples such as protein, peptides, antibodies, and nucleic acids. Furthermore, LAL is a simple and sensitive technique used to detect lipopolysaccharides in the membrane of gram-negative bacteria. The interaction of endotoxin (LPS) with amoebocyte lysate can generate an enzymatic reaction activating factors C, B, and pro-clotting enzymes. Therefore, the activated enzyme breaks p-nitroaniline (pNA) in the colorless chromogenic substrate (Ac-Ile-Glu-Ala-Arg-pNA), resulting in a yellow color which can be measured after stopping the reaction [ThermoSceintific, 144].

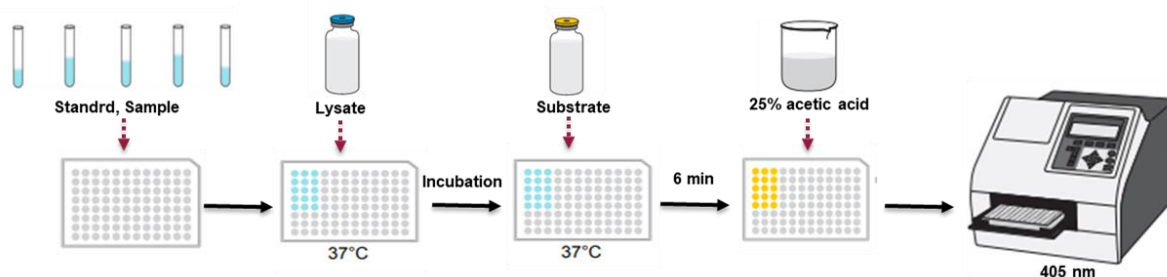


Figure 24| LAL assay measurement of Endotoxin concentrations. Standards and samples were added to a 96-well plate followed by amoebocyte lysate enzymes. After incubation times, the substrate was added and incubated for a specific time. 25 % acetic acid was added to stop the reaction to measure the plate by the reader at 405 nm [ThermoScientific schema modifications].

Briefly, the kit's reagents and standards were prepared before use. The 96-well plate was maintained in the heating block at 37+/-1 °C. Standards, blank (Endotoxin-free water), and samples were added, 50 µl/well, followed by adding amoebocyte lysate reagent, 50 µl/well. The plate was then removed, and the contents were gently mixed before putting the plate back and incubated for the time indicated on the lysate vial. Chromogen substrate solution (100 µl/well) was applied, mixed, and incubated for 6 min. Then, it is followed by adding 50 µl of stop solution (25% acetic acid) and mixing well. Finally, the measurement of the optical density was evaluated at 405 nm. The data were calculated by subtraction the blank average from all individual standards and samples to calculate the mean absorbance.

2.2.13 General schema summarises the experimental workflow:

The shown schema summarises most of the experiments performed in this thesis. Bacterial suspensions were generally centrifuged after growing bacteria to get supernatants as described earlier. Neutrophils were stimulated by supernatants, bacteria, or hydrogel w/wo bacteria and proceeded according to established protocols and followed by performing methods such as zymogram, ELISA, calcium imaging, and ADCC assays described in more detail in later sections.

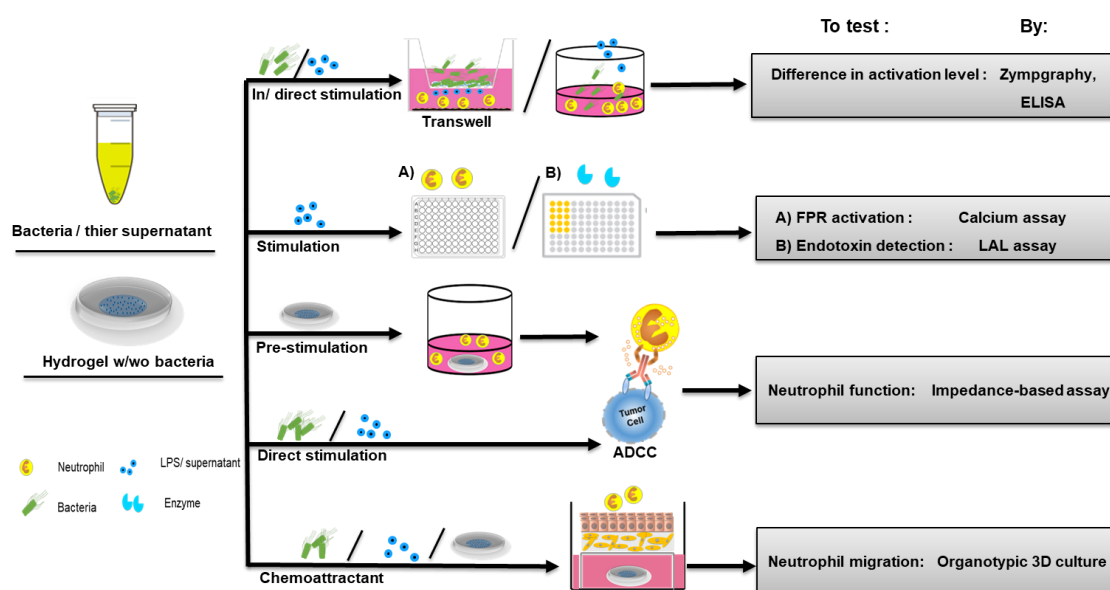


Figure 25| Diagram of neutrophil stimulation procedure *in vitro*. The general procedure was started after (A) collection of bacterial supernatants (Bac.Sup.). (B) Direct stimulation assay (DSA) was performed in a 12-well plate with a concentration of Bac.Sup 1/100 ($OD_{600}=1$) and 4×10^6 cells/1ml medium. After resting neutrophils for 1-2h at 37 °C, they were incubated at 37 °C with 5% CO₂ for indicated time points on the results. (C) Calcium imaging assay was done in a 96-well plate for different FPR –FPR-expressing cells as well as neutrophils. (D) Direct stimulation of neutrophils in ADCC assay, proceeded in a 96-well plate with gold-bottom electrodes.

Section 1:

E. coli B21 and engineered E. coli (LPS-modified ClearColi)

3 Results:

3.1 Investigation of direct and indirect contact of neutrophils with live bacteria.

Neutrophils respond fast to the infection in minutes to hours [50]. Therefore, to determine if physical bacterial separation can decrease neutrophil response compared to nonseparated bacteria. A transwell plate with a microporous membrane was used. It is generally used for cell migration, where cells migrate through the porous membrane of the transwell plate toward the chemotaxis, and for cell invasion, where cells migrate through an extracellular matrix added to the permeable membrane if they have invasive characteristics [145]. Here, the transwell prevents bacteria from direct contact with neutrophils. In this way, it mimics the separation process of bacteria encapsulated by PluDA hydrogel, allowing the exchange of soluble metabolites through membranous transwell with neutrophils.

To do so, fresh neutrophils were placed at the plate bottom, and then *E. coli* strains were mixed in 200 μ l RPMI medium and added to 12 well plates (direct contact) as well as the transwell-insert (indirect contact) containing membrane (0.4- μ m pore size) to maintain the protein exchange between the compartments. Fresh neutrophils were used for a short incubation time (usually 1 h) for transwell and DSA assays. Thus, they are mature cells and have a short lifespan (< 24 h) *in vitro*. Hence, the immunogenic response of neutrophils was measured via co-culturing *E. coli* or *ClearColi* with neutrophils through indirect/ direct contact. Some secretory proteins such as matrix-metalloproteinases (Fig. 26A-D) and cytokines, such as CXCL-8 (Fig. 26I), were analyzed from supernatants after 60 minutes of co-culturing. MMPs facilitate neutrophil recruitment to the site of infection by degrading gelatin and collagen-I and appear as pro and active forms [103, 106, 146]. However, a high level of MMPs causes powerful pathological conditions in tissues [146]. MMP-9 forms including homodimer (200 kDa), NGAL complex (130 kDa), monomer (92 kDa), and MMP-2 (72 kDa) were detected as pro-forms on gelatine gel.

Homodimer MMP9 (Fig. 26E) folds increased in the case of direct contact 1.27 ± 0.33 , (*ClearColi*) and 3.74 ± 1.46 (*E. coli*) indirect contact *ClearColi* to 1.11 ± 0.62 (*ClearColi*) and 1.41 ± 0.85 (*E. coli*) compared to Ctrl (untreated neutrophils). The data was significant between Ctrl vs. direct *E. coli* ($p=0.0005$), direct *E. coli* vs. indirect *E. coli* ($p=0.0028$), and direct *E. coli* vs. direct *ClearColi* ($p=0.0015$). Further, the complex MMP9 (Fig. 26F) elevated in case of direct contact to 1.72 ± 1.39 (*ClearColi*) 3.48 ± 1.4 -fold (*E. coli*) and for indirect contact to 1.2 ± 0.92 (*ClearColi*) 1.46 ± 1.17 -fold (*E. coli*) compared to Ctrl with significant differences of

Ctrl vs. *E. coli* ($p=0.0083$) as well as indirectly and directly contacted *E. coli* ($p=0.0447$). The monomer level (Fig. 26G) increased in the case of direct contact to 1.69 ± 1.24 (*ClearColi*) and 2.6 ± 1.29 (*E. coli*) and for indirect contact reached 1.21 ± 0.82 (*ClearColi*) and 1.43 ± 1 (*E. coli*) compared to Ctrl without significance. However, no change in MMP2 levels (Fig. 26H) was observed in all statues for *E. coli* or *ClearColi*.

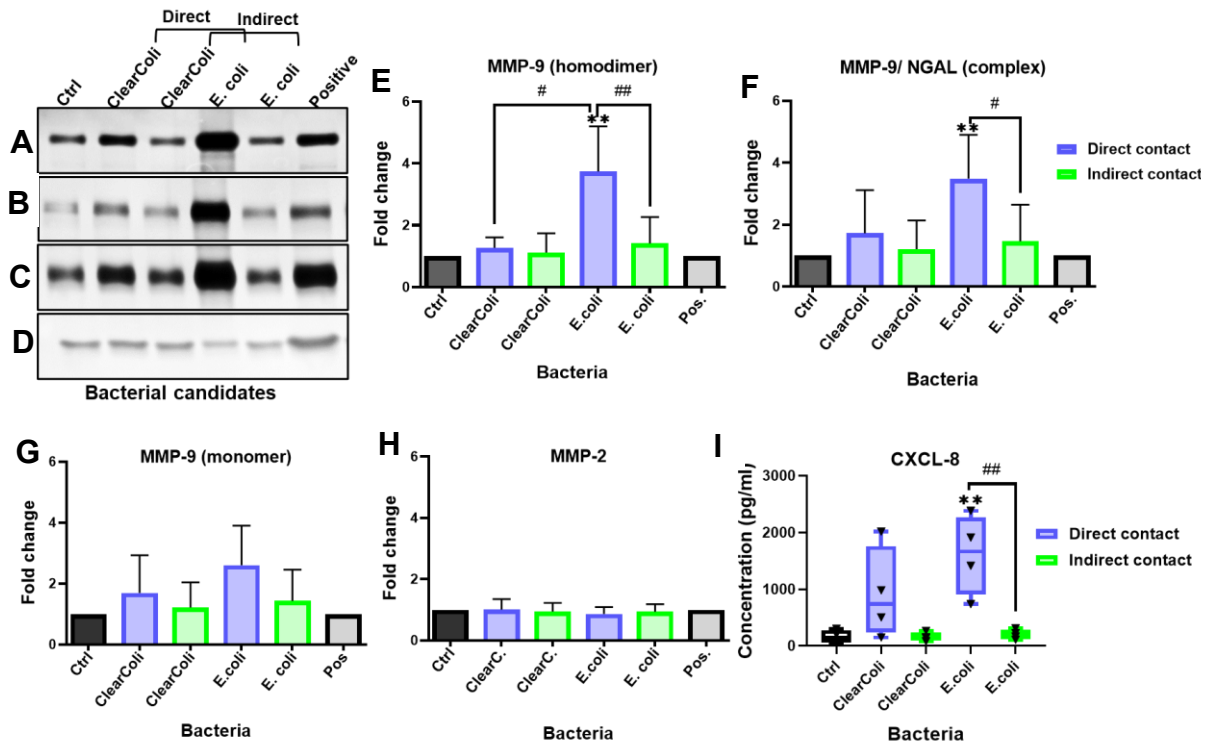


Figure 26I Neutrophil response exposed directly and indirectly to different *E. coli* strains. Neutrophils were cocultured with (treated) and without (Ctrl) live bacteria physically (direct) contact in one well or physically separated (indirect) contact by transwell plate (0.4- μ m pore size) and incubated for 60 min at 37 °C. The bacterial supernatants were collected, centrifuged, and then used for zymography and ELISA. **(A-D)** zymogram gel for MMP detection. **(E-H)** Data analysis of MMP profile. **(I)** CXCL-8 measurement using ELISA. Data were illustrated as mean with SD of at least three independent experiments; E-H: $n \geq 4$, and I: $n=4$. Significant differences were analyzed using GraphPad prism, in which a paired one-way ANOVA with Tukey's multiple comparison tests of untreated neutrophils (Ctrl) with the treated ones (by *ClearColi* and *E. coli*). The significance was illustrated as * (for Ctrl with treated conditions) and # (between treated conditions). GraphPad Prism 8.0.2 [ns ($P > 0.05$) */# ($P \leq 0.05$), **/## ($P \leq 0.01$)]. Concentration/Control: bacteria (1/100 of OD₆₀₀=1), neutrophils (4×10^6 /ml), positive control (Pos., supernatant from CXCL-8-stimulated neutrophils).

CXCL-8 is an effective chemokine for neutrophil migration and guiding during infection and injury [147]. The ELISA measurement showed CXCL-8 secretion (Fig. 26I) increased to about 913 ± 811.3 and 16.12 ± 704.4 pg/ml (direct contact) as well as 160.98 ± 76.48 and $203.3 \pm$

85.47 pg/ml (indirect contact) for *ClearColi* and *E. coli* compared to Ctrl (162.9 ± 111.1). Significant differences were detected for *E. coli* vs. Ctrl ($p=0.0057$) and direct vs. indirect *E. coli* ($p=0.0071$). Furthermore, the CXCL-8 concentration of *ClearColi* has no significant difference. In previous data (Anabels PhD thesis), we saw that the release of ROS and LTB₄ peaked one hour after treatment [138]. Additionally, previous data from the group (Felix Masterthesis) proved that CXCL8 release also peaked 1h after treatment. The data shows various levels of neutrophil response among the four donors. The results illustrated that the process of physical separation of bacteria reduced neutrophil triggering through decreased levels of protein release.

3.2 Preliminary results of pre-stimulated neutrophils by drug-producing LTMs.

In vitro-engineered VEGF mimicking peptides (QK) showed the same characteristics as full VEGF, such as stimulating capillary formation. Besides, an *in vivo* study demonstrated that QK is like VEGF in pro-angiogenesis [151]. Therefore, *ClearColi* bacteria were designed genetically to secrete a QK-bearing fusion protein (YCQ) stimulated by light [114]. The engineered *ClearColi* were then encapsulated in PluDA hydrogel (bacteria-gel), and empty capsules as a control (gel) were also used [152].

To investigate whether LTMs can trigger neutrophil activation, they were co-cultured with fresh neutrophils for 15 and 60 min (short term). This timeframe was selected as neutrophils respond typically in minutes to hours [50]. Then, neutrophils and supernatants were collected separately after centrifugation. Using Zymography (Fig. 27A-C), the supernatant was used to evaluate the degranulation levels by analyzing MMPs (Fig. 27D-F). Neutrophils treated by gel (empty) and *ClearColi* (VEGF_{peptide} yield)-gel (*Clear-gel*) showed degranulation-dependent time compared to control (untreated neutrophils). Homodimer (Fig. 27D) raised to about 1.41 ± 0.4 , 1.95 ± 1.5 (at 15 min) 2.25 ± 0.67 , and 4.38 ± 3.4 -fold (at 60 min) for gel and *Clear-gel*, respectively, compared to Ctrl and without significant differences. Complex levels (Fig. 27E) increased to 1.78 ± 0.8 , 1.87 ± 0.84 (at 15 min) 2.8 ± 1 , and 3.26 ± 1.4 -fold (at 60 min) for gel and *Clear-gel* with different significant at 60 min between Ctrl with gel ($p= 0.0362$) and *Clear-gel* ($p=0.0049$). Further, the level of monomers (Fig. 27F) was approximately 1.65 ± 0.69 , 2 ± 1.17 (at 15 min), 2.25 ± 0.48 , and 3.17 ± 1 -fold (at 60 min) for gel and *Clear-gel*, respectively, and with a significantly different significance at 60 min of Ctrl vs. *Clear-gel* ($p=0.0029$). However, there were no significant differences between gel (empty) and *ClearColi* (Vegf_{pep})-gel in degranulation levels for all results.

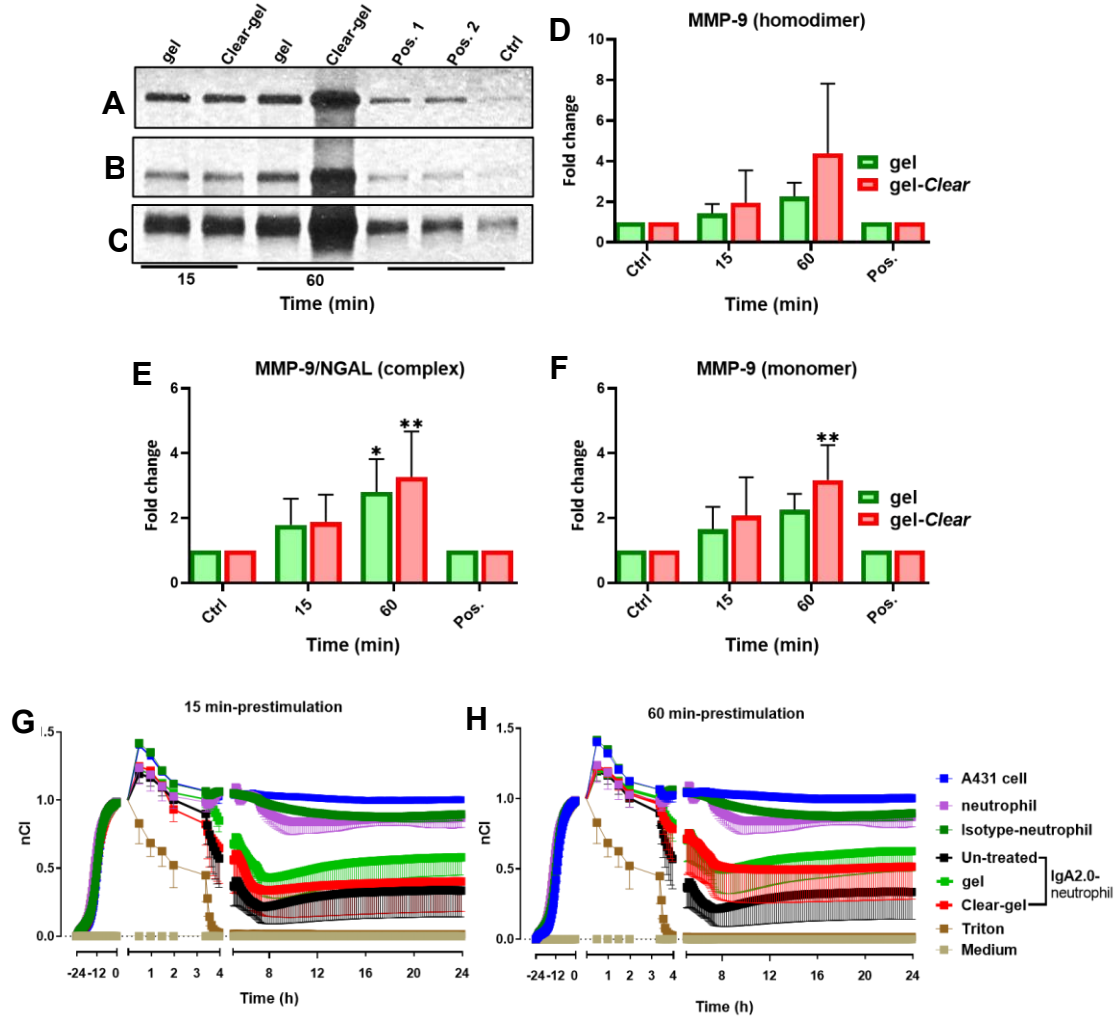


Figure 27I Release of MP9 molecules marks neutrophil degranulation, leading to a decrease in tumour-killing efficacy by ADCC. Supernatant and pre-stimulated neutrophils were collected after treatment by gel (PluDA 30% hydrogel) W/out *ClearColi* (VEGF_{pep}. producing) for specific time points in 24-well at 37 °C. The supernatants were collected from pre-stimulation neutrophils by gel (Green) and by *ClearColi*-gel (Red) and used in the (A-C) Novex zymogram procedure and (D-F) analysis for MMP detection. Positive control represents the supernatant collected from CXCL-8 and GCSF-stimulated neutrophils as Pos.1 and 2, respectively. Data was analyzed using ImageJ software. (G-H) Target cells (A431) were seeded for 24 h in 96-well E-plates. After confluence (high impedance), cells were treated with an antibody (EGFR-specific antibody IgA2.0) and previously pre-stimulated neutrophils by gel or gel-encapsulated *ClearColi* for 15 min (D), and 60 min (E). Data were illustrated as mean with SD (for D-F) and SEM (G-H) of three independent experiments (n=3 for A-H). Significant differences were analyzed, with two-way ANOVA with Tukey's multiple comparison tests of untreated neutrophils (Ctrl) with treated ones (by gel w/out *ClearColi*). The significance was illustrated as * (for Ctrl with treated conditions) and # (Between treated conditions themselves) and as (P > 0.05), */# (P ≤ 0.05), **/## (P ≤ 0.01). Concentration/Control: Neutrophils (4 × 10⁶/ml), positive (Pos., supernatant from CXCL-8-stimulated neutrophils), isotype (non-specific IgA standard, STD), positive (5 µl of 0.2% Triton), negative (untreated A431 cells), PMNs: target cells (neutrophil: A431 cell, Effector: Target) = E: T ratio of 40:1.

PAMPs such as LPS and formyl peptides activate TLR4 and FPR-1/-2, respectively, on neutrophils leading to degranulation, ROS, and migration [85]. To investigate the effect of sensing PAMPs on the crucial biological function of neutrophils after pre-stimulation with gel with/without bacteria. Therefore, IgA2.0 (engineered Ab) was added to neutrophils (stimulated and unstimulated) to kill A431-cells (grown for 24 h) in the ADCC assay as an intermediate term, to monitor the neutrophil activation. The ADCC method is characterized by a label-free real-time and provides information on functional properties. We found a reduction in neutrophil capability for tumor cell killing at indicated time points, 15 and 60 min (Fig. 27G-H), suggesting and ensuring that the pre-treatment with gel w/out *ClearColi* components led to activation of neutrophils, indicated by the release of MMP9 forms including homodimer, monomer, and complex as shown earlier. Consequently, the pre-stimulation reduced neutrophil capacity to kill antibody-opsonized cells (ADCC) compared to untreated neutrophils. However, the reduction was more prominent when we pre-stimulated neutrophils for 60 min (Fig. 27H). The data showed no significant difference between the hydrogel and bacteria-encapsulated hydrogel to stimulate neutrophils mirrored by the release of MMPs.

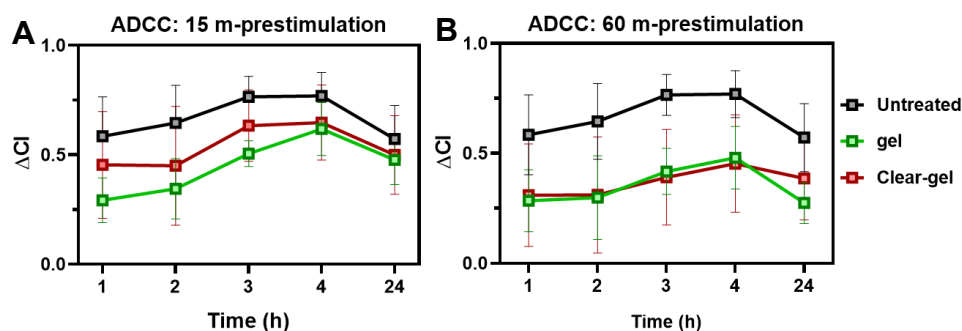


Figure 28I Delta Cell Index calculation. (A, B) The Delta cell index (ΔCI) was evaluated as isotype control (+ neutrophil) - IgA2.0 (+neutrophil) of the respective conditions at 1, 2, 3, 4, and 24 h. Data were illustrated as mean with SEM of three independent experiments (n=3 for A-B). Significant differences were analyzed by two-way ANOVA with Dunnett's multiple comparisons test for each treated condition at 1 h with 2, 3, 4, and 24 h marked as*, and untreated (IgA2.0-neutrophil) with treated conditions (gel/gel-Clear) at each time points.

For further analysis, data was displayed as Delta Cell Index (ΔCI). Therefore, four-time points were chosen after treatment to represent the first hours: 1, 2, 3, and 4 (Fig. 28A-B), and the most effective time for effector cells. However, 24 h was also chosen to show whether neutrophils still can kill tumor cells at a prolonged time. The result of ΔCI showed the same reduction in nCI without significant differences at any time point. The results so far suggest that neutrophils were exhausted. We may speculate that the neutrophils degranulated and thus „lost their

munition“ before ADCC, limiting their capacity to kill tumor cells. Consequently, more investigations are required for the *ClearColi* strain, which does not produce VEGF peptides or the supernatant.

3.3 Bacteria-conditioned supernatants trigger the release of neutrophil proteins.

To test whether soluble components are the responsible mediators for neutrophil activation, we tested the direct contact of neutrophils with bacteria supernatant. Neutrophils were co-cultured with bacterial supernatants at indicated time points 15, 30, and 60 min. MMPs (Fig. 29E-H), cytokines (Fig. 29I, J), and secretion were evaluated using Zymography (A-D) and ELISA, respectively.

Homodimer levels (Fig. 29E) raised for *ClearColi* and *E. coli* to 1.47 ± 0.12 , 2.36 ± 0.74 (15 min), 1.77 ± 0.24 , 8.99 ± 0.92 (30 min), 2.68 ± 1.39 , and 10 ± 1.35 -fold (60 min) with significant differences between Ctrl and *E. coli* at 30 min ($p < 0.0001$) and 60 min ($p < 0.0001$) as well as *ClearColi* and *E. coli* at 30 min ($p < 0.0001$) and 60 min ($p < 0.0001$). Further, the level of NGAL (Fig. 29F) increased to 1.42 ± 0.28 , 1.9 ± 0.17 (15 min) 2.3 ± 0.44 , 13.48 ± 4.6 (30 min) 2.7 ± 2 , and 16.3 ± 5 -fold (60 min) for *ClearColi* and *E. coli*, respectively, with significant differences between Ctrl and *E. coli* at 30 min ($p < 0.0001$) and 60 min ($p < 0.0001$) as well as *ClearColi* and *E. coli* at 30 min ($p = 0.0002$) and 60 min ($p < 0.0001$). Furthermore, monomer levels (Fig. 29G) reached 3.25 ± 2 , 4.57 ± 4 (15 min) 4 ± 3.6 , 9.36 ± 5.4 (30 min) 3.6 ± 1.18 , and 9.9 ± 4.6 -fold (60 min) with significant differences between Ctrl and *E. coli* at 60 min ($p = 0.0361$). Moreover, no change was noticeable in MMP-2 levels in all results. In addition to MMPs, CXCL-8 elevated to a concentration of 97 ± 88 , 58.25 ± 58 (30 min), 200.5 ± 102.4 , and 389.89 ± 75 pg/ml for *ClearColi* and *E. coli* compared to Ctrl (25.4 ± 44) with significant differences between Ctrl and *E. coli* only at 60 min ($p = 0.0005$). Additionally, there was an increased VEGF concentration evaluated by 3 ± 5 , 106.9 ± 28.58 (30 min), 10.3 ± 9.3 , and 151.4 ± 83 pg/ml (60 min) with significant differences between Ctrl and *E. coli* at 30 min ($p = 0.0321$) and 60 min ($p = 0.0026$) as well as *ClearColi* and *E. coli* at 30 min ($p = 0.0385$) and 60 min ($p = 0.0046$).

It was observed that levels of MMPs and CXCL-8, in addition to VEGF release were a time-dependent increase reflecting the increase in neutrophil activation with time. Concerning *ClearColi* supernatant at the different time points, a reduced release of MMP-9 (homodimer, NAGAL, and monomer) and cytokines such as CXCL-8 and VEGF, was noticeable. However, *ClearColi* supernatant induced an increase in the levels of MMPs to more than 2-fold compared to untreated neutrophils (Ctrl). Although there are no significant differences with *ClearColi* supernatant at 15 min, we could observe a slight increase in the MMP9 monomer. This increase indicates that MMP9 release might be before CXCL-8, in which CXCL-8 is treated at the amino

terminus of MMP9, producing an activated form of CXCL-8 [153]. Although, there is a slight increase in VEGF in a concentration of 10 pg/ml at 60 min. These results show that CXCL-8 is secreted before VEGF and in more concentration. Thus, it refers to the crucial role of CXCL-8 as a chemotactic factor guiding neutrophils to the site of infection, inflammation, and injury [111-113].

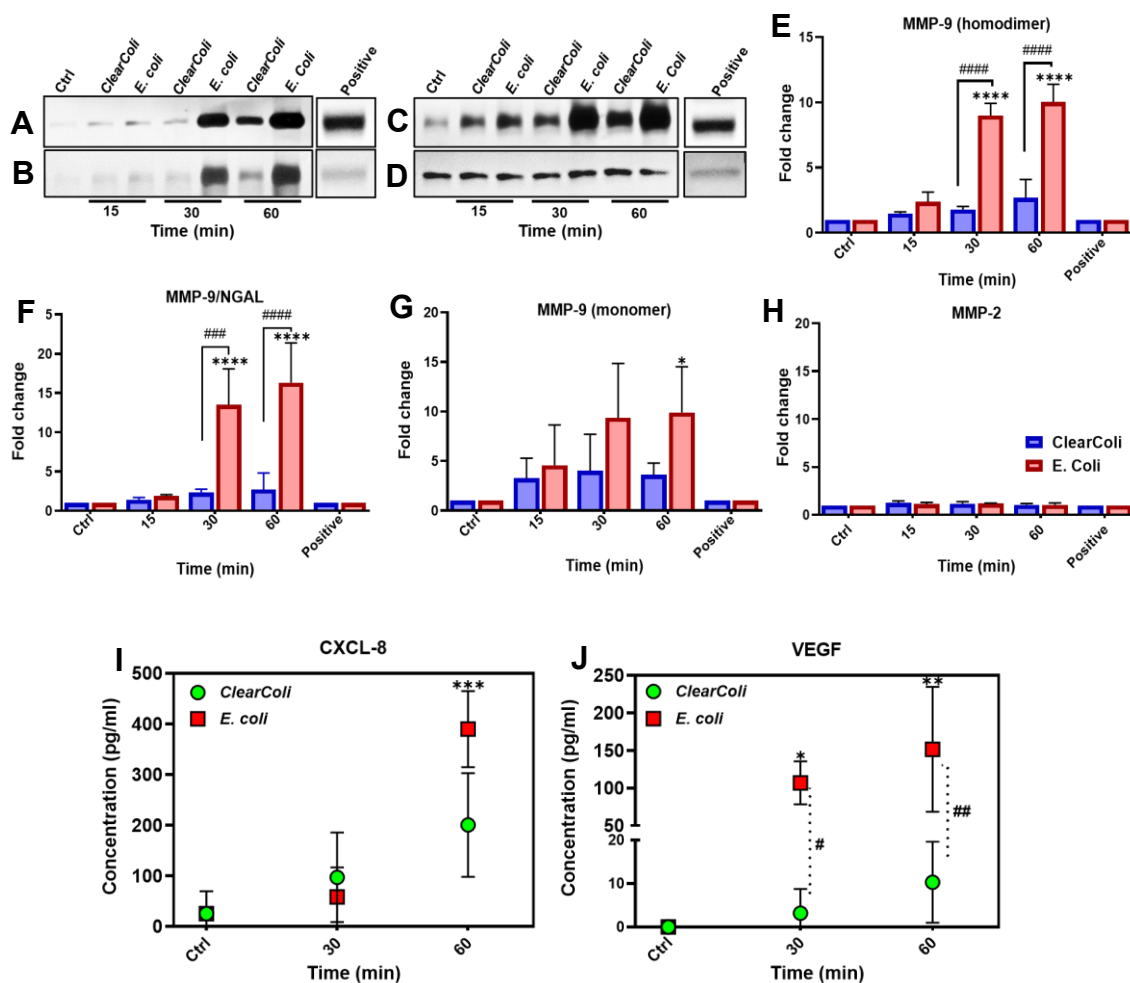


Figure 29I MMPs and cytokines release marks activation and degranulation of neutrophils stimulated by bacterial supernatants. The supernatant was collected and used after stimulation of the neutrophils by supernatant of *E. /ClearColi* in a 24-well plate at 37 °C at different time points. (A-D) Novex zymogram procedure for (E-H) MMPs detection, respectively. (I, J) ELISA for CXCL-8 and VEGF concentration measurement. Data were illustrated as mean with SD of three independent experiments (n=3, A-F) was used. Significant differences were analyzed, with two-way ANOVA with Tukey's multiple comparison tests for untreated neutrophils (Ctrl) and treated ones (by *ClearColi* and *E. coli*). The significance was illustrated as * (for Ctrl and treated conditions) and # (between only treated conditions) and ns ($P > 0.05$), */# ($P \leq 0.05$), **/## ($P \leq 0.01$), ***/### ($P \leq 0.001$), ****/#### ($P \leq 0.0001$). Concentration/Control: bacterial supernatants (1:100, OD₆₀₀=1), neutrophils (4×10^6 /ml), positive (supernatant of CXCL-8-stimulated neutrophils).

To verify the previous finding that the release of MMP9 forms is crucial before CXCL-8 secretion, supernatants of ADCC were investigated by zymogram and ELISA. Tumor cell-engage antibodies led to an increase in the level of neutrophil MMPs (Fig. 30A-C) to about $2.73 (\pm 1.04)$, and $3.28 (\pm 1.67)$ -fold (homodimer), $2.98 (\pm 1.15)$, $3.64 (\pm 1.9)$ -fold (complex), $3 (\pm 0.67)$, and $1.99 (\pm 0.39)$ -fold (monomer), at 1 and 2 h, respectively.

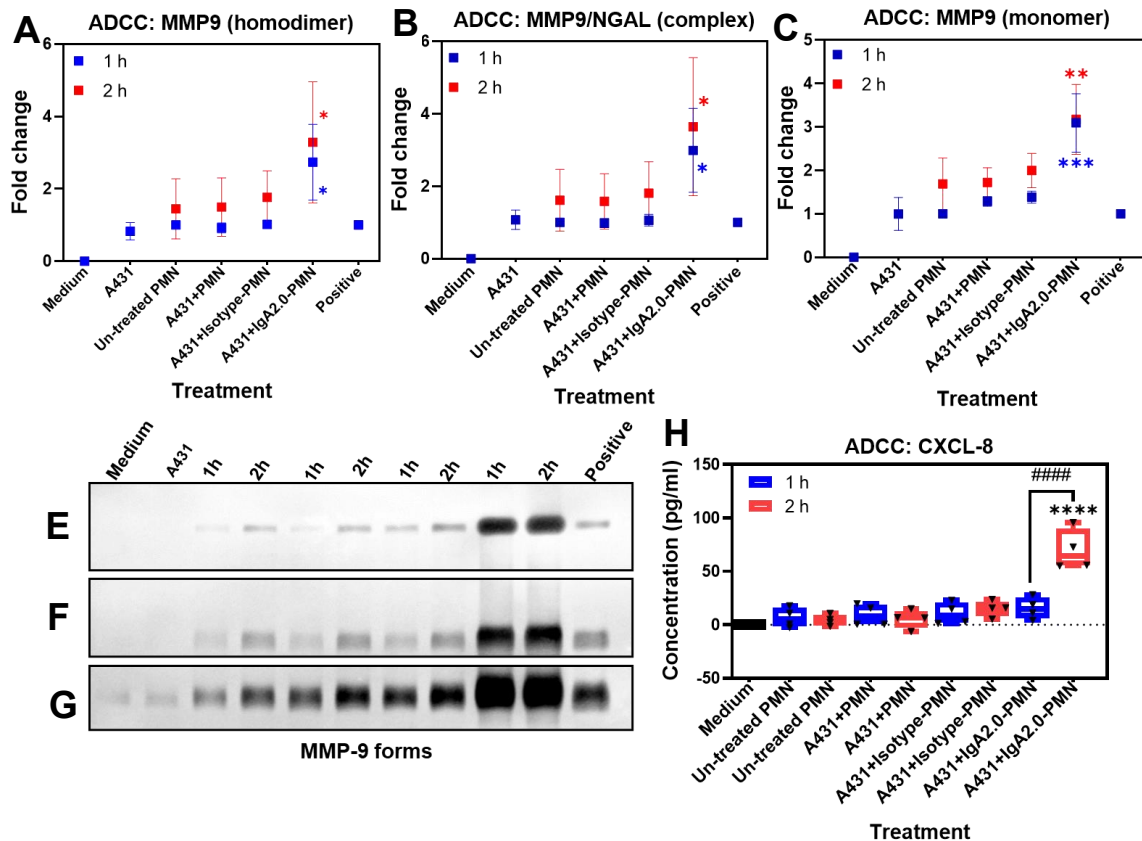


Figure 30 | Release of MMP9 is at an earlier stage of CXCL-8 in ADCC. (A-C) Data analysis of zymogram. (D-G) Zymography of MMP9 forms. (H) CXCL-8 measurement by ELISA. ADCC was performed for 1 and 2 h. Supernatants were collected and centrifuged then used for indicated experiment. Data were illustrated as mean with SD (A-B: $n=3$) and SEM (H: $n=4$) of at least three independent experiments. A paired one-way ANOVA with Dunnett's multiple comparison test between A431-PMN (as control) and other conditions (antibody treated) for 1 h then 2 h. GraphPad Prism 8.0.2 [ns ($P > 0.05$), * ($P \leq 0.05$), ** ($P \leq 0.01$), *** ($P \leq 0.001$), **** ($P \leq 0.0001$)]. Concentration/control/Abb.: negative (medium), neutrophils (4×10^6 /ml), positive (Pos., supernatant of CXCL-8-stimulated neutrophils). PMNs (neutrophils/polymorphonuclear cells).

The significance in MMPs included homodimer (Fig. 30A): A431+PMN vs. A431+IgA2.0-PMN at 1 h ($p=0.0410$) and 2 h ($p=0.0446$), complex (Fig. 30B): A431+PMN vs. A431+IgA2.0-PMN at 1 h ($p=0.0409$) and 2 h ($p=0.0340$) and monomer (Fig. 30C):

A431+PMN vs. A431+IgA2.0-PMN at 2 h ($p = <0.0001$). CXCL-8 (Fig. 30H) concentration was evaluated by an average of 70 pg/ml after 2 h with significance between A431+PMN vs. A431+IgA2.0-PMN 2 h ($p < 0.0001$) and A431+IgA2.0-PMN at 1 vs. 2 h ($p = <0.0001$). The data ensures that MMPs are released before CXCL-8.

3.4 Bacteria-conditioned supernatants enhance neutrophil-mediated ADCC.

To further investigate if soluble bacterial components are the responsible mediators for neutrophil activation and whether neutrophil response changes at lower concentrations, *ClearColi* and *E. coli* supernatants (dil. factor: $1/10^3$ and $1/10^2$) were added to 96-well plates to stimulate freshly isolated neutrophils directly in impedance-based ADCC assays that allow an intermediate term evaluation of neutrophil activation.

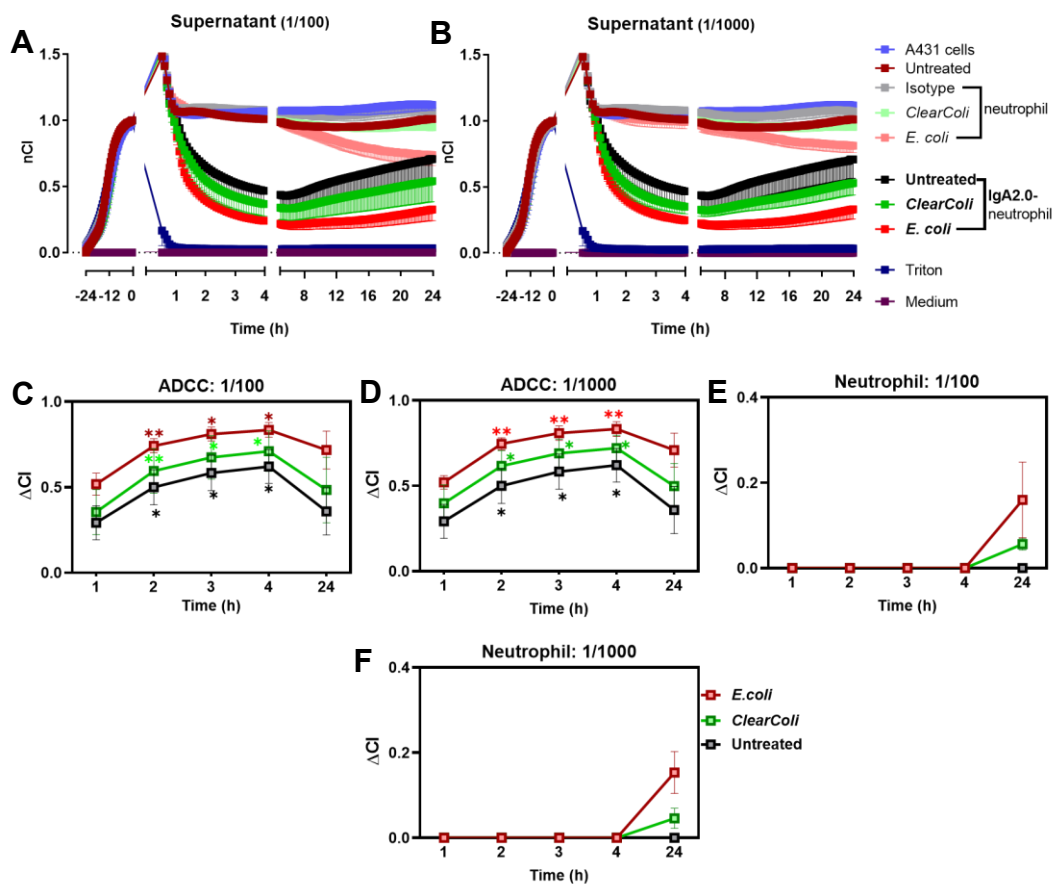


Figure 31 Both *E. coli* and *ClearColi* supernatants enhanced neutrophil activation for tumour-killing by ADCC. Target cells (A431) were seeded and incubated for 24 h in a 96-well E-plate. After confluence (high impedance), cells were treated with antibodies (EGFR-specific antibody IgA2.0) and neutrophils. Further, supernatants of *E. coli*/*ClearColi* were directly added to the ADCC (in 96-well E-plate). (C, D) The Delta cell index (ΔCI) was calculated as (isotype+ neutrophil)–(IgA2.0+neutrophil) of the respective conditions at 1, 2, 3, 4, and 24 h. (E, F) ΔCI = (neutrophil)–(neutrophil) with respective conditions. Measurement of the IBCA was evaluated after 24 h as Cell Index (CI), normalized to treatment time point (nCI). Data were illustrated as mean

with SEM of three independent experiments (A-B: n= at least 3, C-D: n=4, E-F: n=3). Significant differences were analyzed by two-way ANOVA with Dunnett's multiple comparisons test for each treated condition between 1 h with 2, 3, 4, and 24 h marked as *, and untreated (E-F: neutrophil, C-D: IgA2.0-neutrophil) with treated conditions (*E./ClearColi*) at each time points marked as #. The significance was illustrated as * (for Ctrl and treated conditions) and # (Between only treated conditions) and ns ($P > 0.05$), */# ($P \leq 0.05$), **/## ($P \leq 0.01$). Concentration/Control: bacterial supernatants (A: 1/100, B: 1/1000, $OD_{600}=1$), neutrophils ($4 \times 10^6/\text{ml}$), isotype (non-specific IgA standard, STD), positive (5 μl of 0.2% Triton), and negative (untreated A431 cells).

Surprisingly, supernatants of bacterial strains could increase neutrophils' ability to kill (IgA2.0) antibody-opsonized tumor cells for $1/10^2$ (Fig. 31A) and $1/10^3$ (Fig. 31B), and at similar levels for each condition. Moreover, *E. coli* (Red) supernatant was more powerful to enhance neutrophil activation to kill tumor cells (A431) than *ClearColi* (Green) in both dilution factors compared to untreated neutrophils (IgA2.0-neutrophil). After the direct stimulation by bacterial supernatants, antibody-engaged tumor cell killing by neutrophils could last for almost four hours, and then A431 cells started to grow again. Adding the supernatants of bacteria to neutrophils (without antibodies) could cause a cytotoxic impact on tumor cells after 24 h. However, *E. coli* supernatant (Fig. 31A-B) was regarded as more effective than *ClearColi* supernatant compared to neutrophils (untreated). *E. coli* supernatant may have improved cytotoxicity levels at 1/100 more than 1/1000 reached about 0.25 (Fig. 31A) and 0.20 (Fig. 31B) of normalized cell index (nCI=1), respectively. This resulted in tumor cell regression noted one-day incubation.

Delta Cell Index (ΔCI) was also evaluated at the selected time points (1, 2, 3, 4, and 24 h) from normalized cell index (nCI). Therefore, the chosen time points were after treatment with respective conditions (Fig. 31C-F), and the most effective time for effector cells. A time of 24 h can determine for how long neutrophils can kill tumor cells and whether any change occurs as shown by bacterial supernatants with only neutrophils. The result of ΔCI (Fig. 31C-F) showed almost the same enhancement in nCI (Fig. 31A-B) in ADCC. Bacterial supernatant (Fig. 31C) showed significant differences for untreated neutrophils: 1 vs. 2 ($p=0.0163$), 1 vs. 3 ($p=0.0246$) and 1 vs. 4 ($p=0.0330$), for *E. coli*-treated neutrophils: 1 vs. 2 ($p=0.0091$), 1 vs. 3 ($p=0.0204$), and 1 vs. 4 ($p=0.0343$), and for *ClearColi*-treated neutrophils: 1 vs. 2 ($p=0.0045$), 1 vs. 3 ($p=0.0128$), and 1 vs. 4 ($p=0.0257$). Bacterial supernatant (Fig. 31D) had significant differences for untreated neutrophils: 1 vs. 2 ($p=0.0163$), 1 vs. 3 ($p=0.0246$) and 1 vs. 4 ($p=0.0330$), for *ClearColi*-treated neutrophils: 1 vs. 2 ($p=0.0134$), 1 vs. 3 ($p=0.0286$) and 1 vs. 4 ($p=0.0438$) and for *E. coli*-treated neutrophils: 1 vs. 2 ($p=0.003$), 1 vs. 3 ($p=0.0043$) and 1 vs. 4 ($p=0.0052$). Furthermore, bacterial supernatants stimulated neutrophils (without antibody)

after 24 h showed cytotoxicity strongly observed (Fig. 31E-F) with *E. coli* more than *ClearColi* supernatants representing about 0.18 and 0.5 of ΔCI at 1/100 and 1/1000, respectively.

The toxic effect may stem from the capacity of neutrophils to produce ROS, and inflammatory cytokines shown in various research studies. Also, a recent study demonstrated that LPS inoculation into rat tumors led to the triggering and chemoattraction of neutrophils to the tumor microenvironment, resulting in full restriction of the tumor [154]. Thus, the result indicates bacterial supernatants could activate neutrophils (with and without IgA2.0 presence). Furthermore, the effect of *ClearColi* supernatant is more evident in the case of antibody-opsonized tumors (A431 cells).

3.5 Bacteria-conditioned supernatants have similar activation levels of neutrophil FPR1 and similar LPS concentration.

N-formyl peptides from bacteria or mitochondria are signatures recognized by immune cells as pathogen-associated molecular patterns (PAMPs) or damage-associated molecular patterns (DAMPs). Proteins or peptides, having formylated N-terminus, can activate FPRs and initiate inflammation [155, 156]. Therefore, to determine the origin of the difference in activation levels between *ClearColi* and *E. coli* supernatants, we had to measure the activation of FPRs on human-isolated neutrophils. FPRs engage in the G-protein-coupled receptors (GPCRs) family. They are expressed in innate immunity, mainly neutrophils and monocytes, and defend against pathogens. FPR1, 2, and 3 are expressed in humans and can recognize formylated peptides (FPs) broken down by bacteria (like *E. coli*), host cells, or various agonists. FPs include ligands such as *N*-formylated, bacterial, or viral unmodified peptides, peptides from host-endogenous mitochondria, and non-peptide agonists, such as resolvin D1 and lipoxin A4 [157-159]. Thus, we investigated both bacterial supernatants with neutrophils by calcium imaging assay, where ligand activation of FPR leads to the mobilization of intracellular calcium signaling.

To confirm our results by cross-checking, two FPR-expressing model cells and gene-transfected cells for FPR-expressing in addition to neutrophils were applied for our experiments. In research, the human leukemia cell line (HL-60, Fig. 32A) is used as an alternative cell to primary neutrophils and can get neutrophil functional characters after differentiation [160]. Furthermore, the human glioblastoma cell line (U-87, Fig. 32B) expressing FPR can recognize and respond to fMLF by chemotaxis, proliferation, and cytokine production, such as VEGF [157]. Human embryonic kidney cells (HEK293, Fig. 32C) were transfected to express FPR. HEK293 cell line is considered a general cell line applied in considerable research to study G protein-coupled receptors (GPCRs) [161].

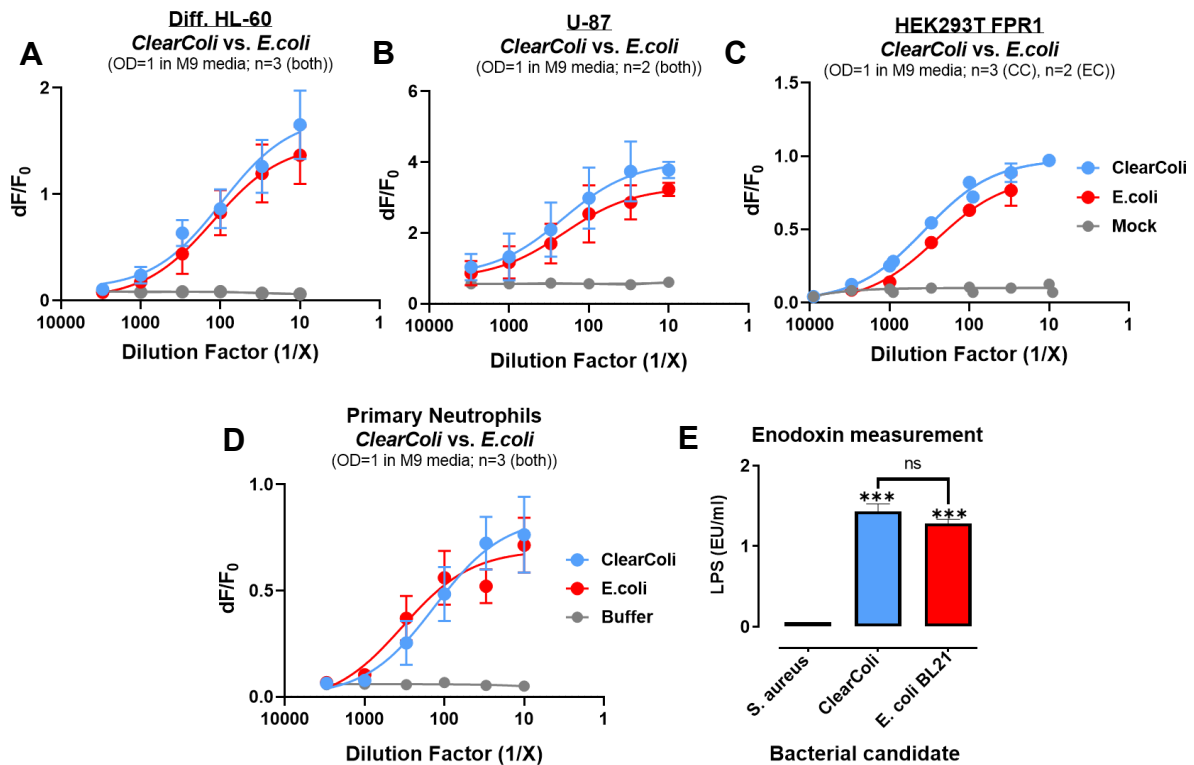


Figure 32 Potential activation in neutrophils is independent of Formyl peptides. (A) Measurement of LPS. (B-E) Calcium imaging. LAL assay evaluated LPS concentration in *E. coli* and *ClearColi* supernatants (n=3). Calcium assay was performed for activation level investigation in neutrophils stimulated by *E. coli* and *ClearColi* supernatants. Data were illustrated as mean with SEM (A, D) and SD (E). Significant differences were analyzed, in which a paired one-way ANOVA with (A, D) a paired one-way ANOVA with a test for Trend investigated between *ClearColi* and *E. coli* with p-value summary (*) for HL-60 and neutrophils and (E) Tukey's multiple comparison tests of negative control (*S. aureus*) and treated ones or between only treated ones (*ClearColi* and *E. coli*). The significant differences were described as * (for Ctrl and treated conditions) and # (between only treated conditions). GraphPad Prism 8.0.2 [ns (P > 0.05), */# (P ≤ 0.05), **/## (P ≤ 0.01), ***/### (P ≤ 0.001)]. Results of (A) and (B-D) were done by Markus Bischoff and AG Bernd Bufo, respectively. Concentration/Control: bacterial supernatants (indicated in results, OD₆₀₀=1), neutrophils (4 × 10⁶ /ml), and negative (Buffer, Mock).

Primary neutrophils (Fig. 32D) in addition to HL-60 and U-87 (Fig. 32A, B) can express naturally FPR [162]. Bacterial signal peptides are N-terminal proteins binding to native proteins such as formyl-methionine. These peptides direct protein transfer through the plasma membrane [162]. Because of cleavage formyl-methionine, the first amino acid released by bacterial protein biosynthesis, all bacteria can release formylated peptides such as N-terminal peptides [163], detected by FPR [159]. Therefore, the equal FPR activation by Ca²⁺ flux assays in the results shown (Fig. 32A-D) did not reflect the functional read-outs. The significant differences were evaluated for HL-60 (p=0.0171) and neutrophils (p=0.0384). Thus, this made

us exclude formyl peptides and pay attention to focus on lipopolysaccharides (LPS). Therefore, LPS secretion levels of both supernatants were measured using an LAL assay to determine Endotoxin units. Surprisingly, both *ClearColi* and *E. coli* supernatants had similar levels of LPS secretion (Fig. 32E). Data was significant between *S. aureus* with *ClearColi* ($p=0.0002$) and *E. coli* ($p=0.0003$). The question came to our mind whether *ClearColi* and *E. coli* supernatants have similar FPR activation levels and similar LPS concentrations, why do they have differences in activation and degranulation levels of neutrophil in addition to enhanced tumor cell killing via *E. coli* than *ClearColi* supernatants?

E. coli has six acyl chains in LPS, which can elicit the complex of toll-like receptor 4 (hTLR4) and myeloid differentiation factor-2 (MD-2) in humans, leading to the release of cytokines. So, *ClearColi* was genetically modified to secrete LPS, which does not trigger the immune response. The modification process included the removal of seven genes such as ΔgutQ , ΔkdsD , ΔlpxL , ΔlpxM , ΔpagP , ΔlpxP , and ΔeptA and thus the removal of carbohydrates binding to LPS. Furthermore, one gene (*msbA148*) was mutated to make bacteria live with the existence of lipid IVA. IVA lipid is a precursor of LPS biosynthesis and loses two secondary acyl chains of hexa-acylated LPS presenting in *E. coli*. Therefore, the IVA lipid of *ClearColi* cannot trigger an immune response [164]. We hypothesized that while the concentration seems rather the same there is a qualitative difference with the mutLPS from *ClearColi* displaying a reduced competence to activate neutrophils via TLR4 signaling.

3.6 LPS increases neutrophil degranulation and activity for tumor cell-killing.

E. coli has about 2×10^6 LPS molecules/ cell, representing 30% of the total outer membrane weight [164]. In addition, traces of LPS can activate neutrophils [165]. To determine if LPS concentrations can close the difference in the activation level between *E. coli* and *ClearColi* supernatants. Further, what are the consequences if we add more LPS concentration to neutrophils? So, we calculated the Endotoxin unit (EU) in *E. coli* BL21(natural) and *ClearColi* (genetically modified) indicated and estimated by approximately 1.25 EU/ml (Fig. 32E) for both strains. 1/100 of these concentrations were used in previous results (zymogram and ADCC assays) which represent 0.0125 EU/ml. In the same way, we adjusted the purified LPS (500×10^3 EU/mg, *Salmonella enterica Typhimurium*, Sigma–Aldrich) to the final concentration of 1.25 EU/ml. Then, a dilution factor of 1/100 was used with the final concentration of 0.0125 EU/ml to compare the new results with previous ones. Additionally, to determine whether 0.0125 EU/ml is enough to induce the maximum activation level in neutrophils, we used a higher concentration: 0.025 and 0.05 EU/ml.

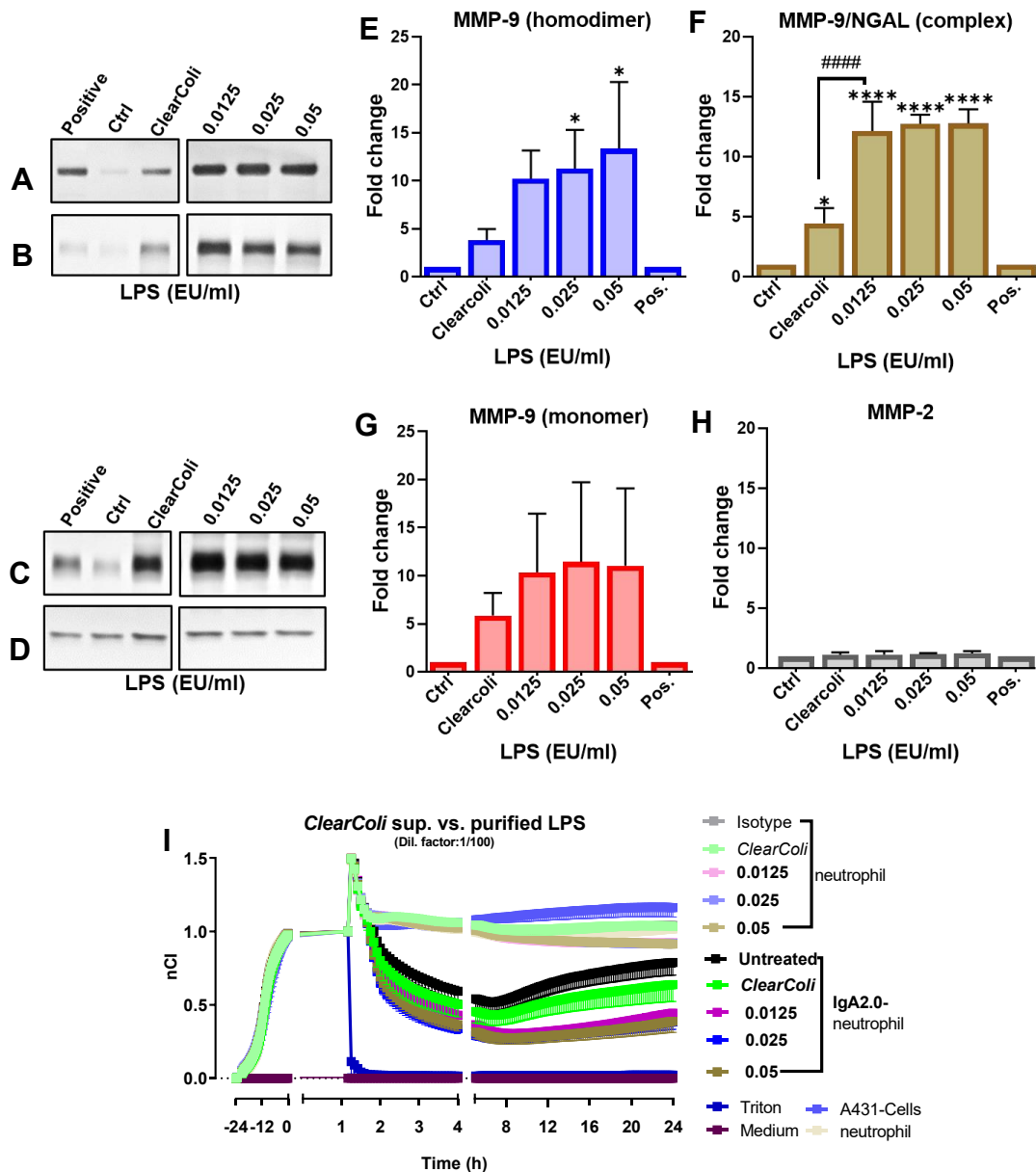


Figure 33 Purified LPS showed neutrophil activation and enhanced ADCC compared to un-purified LPS (*ClearColi* supernatant). (A-D) Zymogram gel. (E-H) Data analysis of LPS effect in different concentrations on neutrophil degranulation. Neutrophils were co-cultured with *ClearColi* supernatants and incubated at 37 °C with the respective concentrations in a 24-well plate. After 1 h, supernatants were collected and used in zymography. (I) Direct stimulation of ADCC by LPS concentrations. The respective concentrations were applied to stimulate neutrophils in the ADCC assay for at least 24 h. Data were illustrated as mean with SD (A-D, n=3), and SEM (E-H, n=at least 4). Significant differences were analyzed using GraphPad prism, in which a paired one-way ANOVA with Tukey's multiple comparison tests of untreated conditions (Ctrl) with treated ones (*ClearColi* and LPS). The significance was illustrated as * (for Ctrl with treated conditions) and # (*ClearColi* and LPS), in which ns ($P > 0.05$) */# ($P \leq 0.05$), ****/##### ($P \leq 0.0001$). Concentration/control: Bacterial supernatants (1/100, OD₆₀₀=1), isotype (non-specific IgA standard, STD), positive (5 μ l of 0.2% Triton), negative (untreated A431 cells), neutrophils (4 x 10⁶/ml), LPS (EU/ml), positive (Pos., supernatant of CXCL-8-stimulated neutrophils).

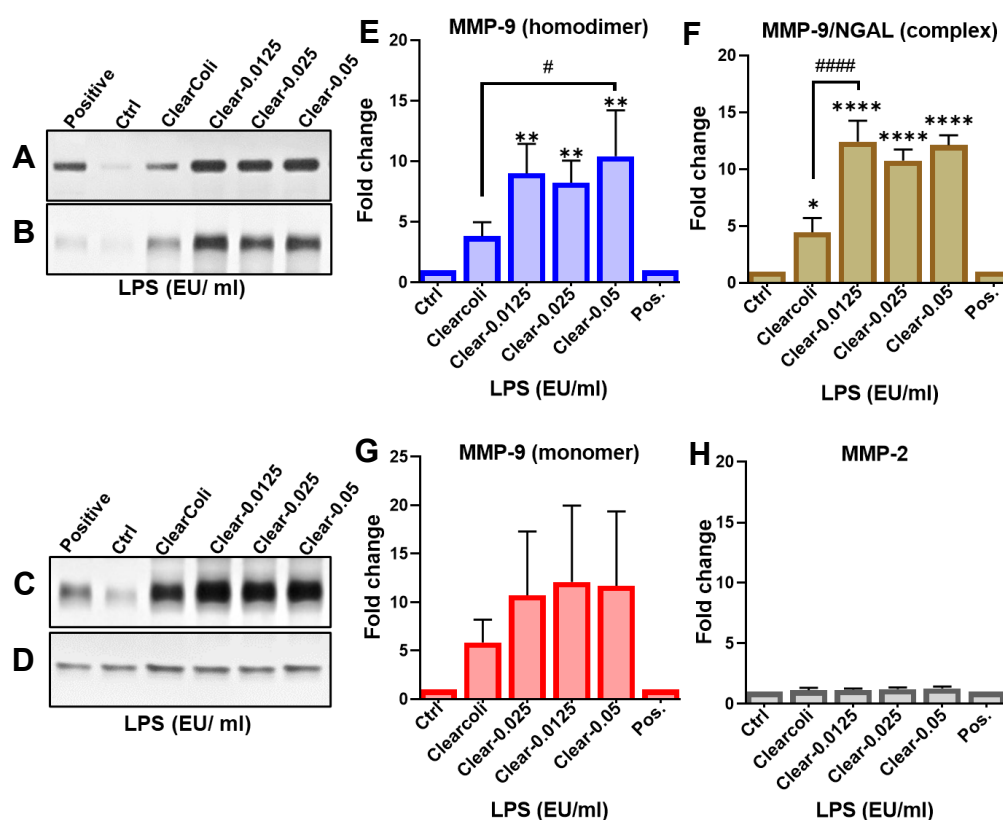
The incubation of neutrophils with purified LPS led to raised activation and degranulation levels. In comparison of untreated neutrophils (Ctrl), *ClearColi* and LPS concentrations of 0.0125, 0.025, and 0.05 EU/ml induced each MMP form, respectively, as follows: (Fig. 33E) homodimer folds were approximately 3.8 (\pm 1.16), 10.2 (\pm 2.9), 11.27 (\pm 4), 13.3 (\pm 6.9)-fold, (Fig. 33F) complex levels reached about 4.45 (\pm 1.25), 12.13 (\pm 2.4), 12.7 (\pm 0.74), 12.77 (\pm 1.16)-fold. Further, the levels of monomer (Fig. 33G) were about 5.86 (\pm 2.3), 10.35 (\pm 6), 11.43 (\pm 8), and 11 (\pm 8)-fold. However, there was no change in MMP-2 level (Fig. 33H). Significant differences were observed with bacterial supernatant and LPS concentration in homodimer (Fig. 33E): Ctrl vs. 2.5 ($p=0.0348$), Ctrl vs. 5 ($p=0.0102$) and complex (Fig. 33E): Ctrl vs. *ClearColi* (0.0485), Ctrl vs. 1.25 ($p<0.0001$), Ctrl vs. 2.5 ($p<0.0001$), Ctrl vs. 5 ($p<0.0001$), *ClearColi* vs. 1.25 ($p<0.0001$), *ClearColi* vs. 2.5 ($p<0.0001$) and *ClearColi* vs. 5 ($p<0.0001$). Further, the capacity of neutrophils in ADCC increased (Fig. 33I) with the three concentrations of LPS at similar levels compared to neutrophils with/without *ClearColi*. So, the results ensure the effect of *ClearColi* supernatants activating neutrophils showed in previous results and demonstrate that relatively 0.0125 EU/ml was already enough to fully activate neutrophils at a concentration of 4×10^6 cells/ml.

3.7 LPS enhances the neutrophil-activating capacity of *ClearColi*.

LPS alone could elevate neutrophil capacity in ADCC and MMP release (Fig. 33). The question was, does the supplementation of LPS to the *ClearColi* conditioned media increase the capacity to activate neutrophils? In the same way in the previous experiment, LPS traces (0.0125, 0.025, and 0.05 EU/ml) were added to *ClearColi* supernatant to simulate neutrophils for 60 min in or directly in ADCC and compared with *ClearColi* (alone) and untreated neutrophil. Adding LPS concentrations increased the level of MMP release. Homodimer (Fig. 34E) elevated to approximately 3.8 (\pm 1.16), 9 (\pm 2.4), 8.2 (\pm 1.8), and 10.4 (\pm 3.79)-fold, and complex levels (Fig. 34F) reached about 4.4 (\pm 1.25), 12.4 (\pm 1.8), 10.7 (\pm 0.9), and 12 (\pm 0.87)-fold. Further, the levels of monomers (Fig. 34G) were estimated to be about 5.86 (\pm 2.34), 12 (\pm 7.8), 10.7 (\pm 6.59), and 11.7 (\pm 7.6)-fold. All MMP folds were estimated respectively for *ClearColi*, without and with 0.0125, 0.025, and 0.05 EU/ (LPS), in comparison to untreated neutrophils (Ctrl). However, there was no change in MMP-2 level (Fig. 34H). Significant differences were evaluated in homodimer (Fig. 34E): Ctrl vs. *ClearColi*-1.25 ($p=0.0044$), Ctrl vs. *ClearColi*-2.5 ($p=0.0096$), Ctrl vs. *ClearColi*- 5 ($p=0.0011$) and *ClearColi* vs. *ClearColi*-5 ($p=0.0179$) and complex (Fig. 34E): Ctrl vs. *ClearColi* ($p=0.0165$), Ctrl vs. *ClearColi*-1.25 ($p<0.0001$), Ctrl vs. *ClearColi*-2.5 ($p<0.0001$), Ctrl vs. *ClearColi*-5 ($p<0.0001$), *ClearColi* vs. *ClearColi*-1.25

($p < 0.0001$), *ClearColi* vs. *ClearColi*-2.5 ($p = 0.0001$), and *ClearColi* vs. *ClearColi*-5 ($p < 0.0001$).

Additionally, 0.0125 EU/ml enhanced killing IgA2.0-opsonized tumor cells in comparison to IgA2.0-neutrophils without (untreated) and with *ClearColi* (treated) in ADCC assay (Fig. 34E). The other two concentrations of purified LPS (0.025, 0.05 EU/ml) did not affect the level of MMP release but slightly raised the ADCC. Surprisingly, all concentrations after the first four hours of treatment reached a similar level of tumor cell killing by neutrophils. The results from zymography are not translated into the functional assays, indicating that MMPs are not critical for ADCC and reflecting that neutrophils kill tumor cells via trogoptosis requiring integrin interactions [235].



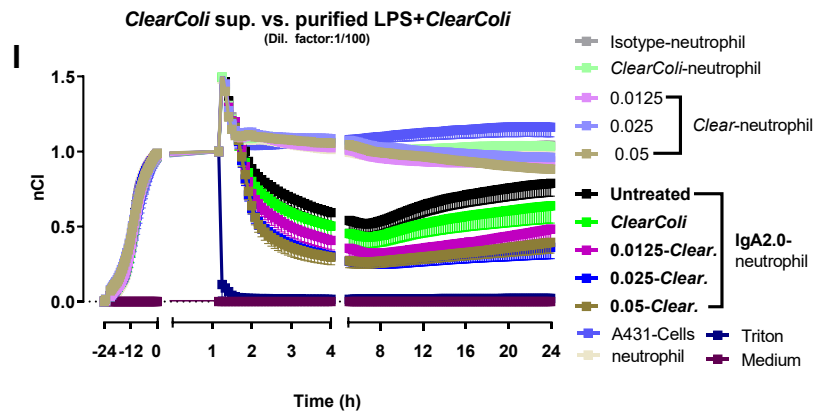


Figure 34I Adding LPS to *ClearColi* supernatant increases MMPs release and efficacy of IgA2.0 to engage neutrophils for ADCC. LPS in different concentrations with/out *ClearColi* supernatant were incubated with neutrophils at 37 °C for 1 h. (A-D) Zymogram gel. (E-H) Degranulation marked by MMP release was analyzed by zymograms. (I) Direct stimulation of neutrophils with the indicated conditions was performed in impedance-based ADCC assays. Data were illustrated as mean with SD (E-H) and SEM (I) of three independent experiments (E-H: n=3, I: at least n=3). Significant differences were analyzed using GraphPad prism, in which a paired one-way ANOVA with Tukey's multiple comparison tests of untreated conditions (Ctrl) with treated ones (*ClearColi* w/out LPS). The significance was illustrated as *(for Ctrl with treated conditions) and # (Between only treated conditions), in which ns ($P > 0.05$), */# ($P \leq 0.05$), **/## ($P \leq 0.01$), ****/#### ($P \leq 0.0001$). Concentration/control/Abb.: bacterial supernatants (1/100, $OD_{600}=1$), Isotype (non-specific IgA standard, STD), positive (5 μ l of 0.2% Triton), negative (untreated A431 cells), neutrophils (4×10^6 /ml), LPS (EU/ml), positive (Pos., supernatant of CXCL-8-stimulated neutrophils), Clear. (*ClearColi*).

3.8 Endotoxin LPS is the essential effector in neutrophil activation by TLR.

The previous result from *E. coli* supernatants had a higher effect than *ClearColi* supernatants. Side-by-side, the addition of LPS alone or with *ClearColi* supernatants to neutrophils had similar enhanced levels of degranulation and ADCC. Therefore, to determine if the differences in activation levels originate from LPS that was higher in *E. coli* supernatant than *ClearColi*. Using the previous condition, neutrophils were incubated with *E. coli* supernatant (dil. factor: 1/100=0.0125 EU/m) with purified LPS (0.0125 E/ml) alone and LPS added to *ClearColi* supernatant (0.125-Clear.) and compared to only *ClearColi* (alternative Ctrl).

Interestingly, LPS w/out *ClearColi* supernatant could raise activation and degranulation levels in the release of all MMPs (Fig. 35E-G) in neutrophils. All MMP folds were estimated respectively for *ClearColi*, *E. coli*, Clear-LPS (0.0125 EU/ml) and LPS (0.0125 EU/ml) as follows: Homodimer (Fig. 35E) $2.9 (\pm 2.4)$, $6 (\pm 4.3)$, $6 (\pm 4)$, $5.58 (\pm 3.8)$ -fold, complex (Fig. 35F) $3.69 (\pm 3.39)$, $9.8 (\pm 8.9)$, $9.7 (\pm 8)$ and $9.38 (\pm 8.4)$ -fold as well as monomer (Fig. 35G) 4.3 ± 2 , $9.78 (\pm 5)$, $9.55 (\pm 4.5)$, and $9.49 (\pm 5.6)$ -fold compared to untreated neutrophils (Ctrl). Further, MMP-2 (Fig. 35H) had no change.

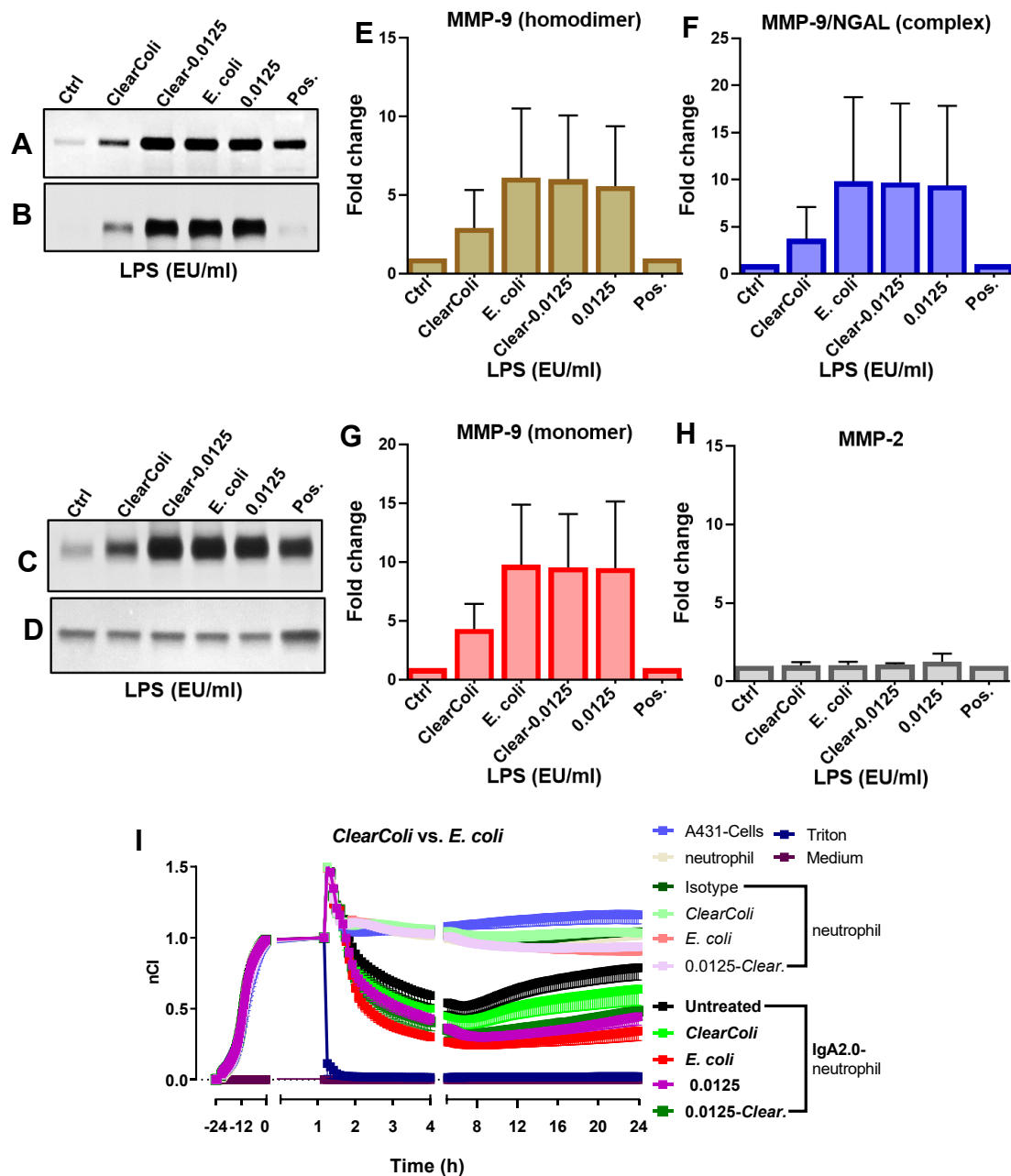


Figure 35I Potential activation in neutrophils possibly relies on TLRs stimulated by LPS. *E. coli*, LPS, and *ClearColi* supernatant w/out LPS were incubated at 37 °C for 1 h with neutrophils. Then, using (A-D) zymography, degranulation level was measured by (E-G) analysis of MMP release. (I) Direct stimulation of neutrophils with the previous conditions was used in impedance-based ADCC assays. Data were illustrated as mean with SD (E-G) and mean with SEM (I). Significant differences were analyzed using GraphPad prism, in which a paired one-way ANOVA with Tukey's multiple comparison tests of untreated conditions (Ctrl) with treated ones (*ClearColi* w/out LPS). The significance was illustrated as * (for Ctrl with treated conditions) and # (Between only treated conditions), in which ns ($P > 0.05$). Concentration/control/Abb.: bacterial supernatants (1/100, $OD_{600}=1$), isotype (non-specific IgA standard, STD), positive (5 μ l of 0.2% Triton), negative (untreated A431 cells), neutrophils (4×10^6 /ml), LPS (EU/ml), positive (Pos., supernatant of CXCL-8-stimulated neutrophils), Clear. (*ClearColi* supernatant).

Furthermore, LPS enhanced ADCC (Fig. 35I) to the level of *E. coli* and purified LPS with a concentration of 0.0125 EU/ml. Rather, the activation of TLR4 seems critical for *E. coli*-based LTMs, causing a more prominent activation of neutrophils.

For further analysis, the Delta Cell Index (ΔCI) was evaluated at the most effective time points; 1, 2, 3, 4, and 24 h. ΔCI from nCI=1 (Fig. 33-35) of treated antibody-neutrophils (ADCC) was shown in (Fig. 36A-E) and treated neutrophils (no antibody, cytotoxicity) were shown in (Fig. 36F, G).

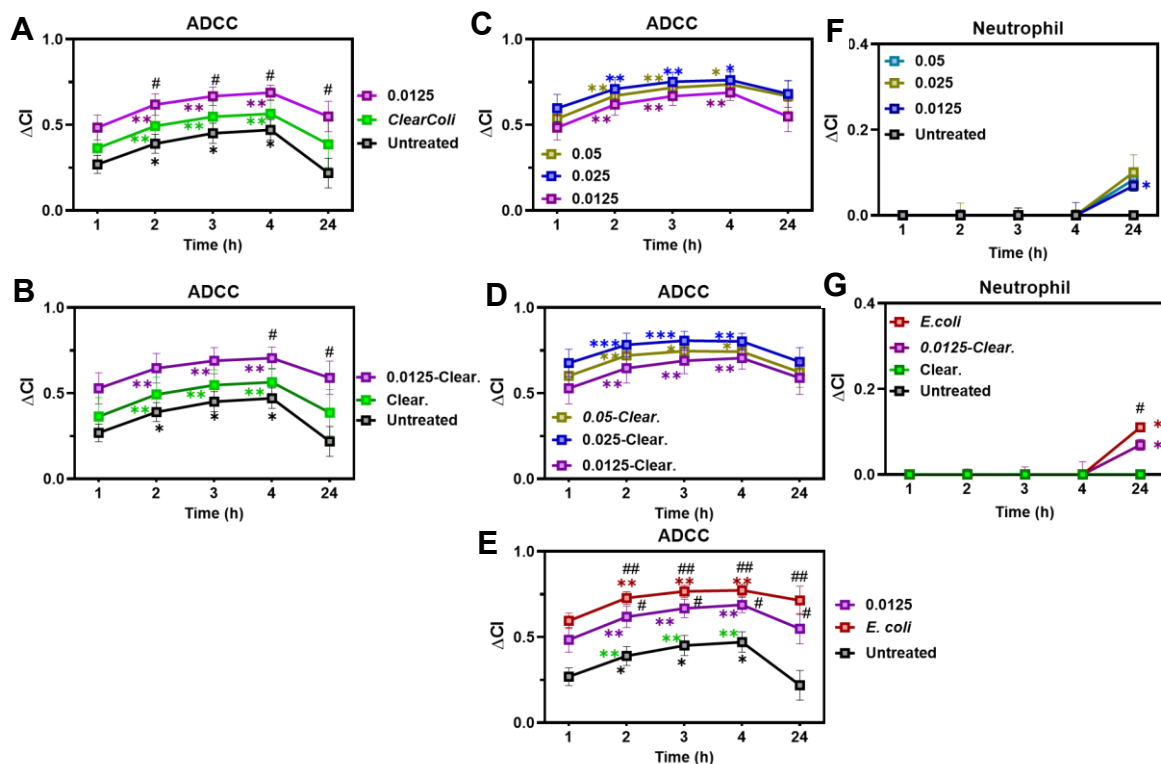


Figure 36I Delta cell index and cytotoxic effect of neutrophils. (A-D, G) ΔCI was evaluated as isotype control (+ neutrophil) - IgA2.0 (+neutrophil) of the respective conditions at 1, 2, 3, 4, and 24 h. Data were illustrated as mean with SEM of three independent experiments (n=3 for 0-0). (E, F) ΔCI = neutrophil- neutrophil with respective conditions. Significant differences were analyzed by two-way ANOVA with Dunnett's multiple comparisons test for each treated condition at 1 h with 2, 3, 4, and 24 h marked as*, and untreated (IgA2.0-neutrophil) with treated conditions (*ClearColi* W/out LPS or LPS concentrations) at each time points marked as #. Abbreviation: ADCC (IgA2.0-neutrophils), Clear. (*ClearColi* supernatant), LPS (EU/ml)

Adding LPS (0.0125) to neutrophils (0.0125, Fig. 36A) or in the presence of *ClearColi* (0.0125-Clear, Fig. 36B) showed significant enhancement in ADCC. P-values were calculated (Table 6) compared to 1 h (Ctrl) with the other time points/each condition. It was also evaluated between untreated neutrophils (Ctrl) with treated conditions/at each time point (1-24 h). Each

condition alone improved tumor killing at a time of 2-4 h compared to 1 h but reduced at 24 h. Moreover, treatment of neutrophils with LPS in the presence or absence of *ClearColi* supernatant was more effective than only *ClearColi*, where the significance appeared at 1 to 24 h (Table 6. A) and 2 and 24 h (Table 6. B) compared to Ctrl.

Table 6: P-values (Fig. 36A, B). *ClearColi* (Clear.) without (out)/with (W) LPS (EU/ml)

Time (h)	A B		A B		A B	
	Untreated		<i>Clear.</i>	<i>Clear.</i>	0.0125	0.0125- <i>Clear.</i>
1 vs. 2	0.0272	0.0165	0.0134	0.0076	0.0059	0.0043
1 vs. 3	0.0194	0.0117	0.0123	0.0070	0.0063	0.0032
1 vs. 4	0.0211	0.0127	0.0146	0.0083	0.0108	0.0079
2	Untreated Vs.		----	----	0.0410	----
3	Untreated Vs.		----	----	0.0423	----
4	Untreated Vs.		----	----	0.0349	0.0449
24	Untreated Vs.		----	----	0.0474	0.0342

Treatment (Fig. 36C) of neutrophils with a high concentration (conc.) of LPS (0.025 and 0.05 EU/ml) showed slight enhancement in ADCC compared to the basic LPS Conc. (0.0125 EU/ml). There are no significant differences even in the presence of *ClearColi* supernatant (Fig. 36D) between the high conc. with the basic conc. However, p-value significance (Table 7) appeared between 1h compared to 2, 3 and 4 h/each conc.

Table 7: P-values (Fig. 36C, B). Different concentrations of LPS (EU/ml) without (Out)/with (W) *ClearColi* (Clear.).

Time (h)	LPS: 0.0125		LPS: 0.025		LPS: 0.05	
	Out	W	Out	W	Out	W
1 vs. 2	0.0033	0.0043	0.0040	0.0018	0.0004	0.0007
1 vs. 3	0.0036	0.0032	0.0063	0.0109	0.0007	0.0004
1 vs. 4	0.0061	0.0079	0.0162	0.0427	0.0014	0.0023

Treatment of neutrophils with LPS (0.0125 EU/ml) and *E. coli* supernatant caused a significantly increased activation during ADCC. P-values (Table 8) were generated from the calculated Δ CI (Fig. 36E) and compared 1 h (Ctrl) to other time points/each condition. Further, it was also evaluated between untreated neutrophils (Ctrl) with treated conditions/at each time point. However, there are no significant differences between *E. coli* and LPS.

Table 8: P-values (Fig. 36E). Significant values of LPS (EU/ml) and *E. coli*.

Time (h)	Untreated	0.0125 EU/ml	<i>E. coli</i>
1 vs. 2	0.0165	0.0033	0.0014
1 vs. 3	0.0117	0.0036	0.0015
1 vs. 4	0.0127	0.0061	0.0023
1	Untreated Vs.	--	0.0022
2	// Vs.	0.0410	0.0024
3	// Vs.	0.0423	0.0048
4	// Vs.	0.0349	0.0065
24	// Vs.	0.0474	0.0051

Finally, adding LPS conc. (Fig. 36F) to only neutrophils (without ab) increased their cytotoxicity at similar levels of 0.0125, 0.025 and 0.05 E/ml. A different significance was noted for 1.25-neutrophils: 1 vs. 24 ($p=0.0340$). Likely, cytotoxicity (Fig. 36G) increased strongly in *ClearColi* with LPS and *E. coli* with significant differences in neutrophil vs. *E. coli*-neutrophil at 1 vs. 24 ($p=0.0138$), 1.25-*ClearColi* neutrophil at 1 vs. 24 ($p=0.0340$) and neutrophil vs. *E. coli*-neutrophil at 24 h ($p=0.0136$). The result indicates that bacterial supernatants can activate neutrophils alone or with IgA2.0 presence. Furthermore, the effect of LPS at 0.0125 EU/ml activates in a similar level of *E. coli* supernatant originating from LPS.

To ensure that *ClearColi* could activate neutrophils, the incubation time was prolonged to check the release of MMPs. An increase in time points led to a rise in MMP release for *ClearColi* at 1, 2, and 4 h. Homodimer (Fig. 37E) was evaluated as 1.13 (± 0.16), 1.54 (± 0.22), and 1.7 (± 0.33)-fold with significant differences for Ctrl vs. *ClearColi* at 2 h ($p=0.0238$) and Ctrl vs. *ClearColi* at 4 h ($p=0.0031$). The complex (Fig. 37F) was 1 (± 0.23), 1.55 (± 0.4), and 1.56 (± 0.44)-fold at the same time points, respectively. Further, the monomer (Fig. 37G) was 1.46 (± 0.3), 1.76 (± 0.5), and 1.69 (± 0.28)-fold with a significant difference for Ctrl vs. *ClearColi* at 2 h ($p=0.0414$). Furthermore, there is no change in MMP2 (Fig. 37H) levels.

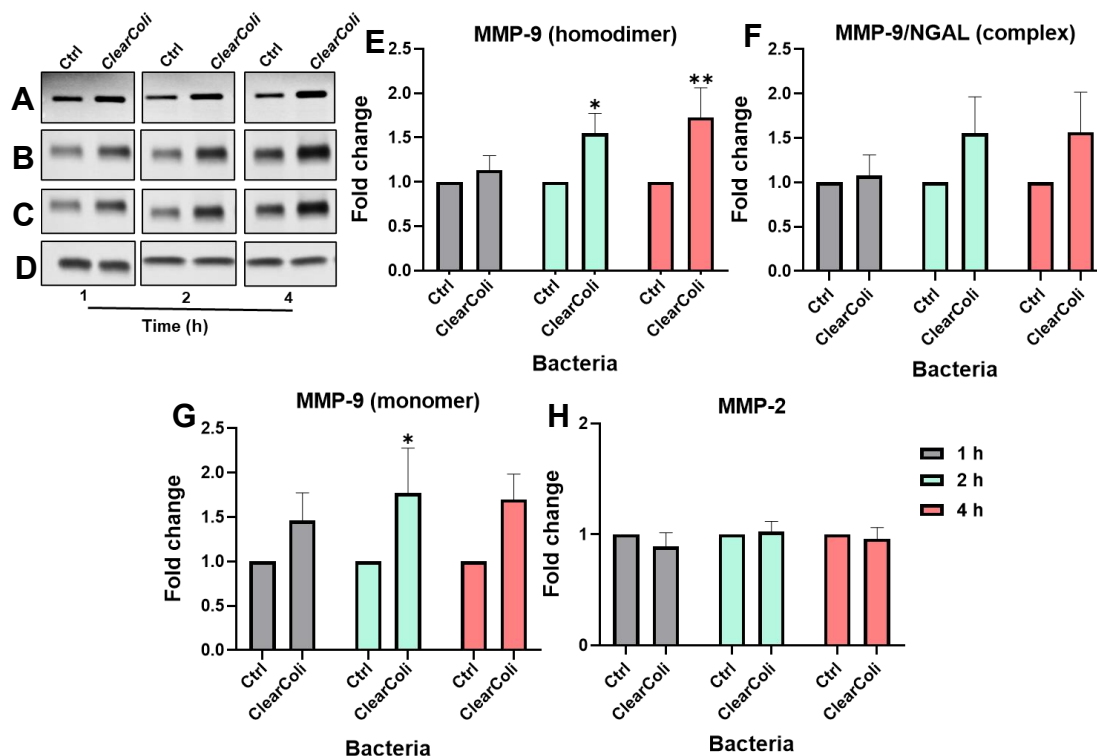


Figure 37 Prolonged incubation of *ClearColi* supernatant may increase neutrophil MMP release. *ClearColi* supernatants were incubated with neutrophils at 37 °C for 1, 2, and 4 h. (A–D) Zymogram gel. (E–H) Degranulation marked by MMP release was analyzed. Data were illustrated as mean with SD (E–H: n=3) of three independent experiments. Significant differences were analyzed using GraphPad prism, in which a paired two-way ANOVA with Tukey’s multiple comparison tests of untreated conditions (Ctrl) with treated ones (*ClearColi*) for each hour. The significance was illustrated as * (for Ctrl with treated conditions) and # (*ClearColi* at 1 h with 2 and 4 h), in which ns ($P > 0.05$) */# ($P \leq 0.05$), **/### ($P \leq 0.01$). Concentration/control/Abb.: bacterial supernatants (1/100, OD₆₀₀=1), neutrophils (4×10^6 cells/ml).

To verify the previous results of neutrophil activation through degranulation levels, CXCL-8 (Fig. 38) was estimated for all conditions to determine cytokine secretion. Adding purified LPS of 0.0125 EU/ml to *ClearColi* supernatant enhanced CXCL-8 secretion to almost the level of *E. coli* supernatant compared to *ClearColi* supernatant alone, ensuring that LPS in *E. coli*, but *ClearColi*, the effective mediator of neutrophil activation. However, doubling the concentration of LPS (0.025 and 0.05 EU/ml) with or without *ClearColi* supernatant led to various responses of neutrophils, resulting in different concentrations of CXCL-8. Measurement of CXCL-8 was determined in pg/ml as follows: 11.25 ± 8.5 (Ctrl), 506 ± 201 (*E. coli*), 226 ± 190 (*ClearColi*), 432.8 ± 165 (*ClearColi*-0.0125), 303 ± 158 (0.0125 EU/ml), 1057 ± 485 (*ClearColi*-0.025), 977 ± 399 (*ClearColi*-0.05), 1208 ± 840 (0.025 EU/ml) and 774 ± 331 (0.05 EU/ml). Significant

differences were found between Ctrl vs. Clear-0.025 ($p=0.0227$), Ctrl vs. Clear-0.05 ($p=0.0385$), and Ctrl vs. 0.025 ($p=0.0082$).

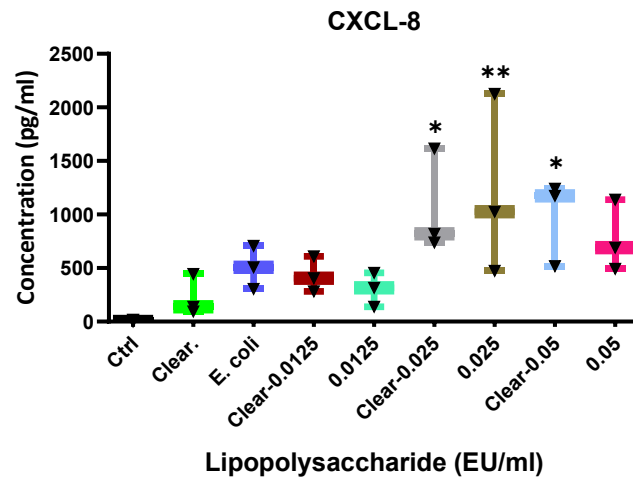


Figure 38I Different doses of LPS enhance neutrophil response to *ClearColi*. Cytokine (CXCL-8) was estimated to use ELIZA for *E. coli* and *ClearColi* w/out LPS at different concentrations. Data was shown as Min to Max. of three independent experiments ($n=3$). Significant differences were analyzed using GraphPad prism, in which a paired one-way ANOVA with Dunnett's multiple comparison test of control/*ClearColi* with treated ones. The significance was illustrated as * (for Ctrl with treated conditions) and # (*ClearColi* with treated conditions), in which ns ($P > 0.05$) */# ($P \leq 0.05$), **/## ($P \leq 0.01$). Concentration/control/Abb.: bacterial supernatants (1/100, OD₆₀₀=1), neutrophils (4×10^6 cell/ml), LPS (EU/ml), positive (Pos., supernatant of CXCL-8-stimulated neutrophils), Clear. (*ClearColi*).

3.9 LPS secreted-trans hydrogel is the main effector of neutrophil activity.

Our investigation for *E. coli*, *ClearColi*, and the bacterial supernatants proved that Lipopolysaccharides are effective stimulators in neutrophil activity. Therefore, we decided to test the whole biomaterial system (LTM) including hydrogel and bacteria-encapsulated hydrogel. Hence, the encapsulated bacteria, non-producers of any proteins, were used. MMPs were evaluated for homodimer (Fig. 39E): 1.54 (± 1.23), 2.4 (± 2) and 3 (± 3.2)-fold, for complex (Fig. 39F): 1.19 (± 0.8), 1.95 (± 1.49), 2.66 (± 2.98)-fold, and for monomer (Fig. 39G): 1.33 (± 0.79), 2 (± 1.22), and 2.18 (± 1.64)-fold for gel, *ClearColi*-gel, and *E. coli*-gel respectively, compared to control. The gel induced a slight MMP release. However, *E. coli* and *ClearColi* involved in hydrogel enhanced MMPs without significant differences compared to Ctrl and gel. Furthermore, there was no change in MMP-2 folds.

Using ELISA, (Fig. 39I) we could also determine CXCL-8 concentrations to prove neutrophil immunogenic activity differently. The average CXCL-8 concentration was measured for unstimulated neutrophils, Ctrl, (304.8 ± 232.6 pg/ml) and gel (232.35 ± 200.7 pg/ml). Further,

there was an increase in CXCL-8 with *Clear-gel* (651.9 ± 155.6 pg/ml) and *E. coli-gel* (1030 ± 378 pg/ml) compared to Ctrl. Although there were various responses between donors, the data was significant in the case of Ctrl vs. gel-*E. coli* ($p=0.0342$) and gel vs. gel-*E. coli* ($p=0.0212$). The results showed that PluDA hydrogel could decrease neutrophil MMPs by separating bacteria contact with neutrophils.

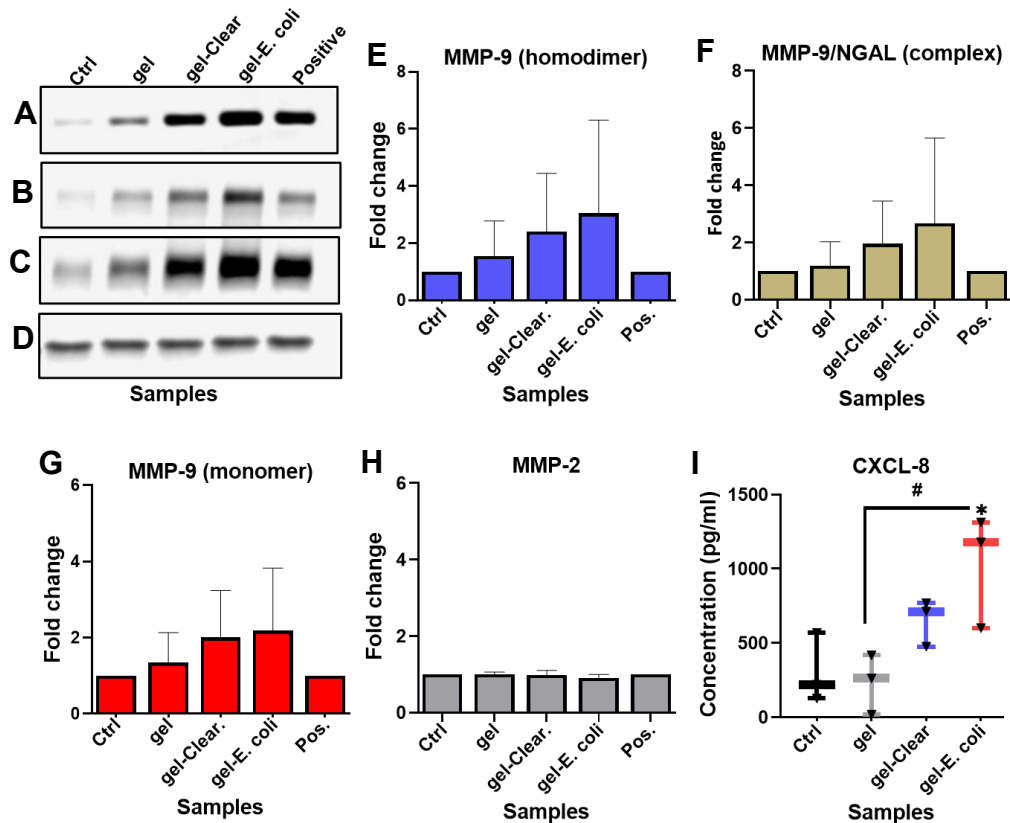


Figure 39 PluDA hydrogel (gel) may reduce neutrophil activation by monitoring soluble protein secretion. Gel w/out bacteria (*E. coli* and *ClearColi*) was incubated with neutrophils at 37 °C for 60 min in a 24-well plate. Supernatants collected after neutrophil stimulation were used in (A–D) the zymogram procedure for (E–H) MMP detection and ELISA for (I) CXCL-8 concentration measurement. Data were illustrated as mean with SD (E–H) and Min to Max. (I) of three independent experiments ($n=3$). Significant differences were analyzed using GraphPad prism, in which a paired one-way ANOVA with Tukey's multiple comparison tests of untreated conditions (Ctrl) with treated ones (gel w/out bacteria). The significance was illustrated as * (for Ctrl with treated conditions) and # (Between only treated conditions), in which ns ($P>0.05$) */# ($P\leq 0.05$). Concentration/control/Abb.: neutrophils (5×10^6 cells/ μ l), LPS (EU/ml), positive (Pos., supernatant of CXCL-8-stimulated neutrophils), Clear. (*ClearColi*), gel (PluDA 50% hydrogel).

3.10 Neutrophils respond to LPS-secreted *E. coli* strongly through migration.

Organotypic 3D cultures are a model system reflecting complex *in vivo* or physiological conditions more closely than classical monolayer cultures [167]. While short-term assays can

provide information on neutrophil activation upon direct contact, freshly isolated, rather young neutrophils were used for these assays. However, neutrophils age during tissue immigration with an extended lifespan from one to several days in vivo. [236, 238-241]. Thus, the 3D cultures can be used as a model system including the temporal dimension of neutrophil aging will allow us to evaluate an altered migration of neutrophils upon sensing bacterial patterns in a more physiologic context. Thus, we aimed to determine the attraction or response of neutrophils towards different LTM components, and bacterial supernatants of PluDA hydrogel with/without bacteria applied in 3D tissue-like cultures.

Therefore, 3D cultures were used to investigate the migration and chemoattraction of neutrophils induced by the supernatant of *E. coli*, *ClearColi* (Fig. 40A-B), and gel (PluDA hydrogel) alone or with *E. coli* (*E. coli*-gel) or *ClearColi* (*ClearColi*-gel) bacteria (Fig. 40C). Neutrophils respond by migration towards *E. coli* more than *ClearColi* supernatants (Fig. 40A-B). Mean \pm SD was calculated (Fig. 40A) 104 (\pm 23.459), 307.6 (\pm 84.91), 562.6 (\pm 62.564), and (Fig. 40B) 103.6 (\pm 52.59), 156.3 (\pm 147.5), 372 (\pm 255.5) for Ctrl (untreated), *ClearColi*, and *E. coli*. Significant differences were in only *ClearColi* and *E. coli* supernatants (Fig. 40A) compared to Ctrl: Ctrl vs. *ClearColi* ($p=0.0170$), Ctrl vs. *E. coli* ($p=0.0003$) and *ClearColi* vs. *E. coli* ($p=0.0058$). Both (Fig. 40C) gel (empty hydrogel) and *Clear*-gel (*ClearColi* encapsulated-hydrogel) could attract neutrophil migration at similar levels but less than *E. coli*-gel (*E. coli* encapsulated-hydrogel). Mean \pm SD was calculated as the following: 82 (\pm 46.22), 302 (\pm 121.54), 325 (\pm 153.48), and 560.3 (\pm 199.40) for Ctrl, gel, *Clear*-gel, and *E. coli*-gel. Data was significant only in the case of *E. coli*-gel ($p=0.0139$) compared to Ctrl. Mean \pm SD (Fig. 40D) of Ctrl, *ClearColi*, 0.0125-*ClearColi* and 0.0125 were 1173 (\pm 31), 252.3 (\pm 22.3), 343.3 (\pm 46.7), and 373.6 (\pm 160.99) with significant differences between Ctrl vs. 0.0125-*ClearColi* ($p=0.0385$) and Ctrl vs. 0.0125 ($p=0.0180$)

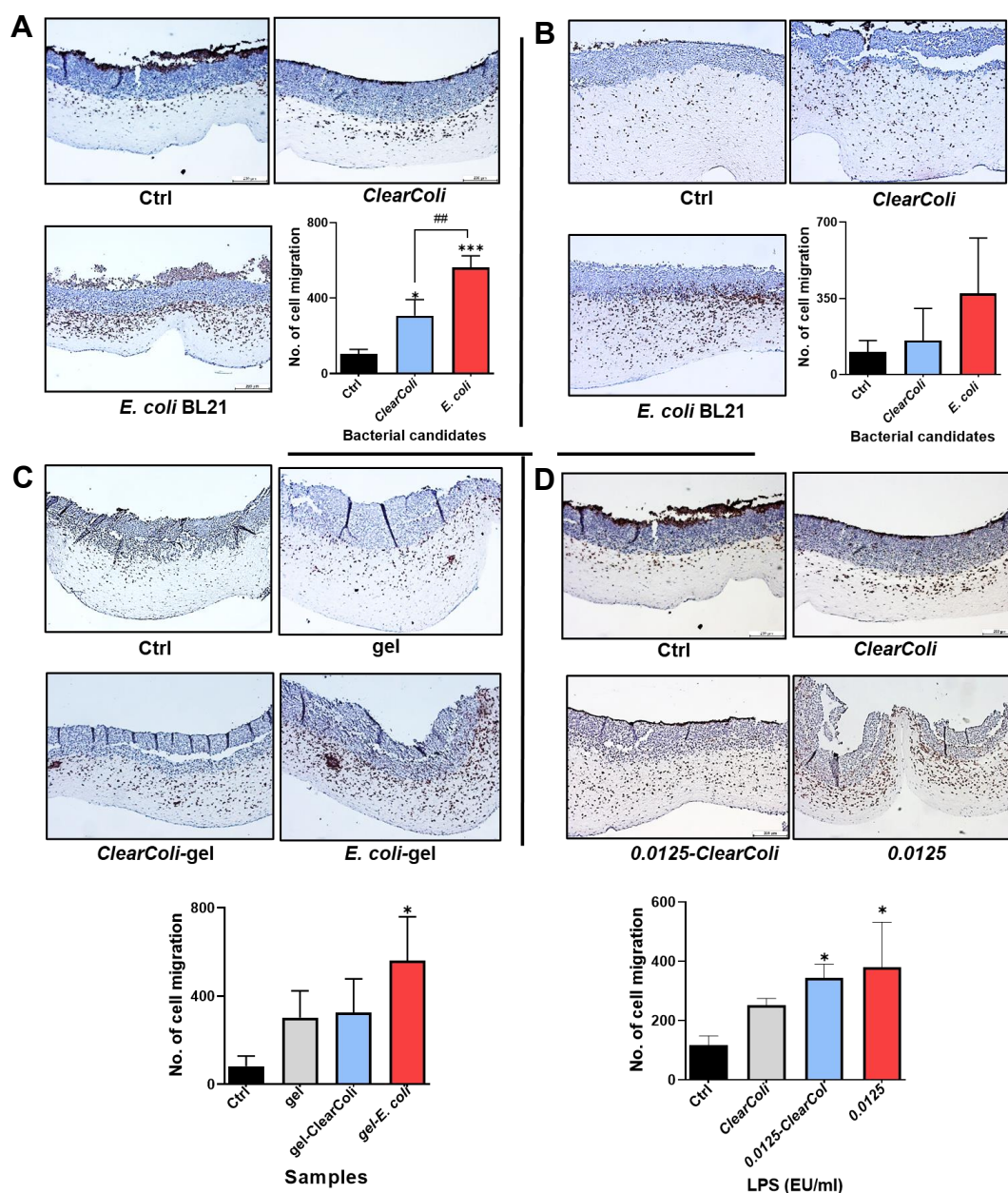


Figure 40| Bacterial supernatants/LPS and gel with/without bacteria attracted neutrophil transmigration in organotypic 3D culture. Collagen and fibroblasts were mixed and incubated with a proper medium at 37 °C. After 24 h, HPK1A cells (A, C, D: Human foreskin Keratinocytes, HPV16 positive) or P2 (B: penile cancer cell line) were seeded in concentration of $5-7 \times 10^5$ and incubated for 24 h before transferring the 3D cultures on a metal grid. The air-phase cultures were incubated for 7 days (A and C) or 14 days (B) with medium change every 2 days. (A, B) bacterial supernatant or (C) gel (PluDA 50%) with/without bacteria (D) *ClearColi* w/wo LPS were placed into the medium (beneath a metal grid). Neutrophils were added to the 3D culture top in a concentration of 5×10^6 cells/culture for 24 h. 3D cultures were then collected, fixed in FFPE, sectioned, and stained for CD15 (neutrophil marker) by IHC. The migrated neutrophils were counted using ImageJ, and the average was calculated as indicated above. Data were illustrated as mean with SD of three experiments (n=3). Significant differences in data analysis were evaluated using GraphPad prism, in which a paired one-way ANOVA with Tukey's multiple comparison tests of untreated condition (Ctrl) with treated ones (*ClearColi* and *E. coli* and or W/out gel). The significance

was illustrated as *(for Ctrl with treated conditions) and # (between treated conditions themselves). GraphPad Prism 8.0.2 [ns ($P > 0.05$) */# ($P \leq 0.05$), **/## ($P \leq 0.01$) ***/### ($P \leq 0.001$)]. Concentration/control/Abb.: bacterial supernatants (1/100, OD₆₀₀=1), LPS (EU/ml), neutrophils (5×10^6 cell/ μ l), Clear. (*ClearColi*), gel (PluDA hydrogel).

This result demonstrates that neutrophils can also respond to PluDA hydrogel compared to Ctrl (migrated neutrophil without treatment) shown in C (Fig. 40). Also, these results reflect and confirm the ones above, showing that LPS influences activation, degranulation, and migration through TLRs. It suggests that the reduced capacity of *ClearColi* to activate neutrophils is related to an impaired toll-like receptor (TLR)-signaling due to the mutated endotoxin. Besides, the Pluronic hydrogel can trigger neutrophils, and these results need to be verified with other methods.

Section 2:

***Lactobacillus planetarium* candidates.**

This section thoroughly examined the immune response utilizing granulocytes (neutrophils) to investigate five candidates (mCherry, I6P7, KCF18, NGF, and Nuclease) derived from *L. Plantarum*.

3 Results:

3.11 *L. plantarum*-conditioned supernatants trigger neutrophil degranulation and enhance ADCC.

Lactobacillus sp. is a facultative anaerobic and gram-positive bacterium with health benefits, and it is involved in food fermentation, for example [168, 169]. Probiotic bacteria pay attention to scientists as a novel therapeutic factor for inflammation caused by trauma or sepsis because of their impact on immune response modulating [170]. *L. plantarum* WCFS1 may have genes for 223 extracellular proteins including 48 covalently bound to a lipobox, 81 membrane-anchored, and 37 bound to cell wall. Extracellular proteins participate in cellular processes such as recognition, adherence to the host, and signaling pathway transduction [171]. Four gene clusters are involved in the *L. p* (WCFS1). Genes of *cps2A-J* and *cps4A-J* create surface polysaccharides including monomers that bind with glycosidic linkage [172, 173]. WCFS1 is a type II TA system (2 genes as an operon) containing toxin and antitoxin. While the toxin is an endoribonuclease weakening the growth, the antitoxin is its inhibitory protein, neutralizing the activity [169, 174]. However, their polysaccharides, recognized by the immune system causing immunogenic response, effectively treat many human diseases [173].

To investigate more possible therapeutic bacteria against neutrophils. Five candidates of *Lactobacillus plantarum* (*L. p*) were engineered to produce peptides (P-producing *L. p*.) in addition to vector (P non-producing *L. p*.) as an alternative control. This includes mCherry, I6P7, KCF18, NGF, and nuclease peptides. mCherry is a photostable gene that encodes red fluorescence protein (RFP) stimulated at longer than 600 nm [175]. I6P7 is a peptide, binding to particularly interleukin-6 receptors, expressed highly on various cancer cells, such as U-87 cells. Thus, I6P7 prevents IL-6 binding with IL-6R [177]. IL-6 is produced by tumors such as HPV-transformed keratinocytes with a high expression level. IL-6 suppresses myeloid cells promoting tumors such as cervical cancer through binding IL-6 with IL-6R [177-178, 201-202]. KCF18 is a peptide derived from pro-inflammatory cytokine receptors and has amphiphilic characteristics. It was reported that the KCF18 protein binds tumor necrosis factor- α (TNF- α) and interleukin-6 and thus reduces the engagement with their receptors [179]. Nerve growth factor (NGF) is an insulin-like protein. NGF maintains the survival of neurons, where it aids in the growth and development of embryonic sensory neurons [180, 181]. Nucleases are enzymes such as DNases and RNases that can catalyze nucleic acids like DNA and RNA, respectively [182]. Nuclease deficiency may lead to immunodeficiency or genetic instability. DNA

nucleases, for example, are essential in DNA repair, including excision repair of base and nucleotide in addition to DNA replication [183].

L. plantarium (*L. p.*) candidates were cultured in MRS (Man, Rogosa, and Sharpe) agar at 37 °C with shaking at 100-300 rpm for one day. Bacteria were sub-cultured more than two times to take and use the third generation for the experiments. After adjusting the optical density to $OD_{600}=1$, the supernatant of each candidate was collected. In dilution factor 1:100, bacterial supernatants were used in all experiments to investigate neutrophil response. Furthermore, it is to understand whether the bacterial contact or their soluble protein are the responsible mediators of activation. After a neutrophil resting time of 1-2 h at 37 °C, all supernatants were co-cultured with neutrophils for 1 h at 37 °C. After supernatant collection and running in a zymogram gel, it was followed by an analysis of MMPs, marking degranulation. The zymogram results indicate that the bacterial candidates' supernatants slightly increased MMP9 at similar levels. MMP (Fig. 41) levels were evaluated for vector, mCherry, I6P7, KCF, NGF, and nuclease, respectively, as follows. The homodimer (Fig. 41E) was 1.67 (± 0.3), 1.67 (± 0.4), 1.72 (± 0.29), 1.92 (± 0.3), 2.12 (± 0.9), and 3.10 (± 2.13)- folds. The complex (Fig. 41F) levels were 1.43 (± 0.11), 1.24 (± 0.2), 1.94 (± 0.58), 1.59 (± 0.42), 1.64 (± 0.35) and 2.3 (± 0.78)-folds. Levels of monomer (Fig. 41G) were 2.72 (± 0.62), 2.61 (± 0.69), 2.84 (± 0.9), 2.94 (± 0.68), 2.9 (± 0.82), 3.56 (± 1)-folds. MMP-2 (Fig. 41G) levels did not change. All MMPs were compared to control (Ctrl). The significance was detected in homodimer: Ctrl vs. Nuclease ($p=0.0341$), in complex: Ctrl vs. I6P7 ($p=0.0174$) Ctrl vs. nuclease ($p=0.0008$) and vector vs. nuclease ($p=0.0437$), in monomer: Ctrl vs. vector ($p=0.0126$), mCherry ($p=0.0204$), I6P7 ($p=0.0070$), KFC18 ($p=0.0044$), NGF ($p=0.0053$) and nuclease ($p=0.0002$).

Next, to investigate whether neutrophils respond differently to heat-killed bacteria at a similar level to their supernatants. The bacteria were adapted and killed according to the protocol (Junhua Jin et al., 2020). The supernatants (Fig. 41I, K) and heat-killed (Fig. 41J, L) *L. plantarium* candidates were directly added to neutrophils to assess the biological function of neutrophils in ADCC. When candidates' supernatants (Fig. 41K, I) were added to only neutrophils (without Ab), they did not cause any observed changes. However, all heat-killed *L. plantarium* candidates (Fig. 41J, L) resulted in a cytotoxic effect when added to only neutrophils reaching about 2.5 of $nCI=1$ after 24 h. In ADCC, candidates' supernatants may cause slight enhancement. However, all *L. plantarium* candidates (heat-killed) were found to improve the capacity of ADCC to kill tumors (A431 cells).

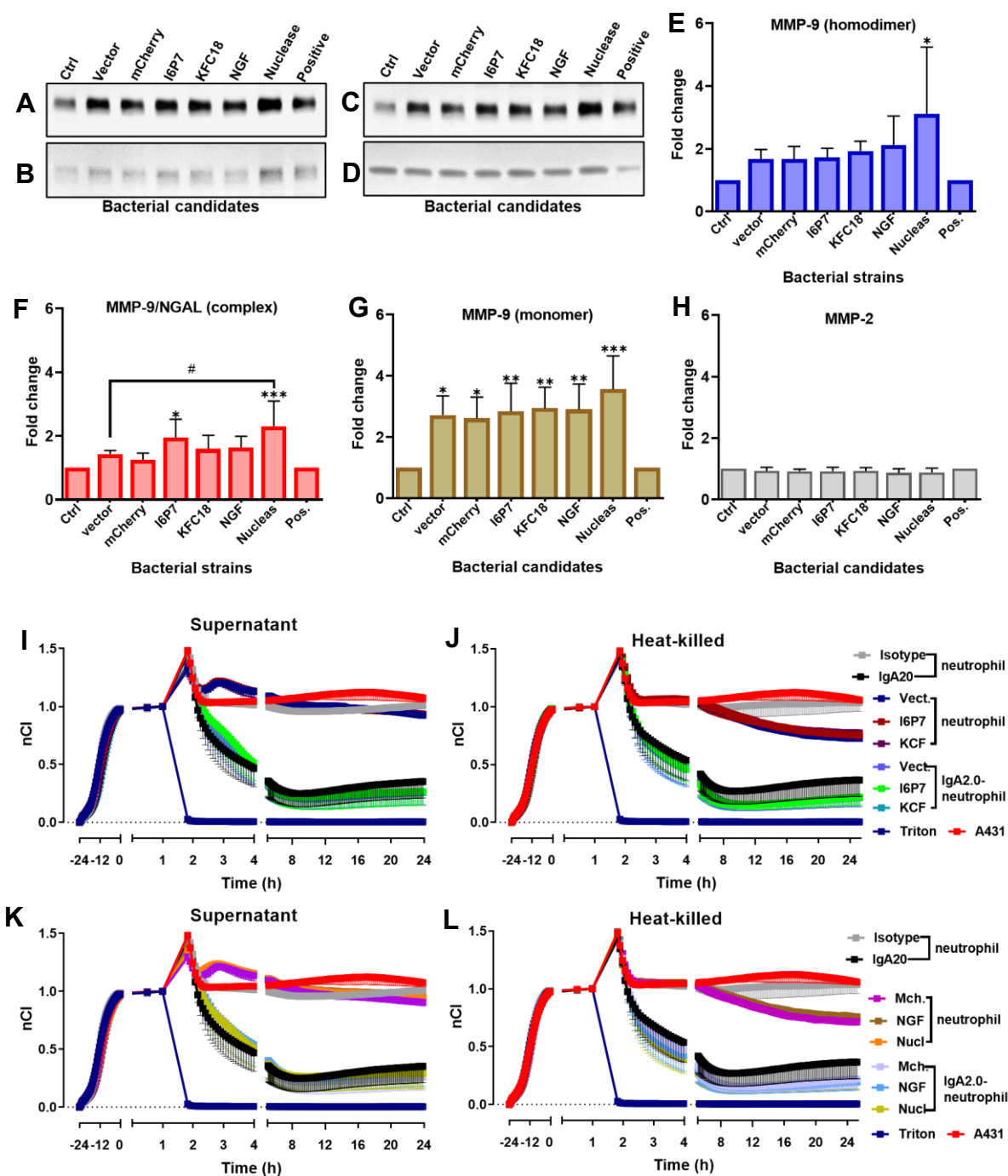


Figure 4I | Supernatant/ heat-killed of *L. plantarum* may enhance neutrophil degranulation and activation for tumor cell-killing by ADCC. (A-D) *L. plantarum* candidate's supernatant was incubated at 37 °C for 1 h with neutrophils in a 24-well plate. Then, (A-D) using zymography, the Level of neutrophil activation was measured neutrophil degranulation through (E-H) analysis of MMP release was analyzed. (I-L) Direct stimulation of neutrophils was used in the ADCC assay with (I, K) the supernatants and (J, L) bacterial candidates killed by heating at 121 °C for 15 min. Data were illustrated as mean with SD (E-H) and SEM (I-L) of three independent experiments (n=3). The significant differences were evaluated using GraphPad prism, in which a paired one-way ANOVA with Dunnett's multiple comparisons test of untreated condition (Ctrl) with the five candidates as well as vector (alternative Ctrl/ P non-producing *L. p.*) with the candidates. The significance was illustrated as *(Ctrl and candidates) and # (vector and candidates), in which ns (P > 0.05) */#

($P \leq 0.05$), **/### ($P \leq 0.01$) *** /### ($P \leq 0.001$]). Concentration/control/Abb.: Concentration/control/Abb.: bacteria/supernatant (1/100, OD₆₀₀=1), isotype (non-specific IgA standard, STD), positive (5 μ l of 0.2% Triton), negative (untreated A431 cells), neutrophils (4 x 10⁶ cell/ml), positive (Pos., supernatant of CXCL-8-stimulated neutrophils).

For further analysis, the delta cell index was calculated. *L. plantarum* candidates' supernatants (Fig. 42A, C) may improve ADCC at 24 h. The significance was evaluated for each condition between 1 h (control) with 2, 3, 4 and 24 h as follows; for untreated: 1 vs. 2 ($p=0.0176$), 1 vs. 3 ($p=0.0235$), 1 vs. 4 ($p=0.0356$) and 1 vs. 24 ($p=0.0151$), for mCH: 1 vs. 2 ($p=0.0271$) and 1 vs. 3 ($p=0.0432$), for I6P7: 1 vs. 2 ($p=0.0461$), for Vector: 1 vs. 2 ($p=0.0383$), for KFC: 1 vs. 2 ($p=0.0255$), 1 vs. 3 ($p=0.0249$), 1 vs. 4 ($p=0.0340$) and 1 vs. 24 ($p=0.0426$) and for NGF: 1 vs. 2 ($p=0.0278$) and 1 vs. 3 ($p=0.0457$). Data was without a significant difference between untreated with treated conditions. Furthermore, the delta cell index showed enhancement with heat-killed bacteria candidates (Fig. 42B, D) without significance. The results of the enhancement of tumor killing may stem from the activation of toll-like receptor (TLR) signaling from both live and killed bacteria [232], where killed bacteria are recognized as PAMPs. These results also indicate that proteins from different *L. plantarum* candidate supernatants may have varying effects on neutrophil degranulation, but their impact on neutrophil function does not differ in addition, results confirm that MMP release is not associated functionally with ADCC.

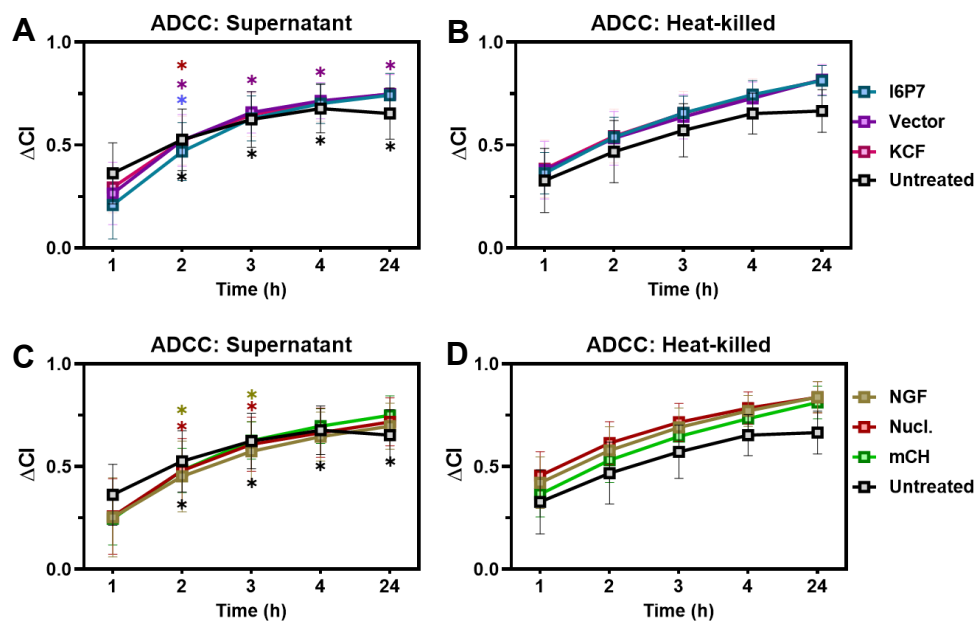


Figure 42| Delta cell index calculation. (A, C) Supernatant. (B, D) Heat-killed bacteria. ΔCI was evaluated as (isotype + neutrophil) – (IgA2.0 + neutrophil) of the respective conditions at 1, 2, 3, 4, and 24 h. Data were illustrated as mean with SEM of three independent experiments (n=3). Significant differences were analyzed

by two-way ANOVA with Dunnett's multiple comparisons test for each treated condition at 1 h with 2, 3, 4, and 24 h marked as*, and untreated (IgA2.0-neutrophil) with treated conditions (*L. Plantarum* candidates) at each time points marked as #.

3.12 Supernatant and heat-killed *L. plantarum* increase neutrophil migration.

Organotypic 3D cultures mimic the complex model *in vivo*, being closer to natural conditions than classical monolayer cultures [167]. To verify our results, neutrophil chemoattraction towards *L. plantarum* was investigated through 3-D cultures (Fig. 43). Neutrophil migration was evaluated to investigate cell functions such as response to bacterial supernatants and heat-killed bacteria. In this experiment, we aimed to assess the efficacy of the vector (peptide non-producing *L. plantarum*) inducing neutrophil migration under two conditions: the supernatant and heat-killed bacteria. When neutrophils migrated alone or with MRS medium, the average number of cells was 130 (± 59.6), and 140.3 (± 13.3), respectively. However, the supernatant and heat-killed bacteria (vector) were able to attract more neutrophils with an average of about 368.3 (± 27.9), and 355 (± 127.9) cells. Data showed significant differences compared to untreated neutrophils (Ctrl) with supernatant ($p=0.0200$) and heat-killed ($p=0.0270$) and compared to MRS with supernatant ($p=0.0158$) and heat-killed bacteria ($p=0.0212$). Moreover, no significant differences existed between the Ctrl and MRS or the supernatant and heat-killed bacteria.

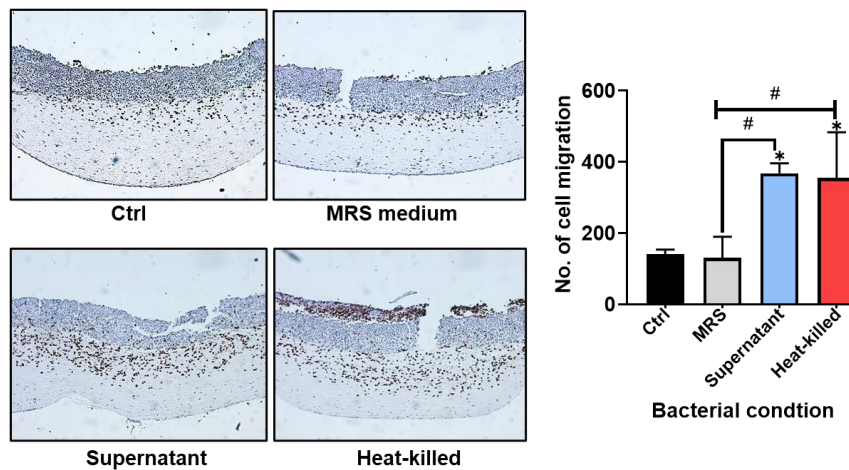


Figure 43| Strong chemoattraction of neutrophils towards supernatant and heat-killed *L. plantarum* (vector/P non-producing *L. p.*). A mixture of Collagen and fibroblasts were incubated with a proper medium at 37 °C for 24 h. HPK1A Cells (Human foreskin Keratinocytes, HPV16 positive) were added ($5-7 \times 10^5$ cell/culture) and incubated for 24 h before transferring 3D cultures onto a metal grid. Air-phase cultures were incubated for 7 days for 14 days with medium change/ 2 days. Bacterial supernatant or heat-killed bacteria ($1/100$, $OD_{600}=1$) were placed in a medium (beneath a metal grid) and neutrophils were added on top of the 3D cultures in 5×10^6 cell/culture for 24 h. 3D cultures were then collected, fixed in FFPE, sectioned, and stained for CD15 (neutrophil marker) by IHC. The migrated neutrophils were counted using ImageJ and their average

was calculated as indicated above. Data were illustrated as mean with SD of three independent experiments (n=3). Significant differences in data analysis were evaluated using GraphPad prism, in which a paired one-way ANOVA with Tukey's multiple comparisons test of untreated condition (Ctrl, MRS) with treated conditions (supernatant and Heat-killed of vector). The significance was illustrated as * (Ctrl and treated ones) and # (MRS and treated ones), in which ns ($P > 0.05$) */# ($P \leq 0.05$).

3.13 Capabilities of *L. plantarum* to enhance neutrophil degranulation.

Based on our previous findings, we have chosen vector (Ctrl/ P non-producing *L. p.*) and nuclease candidates of *L. plantarum* for further detailed investigation. This time, we tested bacteria in different phases, including heat-killed and live bacteria, as well as their supernatants to observe degranulation and cytokine release. Vector and nuclease (Fig. 44D-F) at different conditions including supernatant, heat-killed, and live bacteria, resulted in a slight increase of homodimer to about 2-fold in (Fig. 44D) homodimer, to less than 2-fold in (Fig. 44E) complex, and to about 2-fold in (Fig. 44F) monomer. Results (Fig. 44D-F) indicate that the MRS medium did not prompt neutrophil degranulation. Also, our assessment of cytokines (Fig. 44G) for vector (Peptide non-producing *L. p.*) showed a notable rise in CXCL-8 levels to an average of 72, 68, 183, 129, and 139 pg/ml for MRS, Ctrl, supernatant, heat-killed, and live vector, respectively, compared to the control. In the case of nuclease (Fig. 44H), CXCL-8 had an average of 242, 188, 525, 324, and 272 pg/ml for the same conditions. However, the change in CXL-8 concentrations was not significant.

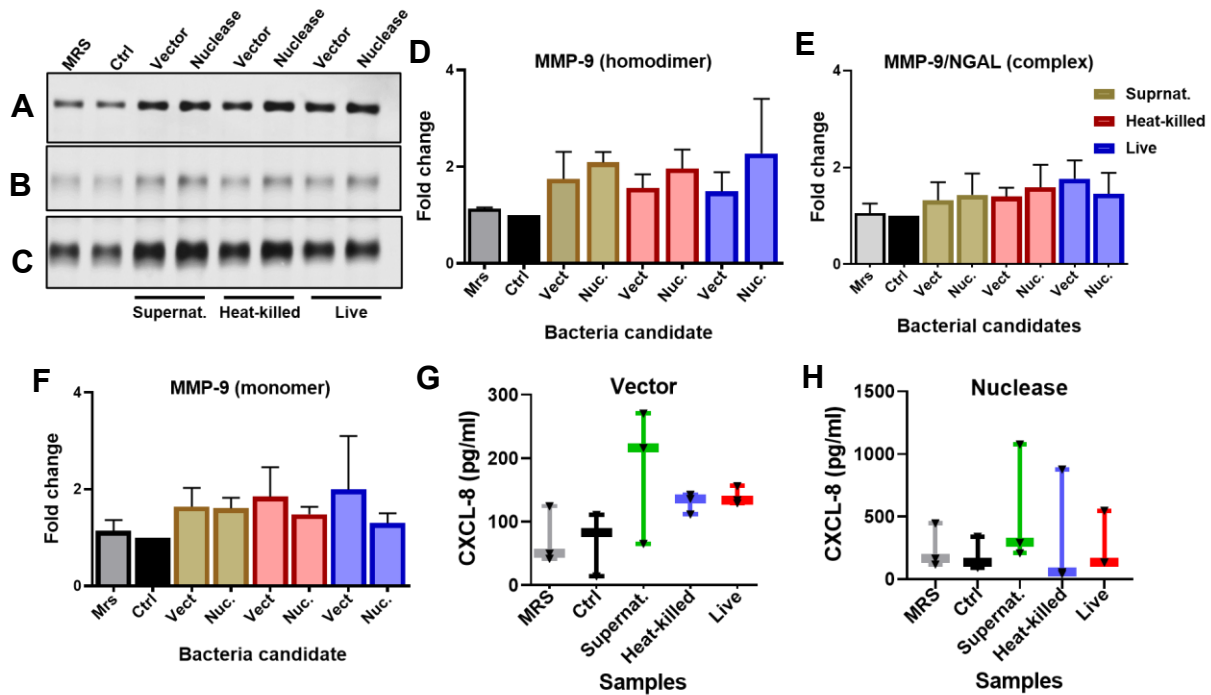


Figure 44| Various levels of protein secretion can be triggered by bacterial phases. Vector and Nuclease candidates were incubated with neutrophils at 37 °C for 60 min in different states (supernatant, heat-killed, and live bacteria) in a 24-well plate. Supernatants collected after neutrophil stimulation were used in the zymogram procedure for (A-C) MMP detection and ELISA for (D-E) CXCL-8 concentration measurement. Data were illustrated as mean with SD of three independent experiments (n=3, A-E). Significant differences were analyzed using GraphPad prism, in which a paired one-way ANOVA with Tukey's multiple comparison tests of untreated conditions (Ctrl) with treated ones (gel w/out bacteria). The significance was illustrated as * (for Ctrl with treated conditions) and # (between only treated conditions), in which ns ($P > 0.05$). MRS: medium

3.14 Under various conditions, the status of *L. plantarum* increases the capacity of neutrophils in ADCC.

We conducted further investigations on *L. plantarum*, vector, and nuclease under previous conditions to assess their functionality in ADCC assay. Additionally, we aimed to determine whether live and heat-killed bacteria are associated with the release of MMPs, which demonstrated neutrophils' ability to kill tumors through trogoptosis [253]. Our experiment focuses on assessing the impact of introducing bacterial components to IgA2.0-bound neutrophils, as untreated/experiment control. The results of ADCC (Fig. 45A, B) demonstrate clearly that untreated (IgA2.0-neutrophils) exhibit potent tumor-killing capacity, reaching approximately 0.5 (nCI=1) compared to isotype-neutrophils (control) showing no effect. However, in vector (Fig. 45A), the addition of supernatant, heat-killed, and live bacteria importantly enhanced the ADCC (treated condition) compared to the untreated control, with consistent levels of tumor cell-killing. Additionally, enhancement of isotype-neutrophils

(control) was observed when adding heat-killed and live bacteria. Regarding the nuclease (Fig. 45B), all treated conditions also improved ADCC, with varying levels compared to the control. The heat-killed, and live bacteria may be the supernatant elevated cytotoxicity of isotype-neutrophils and neutrophils.

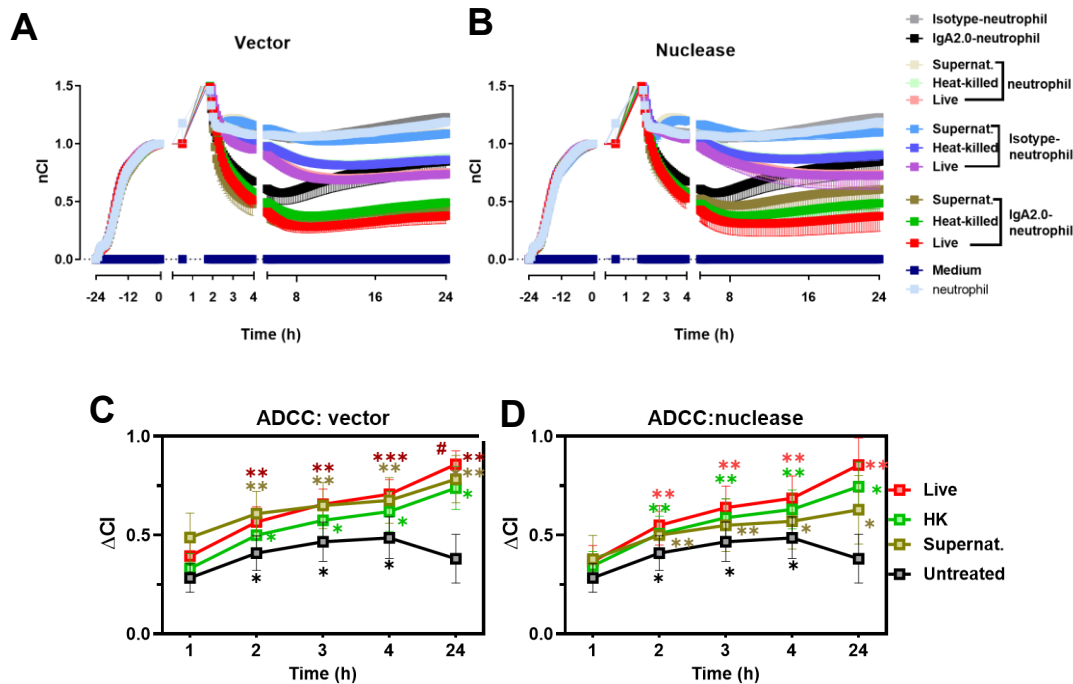


Figure 45| Elevation in neutrophil capacity to kill the tumor cells in impedance-based ADCC assay. The supernatant, Heat-killed, and Live *L. plantarum* ($OD_{600}=1$, 1/100) of (A) vector and (B) Nuclease were added to neutrophils w/out antibodies (IgA2.0 and Isotype) in 96-well plate for ADCC assay. (C, D) The Delta cell index (ΔCI) was calculated as isotype+ neutrophil - IgA2.0+neutrophil of the respective conditions at 1, 2, 3, 4, and 24 h. Data were illustrated as mean with SEM of three independent experiments ($n=3$). Significant differences were analyzed by two-way ANOVA with Dunnett's multiple comparisons test for each treated condition at 1 h with 2, 3, 4, and 24 h marked as*, and untreated (IgA2.0-neutrophil) with treated conditions (*L. Plantarum* vector/Nuclease) at each time points marked as #. Control/dilution: isotype (non-specific IgA standard, STD), positive (5 μ l of 0.2% Triton), negative (untreated A431 cells), HK (Heat-killed bacteria). Some data was not shown for a clearer view.

For further analysis, the delta cell index was evaluated for ADCC assay. ΔCI showed enhancement in for vector (Fig. 45C) and nuclease (Fig. 45D) for all treated condition/each time point compared to 1 h. The significance was evaluated in vector and nuclease (Table 9).

Table 9: P- value of Vector and nuclease candidates (Fig. 45C, D).

Time (h): C	Untreated		Supernatant		heat-killed		Live	
	C	D	C	D	C	D	C	D
1 vs. 2	0.0110	0.0110	0.0024	0.0040	0.016	0.0059	0.0035	0.0075
1 vs. 3	0.0181	0.0181	0.0054	0.0076	0.0147	0.0052	0.0019	0.0081
1 vs. 4	0.0226	0.0226	0.0049	0.0110	0.0108	0.0054	0.0009	0.0074
1 vs. 24			0.0006	0.0464	0.0111	0.0137	0.0018	0.0092

Furthermore, Δ CI demonstrated that adding bacteria or their components to neutrophils with Isotype (Fig. 46A-B) or neutrophils alone (Fig. 46C, D) led to observed cytotoxic effects on cancer cells in both vector and nuclease at similar levels. The effect was observed in the order of low, medium, and high for supernatant, heat-killed, and live bacteria, respectively. The significance was found in (Fig. 46A) heat-killed vector at 1 vs. 2 ($p=0.0010$), 3 ($p=0.0028$), 4 ($p=0.0079$), and 24 ($p=0.0029$) as well as live vector: between 1 with 2 ($p=0.0461$), 4 h ($p=0.0406$), and 24 ($p=0.0042$). Also, untreated with heat-killed were significant at 2 h ($p=0.0108$), at 3 h ($p=0.0034$), at 4 h ($p=0.0053$), and 24 h ($p=0.0028$) as well as untreated with live at 2 h ($p=0.0270$), at 3 h ($p=0.0177$), at 4 h ($p=0.0053$) and 24 h ($p=0.0008$). The significance was found in nuclease (Fig. 46B) for heat-killed: 1 vs. 2 ($p=0.0414$) and 1 vs. 24 ($p=0.0264$). Further, nuclease has significant differences between untreated with supernatant at 2 ($p=0.0040$) and heat-killed at 2 ($p=0.0103$) and live at 24 ($p=0.0236$). Adding bacterial conditions to neutrophils (without Ab) elevated cytotoxicity which was observed at 24 h. The significance was evaluated for the (Fig. 46C) vector live 1 vs. 24 ($p=0.0119$) and neutrophil with heat-killed at 24 h ($p=0.0173$). Also, significance was found in (Fig. 46D) nuclease heat-killed 1 vs. 24 ($p=0.0477$) and live 1 vs. 24 ($p=0.0485$) and between neutrophil vs. live at 2 ($p=0.0374$), at 3h ($p=0.0221$) and 4 h ($p=0.0242$). These findings (Fig. 46C, D) conclusively demonstrate that the observed impact is solely attributed to the bacteria and their components on neutrophils, without the effect of isotype antibody.

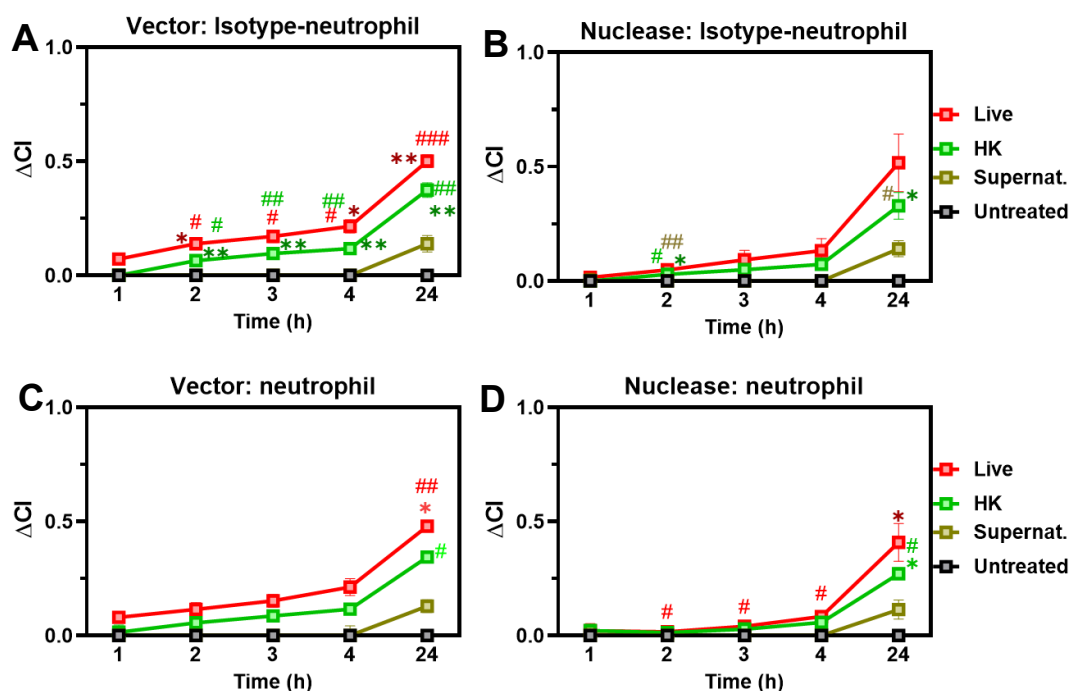


Figure 46I Cytotoxic effect of bacterial status with neutrophils with and without nonspecific antibodies.

(A, B) The Delta cell index (ΔCI) was calculated as (isotype+ neutrophil) – (Isotype+ neutrophil) w/out the respective conditions at 1, 2, 3, 4, and 24 h. (C, D) $\Delta CI = (\text{neutrophil}) - (\text{neutrophil})$ with respective conditions at the same time points. Data were illustrated as mean with SEM of three independent experiments ($n=3$). Significant differences were analyzed by two-way ANOVA with Dunnett's multiple comparisons test for each treated condition at 1 h with 2, 3, 4, and 24 h marked as*, and untreated (neutrophil/ isotype-neutrophil) with treated conditions (*L. Plantarum* vector/ nuclease) at each time points marked as #. HK (Heat-killed bacteria).

4 Discussion:

Living therapeutic materials (LTM) are being used in medicine. Because of the potential activation of the immune system, they are always developed to meet the best-needed requirements of the human immune system. In this work, LTMs were developed, and obtained from the INM institute, where potential therapeutic bacteria were loaded on Plu/PluDA hydrogel (central core) crosslinking with the PluDA (shell) covering the core. This includes empty gel (hydrogel), bacterial-gel (hydrogel-containing bacteria) and only bacteria such as *E. coli* and *ClearColi*. To investigate the immune cell response to LTMs, cytokines, functional characteristics and transmigration of neutrophils were evaluated using ELISA, ADCC and organotypic 3D cultures, respectively. All constructs could activate neutrophils. Then I shifted to using only *E. coli* and *ClearColi* (conditioned media) without hydrogel to stimulate neutrophils. Both strains could activate neutrophils and were higher with *E. coli* than *ClearColi*, translated to the release of MMPs, and cytokines, enhancing the killing of tumor cells and increasing the immigration of neutrophils through 3D culture. To define the difference in activation level between both strains, I applied Lipopolysaccharides (LPS) in the same concentration measured in both strains' supernatants. As expected, by comparison between *ClearColi* (modified LPS), *E. coli* (natural LPS) and pure LPS (commercial), we could prove that the higher activation level of *E. coli* supernatants originated from LPS that activates TLR-signalling. In contrast, the lower activation by *ClearColi* may rely on FPR-signalling.

4.1 Interaction of neutrophils with *E. coli* and *ClearColi* strain.

Among the bacteria used in a drug-delivery system is the engineered *E. coli* known as *ClearColi*. This strain is characterized by the release of modified lipopolysaccharides, genetically engineered not to elicit human immune response [134]. In a recent study, T cells couldn't differentiate (CD4+ and CD8+) based on activation after direct contact with bacteria (*E. coli*/*ClearColi*). However, both bacteria induced the secretion of IL-6 and led to PBMC apoptosis, which may originate from innate immune cells such as monocytes and NK cells [150]. Therefore, this is the first evaluation of the potential activation of neutrophils by LTM, which is the relevant immune cell population *in vivo*. Neutrophils are characterized by immediate response to hours or days [50]. So, the incubation time was 60 min in most experiments. It is comprehended that *E. coli* can secrete LPS during division every 20 minutes or by death [184]. Therefore, bacteria (Fig. 26) were washed and incubated with neutrophils (in/direct contact) by transwell inserts in RPMI with supplements for 60 min. This medium is appropriate for neutrophil life and not proper for bacterial growth, indicating that there is no

production of LPS in the medium except those in the bacterial wall, which neutrophils can sense. Investigation *in vitro* showed activation which differentiates between direct and indirect contact with bacteria. However, the application *in vivo* would increase PAMP concentration which activates and increases neutrophil recruitment triggering other immune cells. Thus, extending the incubation time probably increases the activation of neutrophils with *ClearColi* but more with *E. coli*. RPMI medium was tested and suited for neutrophils but bacteria, so, using a proper medium for bacteria would be the best solution for both in/direct contact at 60 min and long-term incubation, enabling bacteria to produce soluble metabolic factors activating neutrophils with *ClearColi* and *E. coli*. Further, neutrophils can modulate their response to Gram-positive and negative bacteria. For instance, neutrophils produce ROS against LPS-containing bacteria (Gram-: *P. aeruginosa*, *S. enterica*) more than bacteria (Gram+: *L. monocytogenes*, *S. aureus*) that do not produce LPS. However, even with those two Gram-positive bacteria, neutrophils showed more extravasation toward *L. monocytogenes* than *S. aureus* [185]. Because of LPS mutation, applying *ClearColi in vivo* would trigger a neutrophil response similar to that triggered via Gram-positive bacteria. We demonstrate that we are the first to investigate *ClearColi* with neutrophils and saw activation as neutrophils are the relevant first responders.

4.2 Bacterial LPS and other PAMPs are mediators of neutrophil activation.

During cellular division and invasion, microorganisms produce exogenic factors called PAMPs such as peptidoglycan, formylated peptides, LPS, and others [58]. Gram-negative bacteria including *E. coli*, have a thin layer of peptidoglycan which predominantly exists as mesoDAP-peptidoglycan recognized by the NOD1 receptor activating neutrophils through NF- κ B signaling. However, a thicker peptidoglycan layer exists in gram-positive bacteria [242, 243]. Further, the NOD2 receptor can detect Gram+/- bacterial peptidoglycan [243]. The bacterial DNA derived from *E. coli* can activate neutrophils and reduce L-selectin expression significantly. Further, neutrophils could produce CXCL-8 and change their shape. CpG DNA is engulfed to interact with endosomal TLR9 activating neutrophils. Bacterial DNA stimulates human and murine-model immune cells such as monocytes, macrophages, dendritic and NK cells [71, 244]. Formylated peptides (fMLP) secreted by bacteria can also activate neutrophils via FPR1 [188, 245]. This activation results in the release of MMPs such as MMP-9 and the secretion of cytokines such as CXCL-8 [189, 190]. Neutrophils follow guidance cues hierarchically. Neutrophils prioritize an fMLP gradient when they are subjected to competing gradients between fMLP (end-target) and CXCL-8 (intermediate-target). *In vivo* study, neutrophils were shown to respond to MIP-2 in sinusoidal tissue. However, by the presence of

fMLP, neutrophils preferred the response to the new gradient which directed them to the infection site [245]. *E. coli* produces LPS, an essential mediator in neutrophil activation and a critical cell wall component of Gram-negative bacteria [164, 186]. Death or multiplication of bacteria causes the release of LPS molecules into the microenvironment [187]. Under laboratory aerobic, nutrient-rich circumstances, LPS is produced from *E. coli* each 20 min during division [184]. *ClearColi* strains (engineered *E. coli*) can also produce LPS, but they are genetically modified not to trigger an endotoxin response in the human body making the only difference between the two strains [164]. Six acyl chains (in LPS) of *E. coli* are agonist to TLR4. The oligosaccharide chain and two acyl chains were removed. Hence, *ClearColi* does not contain the outer membrane agonist to hTLR4/MD-2 reducing signaling compared to *E. coli* [164].

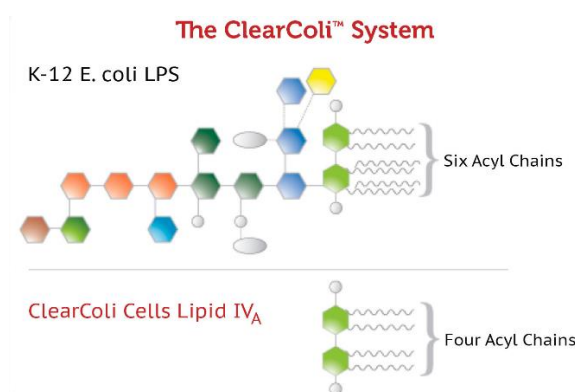


Fig. 47I Comparison of LPS in *E. coli* and Engineered *E. coli* strain (*ClearColi*). Oligosaccharides were removed through the deletion of seven genes (Δ gutQ, Δ kdsD, Δ lpxL, Δ lpxM, Δ pagP, Δ lpxP and Δ eptA. One gene (msbA148) was added. [BIORESERCH TECHNOLOIES, 164].

Moreover, neutrophils are sensitive to endotoxins such as LPS (TL4 ligand) because it is a firm indicator of infection [242]. This leads to endotoxic shock or even cell death [164]. The presence of LPS reduces CXCR2 expression on neutrophils which leads to preventing neutrophil migration toward CXCL-8 (humans) and MIP-2 (mice) [245]. Investigation of PAMPs (fMPL, LPS) involved bacterial supernatants (Fig. 27-38, 43A, B, D) or adding them demonstrated the activation of neutrophils via *ClearColi* and *E. coli*. However, the activation is predominant with *E. coli*. By neglecting the other PMPs secreted by both strains, the results confirm that engineering LPS in *ClearColi* led to a significant reduction in neutrophil activation reflecting the importance of LPS as a major activating factor. Further, extending the time to 2 and 4 hours enhanced the level of degranulation. Thus, *ClearColi* would induce more response if the time was prolonged.

4.3 Immune response to *E. coli* and *CleareColi* in case of the encapsulation (gel).

Biomaterial encapsulation is a good tool for viral vector delivery to specific organs. It is characterized by the ability to reduce immune response [191]. Pluronic F127 gel application in cutaneous wounds causes the production of vascular endothelial growth factor (VEGF) and transforming growth factor-beta1 (TGF- β_1) on days 3 and 7 [192]. Pluronic® F127 is one of the biomaterial encapsulations taxonomized as non-toxic and approved by the FDA. Pluronic® F127 is also water-soluble, where hydrophilic segments (PEO₁₀₀–PPO₆₅–PEO₁₀₀) contain hydrophilic polyethylene oxide (2 blocks) and polypropylene oxide (1 block) [193]. Therefore, bacteria should be prevented and controlled from direct contact with immune cells, avoiding the protein cascade release leading to tissue damage. Encapsulation of bacteria with Pluronic hydrogel, including Pluronic diacrylate (PluDA) core can prevent bacterial outgrowth and hydrogel shell, preventing physical contact with neutrophils. The encapsulated-therapeutic bacteria are known as living therapeutic materials (LTMs) [150, 194].

Freshly isolated neutrophils live a short half-life in the bloodstream of less than one day, then proceed to the aging process [236, 237-239]. Therefore, the first time of investigation (Fig. 27), neutrophils incubated for short- and intermediate-terms where the gel of PluDA (30%) w/out bacteria (VEGF_{peptide} producing) could activate neutrophils marked by degranulation and decrease in ADCC in case of the pre-stimulation. Testing the gel of PluDA (50%), encapsulated bacteria (non-protein-producing) for the second time (Fig. 46) showed that PluDA hydrogel could modulate fresh isolated-neutrophil immunogenicity marked by a reduction in MMP release. Neutrophils can survive after immigration into tissue for one to several days where they are aged. However, maybe their lifespan extends for weeks [236, 238-242]. To test, *in vitro*, the response of aged neutrophils to PluDA, a system close to *in vivo* conditions, 3D culture/tissue-like culture (Fig. 40C), was used. Neutrophils immigrated toward PluDA (50%), where they could meet after one day as a long-term incubation. To my knowledge, I am the first to investigate the direct interaction between PluDA and neutrophils and report neutrophil activation. Some studies showed that Pluronic, containing elevated levels of PPO content, caused cytotoxicity through cell membrane incorporation, change in viscosity, and concentration of adenosine triphosphate (ATP) [193]. Further studies proved that the encapsulation of bacteria in Pluronic F127 diacrylate hydrogel (30%) decreased PBMC response [150]. Furthermore, histopathology showed that Pluronic gel 127-treated wounds attracted leukocytes after 2 days compared to saline-treated ones [192]. Gel-encapsulated bacteria (Fig. 27) produce QK peptides mimicking VEGF *in vivo*. These peptides could activate endothelial cells by upregulation of the VEGF receptor as well as the VEGFR2-dependant

pathway leading to cellular proliferation migration and Survival [195]. So, neutrophil activation might be by formylated peptides or other molecules. Further, extending the incubation time of gel (Fig. 38) would increase neutrophil response. Our results demonstrated that bacterial-soluble components could activate neutrophils. However, the activation level in *ClearColi* was less than in *E. coli*, likely related to LPS. In addition to that different gel contents could activate neutrophils differently.

The *ClearColi* strain might be used for drug-delivery systems if we can optimize the LTM concept and thus modulate its contents. For instance, neutrophils and macrophages express an intensive number of formyl peptide receptors (FPRs) recognizing formylated peptides (bacteria/mitochondria) and endogenous non-formylated peptides leading to their activation [243]. Further, deformylation is an essential process that enables bacteria to live. It is also required for N-terminal methionine cleavage that occurs by methionine aminopeptidase (MAP), which may occur for about 50% of all proteins [244]. Thus, introducing peptide deformylases (PDF) can modulate encapsulated bacterial content. PDF catalyzes the formyl group of N-terminal formylmethionine (fMet) of the nascent peptide, with exceptions including secretory proteins as well as membranous proteins, leading to the production of formic acid [244]. It was observed the presence of a low amount of SCFA in inflammatory bowel diseases (IBD) and vice versa under active inflammatory conditions. Therefore, short-chain fatty acids (SCFA) including propionate and butyrate are considered anti-inflammatory metabolites of gut microbiota, playing an important role in maintaining intestine homeostasis. Thus, designing and introducing genetic circuits that sense low SCFA concentration and release biotherapeutic SCFA would be an interesting strategy [245]. SCFAs can weaken the activation of neutrophils and other immune cells such as macrophages, dendritic and Th1/17 cells. SCFAs activate G-protein-coupled receptor (GPCR) signaling inhibiting histone deacetylase (HDAC) and producing acetyl-CoA [246, 249]. SCFAs activate GPR-41 and -43 inhibiting nuclear factor- κ B (NF- κ B) signaling, leading to anti-inflammatory factor production [249]. Peptidoglycan is recognized principally through the connection of the whole bacteria by intracellular cytosolic innate immune receptors [247]. The shedding of peptidoglycan fragments (ligands) occurs by host lysozyme catalyzing unmodified peptidoglycan, in which ligands exist in blood circulation caused by infection or the presence of gut microbiota [247, 248]. Neutrophils, for instance, respond to mesoDAP-peptidoglycan of *E. coli* (thin layer) by NOD-1 and -2 (PRRs) [242, 243]. Modifying stem peptides such as amidation of meso-DAP (l-ornithine instead) or glutamic acid enables bacteria to replicate and minimize peptidoglycan release, thus changing the host response by reducing the Nod1 response. NamH can modify stem peptides related to host lysozyme resistance and

resistance to β -lactam antibiotics. For instance, a gene of *pgdA* (70) (peptidoglycan deacetylase A) for N-deacetylation of GlcNAc (N-Acetylglucosamine) in *Streptococcus suis* resists neutrophil killing. After modification, peptidoglycan becomes more intact where bacteria can resist lysozyme hydrolysis and thus it is not sensed as PAMP [248].

4.4 Impact of *L. plantarum* strain on the immune cell response:

Lactobacillus plantarum was reported to be generally recognized as safe (GRAS) status. Vaccination of *plantarum* strains (derived from WCFS1) regulates the immune system positively, in which the bacteria can induce cellular tolerance in mucosal intestinal cells [196]. They can protect the intestine from damage caused by infection. *L. probiotics*, for example, inhibit *C. difficile* and *C. perfringens* growth [168].

Possible metabolites of non-engineered and engineered *L. plantarum* that trigger immune response:

The investigation of *L. p.* (vector/wt) showed an immune response of neutrophils (Fig. 41-46). This may originate from antigens varying with *L. plantarum* activating the host toll-like receptors (TLR-2, -4) and CD14 [196]. Lipoteichoic acid (LTA) exists in Gram-positive cell wall bacteria as an endotoxin interacting with TLR2-inducing proinflammatory proteins [171, 197]. LTA contains anionic amphipaths with similar chemical characteristics to LPS of Gram-negative bacteria [197]. Therefore, it was suggested that LTA may have the same impact as LPS in Gram-negative bacteria [171]. LTA can induce a neutrophil response during the inflammation process. Such response was observed in 6 to 24 hours where LTA concentration affects the number of neutrophils [198]. Other studies showed that *Lactobacillus plantarum* had various impacts on human dendritic and peripheral blood mononuclear cells [196]. *L. plantarum* WCFS1 could stimulate immature monocyte-derived dendritic cells *in vitro* producing IL-10, TNF- α , and the TH1-inducing cytokine IL-12p70 [171]. Modification of LTA in *pneumococci sp.* through d-alanylation (*dltA* mutant) alters the LTA structure which acts as an antagonist and could decrease NETs and antimicrobial peptides (AMPs) [250]. Lipoproteins in *L. plantarum* WCFS1 are recognized as PAMPs and are crucial mediators of TLR2 (heterodimer) activation in the innate immune system. Bacterial di- and tri-acyl lipoproteins are recognized by distinct TLR2/6 and TLR1/2, respectively. Modifying lipoprotein by *lgt* deletion could stimulate lower TLR1/2 signaling. Furthermore, *lgt* deletion mutant increased pro-inflammatory responses and decreased anti-inflammatory in PBMCs. It is known that *lgt* or *lsp* deletions can weaken the immune activation and/or the virulence of Gram-positive pathogens *in vitro* and *in vivo* [199]. Probiotic bacterial exopolysaccharides (EPS) may act on different

receptors including (TLR)2, TLR4, C-type lectins, or scavenger receptors. For instance, *Lactobacilli* can induce TLR2 and/or TLR4. EPS of *Bacillus subtilis* could stimulate TLR4-dependent manner in M2 macrophages (anti-inflammatory) which prevents T cell-mediated disease whereas EPS of *Bacteroides fragilis* acts on TLR2. It was reported that EPS-37 could prevent T-cell proliferation and IFN- γ production. Bacterial pathogens that form EPS-containing capsules can decrease the inflammatory response of the immune system [200]. More studies are required to understand the actual mechanism of EPS as well as the effects originating from probiotic bacterial products [168, 200].

In addition to metabolites of non-engineered bacteria, other contents of engineered ones may activate immune cells. The investigation of *L. p.* (candidates) enhanced the immune response of neutrophils (Fig. 41-42). In nature, interleukin-6 (IL-6) is the inflammatory cytokine and ligand of the IL-6 receptor (IL-6R). It has been reported that IL-6 mediates mainly inflammation, hematopoiesis, and immune cells [177, 178]. Cervical cancer (HPV-transformed keratinocytes) showed a high level of IL-6 production. It functions as a myeloid cell suppressor (dendritic cells) in the last phases of cervical cancer and increases myeloid cell activity to promote tumors through the production of MMP-9 [201, 202]. As a response to inflammation, many cytokines are released in the environment to modulate immune cell activation and may cause tissue damage such as human respiratory syncytial virus (hRSV) infection, where a higher number of cytokines were detected, including CXCL-8 and IL-6 [203]. KCF18 functions as a blocking peptide (anti-inflammatory) by connecting to proinflammatory cytokines such as TNF- α , IL-1 β , and IL-6, preventing the binding with their receptors and gene expression [204]. IL-6 binding to the neutrophil receptor (IL-6R) leads to IL-8 and MCP-1 production and thus neutrophil migration [205]. Further, injection of IL-6 results in neutrophilia, and inhibition of IL-6 can decrease neutrophils in monkey models [205]. Further, it was reported that KCF18 reduced human monocyte ROS. Moreover, it could reduce the increase of mice leukocytes stimulated by LPS [204]. NGF is a cytokine produced by human neutrophils [64]. It can bind to Trk A, B, and/or C (high-affinity) receptors triggering Ras, PI3-kinase signaling pathways in innate immune cells. It induces chemotaxis, survival phagocytosis in neutrophils, and response of eosinophils through peroxidase and interleukin-4 secretion [206]. Some studies showed the binding of NGF with human basophils, indicating a high affinity for NGF receptors [231]. NGF stimulates basophil activation and interleukin-13 secretion. Adaptive immune cells (lymphocyte T, B) can respond to NGF through p75NTR (low affinity) by survival and differentiation [206]. Nucleases are hydrolytic enzymes secreted as ex- or endo enzymes. It is a strategy for escaping from immune cells by degrading neutrophil NETs [207]. Nucleases

produced by *S. aureus* can render neutrophil NETosis and thus delay antimicrobial activity, leading to pathogenicity *in vivo* [208]. However, neutrophils showed activation with only the nuclease candidate compared to the vector. One possible explanation is that histones derived from DNA degradation by DNases might be considered proinflammatory factors [209]. For example, H4 raised neutrophil intracellular calcium, which is crucial for respiratory burst activation and degranulation [210]. Histone existence at high levels was found in inflammatory diseases. Histone injection in mice increased activated (CD44⁺CD69⁺) CD4⁺ T cells in the blood [209].

Furthermore, neutrophils may respond (Fig. 41F, H) to the heat-killed vector more than supernatant. Heat-killed *Lactobacillus plantarum* N14 (LP14) and their EPS were reported to activate TLR2 (receptor for peptidoglycan) and 4 (receptor for LPS). Also, UV-killed *Lactobacillus* strains and EPS could trigger human Th1 cells [211]. Heat-killed *L. plantarum* (HKLP) could activate neutrophils by inducing the production of cytokines (pro-and anti-inflammatory) and high levels of G-CSF. Furthermore, it increased neutrophil apoptosis. However, HKPL could not influence function including phagocytosis, oxidative burst, and NETosis [170]. *L. plantarum* might be used as therapy for IBD, as it has been shown to survive gastric vectors, regulate microbiota, and respond to immune cells [212]. Twenty research studies (3 in humans and 17 in animal models) showed that *L. plantarum* positively affects the symptoms of neurogenerative diseases such as Alzheimer's, Parkinson's, and Multiple Sclerosis. However, one study showed a negative impact [213]. Results of *L. plantarum* (Fig. 45, 46), particularly the nuclease candidate, demonstrated that bacterial supernatants (soluble proteins), heat-killed or live bacteria could activate neutrophils at various levels. However, the activation orders were lower, medium, and higher. Increasing the time of incubation would enhance the activation level of candidates. So, application *in vivo* would also trigger the immune response. Therefore, more studies are required to study how differences in signals originating from bacteria statuses including function assays, and encapsulation in materials such as alginate-gelatine (ALG-GE) hydrogel beads can increase the viability of *L. plantarum* [214] as well as may reduce activation of neutrophils.

4.5 Factors may affect immunogenic response and thus influence the outcomes.

In this study, peripheral blood was collected from healthy adult donors. Non-considering some factors could potentially make a difference in neutrophil responses between donors, affecting the significance of the data in certain instances. Here, we aim to explore various factors that may influence neutrophils (granulocytes) and potentially other immune cells. These factors

represent crucial areas for future research, particularly in the context of long-term monitoring system implantation, when applied to the human body. We can categorize these factors into three main areas: a) microenvironment, encompassing elements within the human body, such as different cell subsets. b) The small or macro-environment, including factors such as sex differences, cultural nuances, and societal influences within a given country. c) The broader environment, or what could be termed the "global environment," encompasses geographical disparities between countries, such as variations from colder to hotter climates.

4.5.1 Cell subsets (neutrophils):

Neutrophil subsets have distinct markers and may represent a central role by making a difference in response during inflammation. For instance, it has been observed that PD-L1⁺ neutrophils are developed during SARS-CoV-2 and rheumatoid arthritis. These subsets participate in elevated responsiveness to infection in pancreatic cancer after injury of tissue or metastasis in the liver. Additionally, mature hyper-segmented neutrophils, characterized by high responsiveness expressing PD-L1⁺ and arginase-1, were reported to be stimulated by human endotoxemia [82].

CD177 marker of neutrophil is a glycosylphosphatidylinositol (GPI)-linked glycoprotein and called neutrophil antigen B1 (NB1) or human neutrophil antigen 2a (HNA-2a) [215-217]. CD177 marker exists in the membrane of plasma and granules of neutrophils. The expression percentage of CD177 on circulating neutrophils varies among individuals and ranges between 0% and 100%, depending on the donor. It was reported that neutrophil CD177⁺ can connect to PECAM-1 of other cells, such as endothelial, monocytes, and granulocytes, in which it participates in transmigration from vasculature to tissue. It can also interact immediately with protease 3 (PR3) on the surface membrane of neutrophils to play a possible role in the canalization of ECM. *In vitro* Chemotaxis experiments showed an increase in the level of neutrophil migration with Pos. CD177, but not Neg. [215, 217]. Furthermore, neutrophils with Pos. CD177 showed elevated bactericidal activity more than those with Neg. CD177 [217]. Additionally, some studies showed that the immunogenic response of neutrophils is coordinated between healthy people with low and high traits. For instance, the response to lipopolysaccharides (LPS) and N-Formyl methionine-leucyl-phenylalanine (fMLP) might be associated with the host immune system of individuals [218].

4.5.2 Sex differences:

Sex is determined by the difference in chromosomes, genital organs, and steroid levels [219]. The sex difference originates from the difference in anatomy and physiology. Thus, sex may

make variable immune responses due to the variable sex hormones [220, 219]. In general, the response of innate and adaptive immune systems is better in females than males. For example, men are more exposed to death resulting from cancer than women as well as response to influenza virus vaccine by antibody is about 2 folds stronger in women. Another example, women, during HIV infection, have lower blood viral RNA compared to men. However, women have the bigger percentage, 80%, of autoimmune diseases resulting from faster response [219]. At the molecular level, genes of human leukocyte antigen (HLA class I and II) expression were investigated after inducing by LPS and approximately 47% differentiate between sexes [221]. The difference may originate also from temperature which differentiates among coldest and warmest organs such as the skin and ear canal, respectively, in females compared to males as well as inside the body in 10 C grade [222].

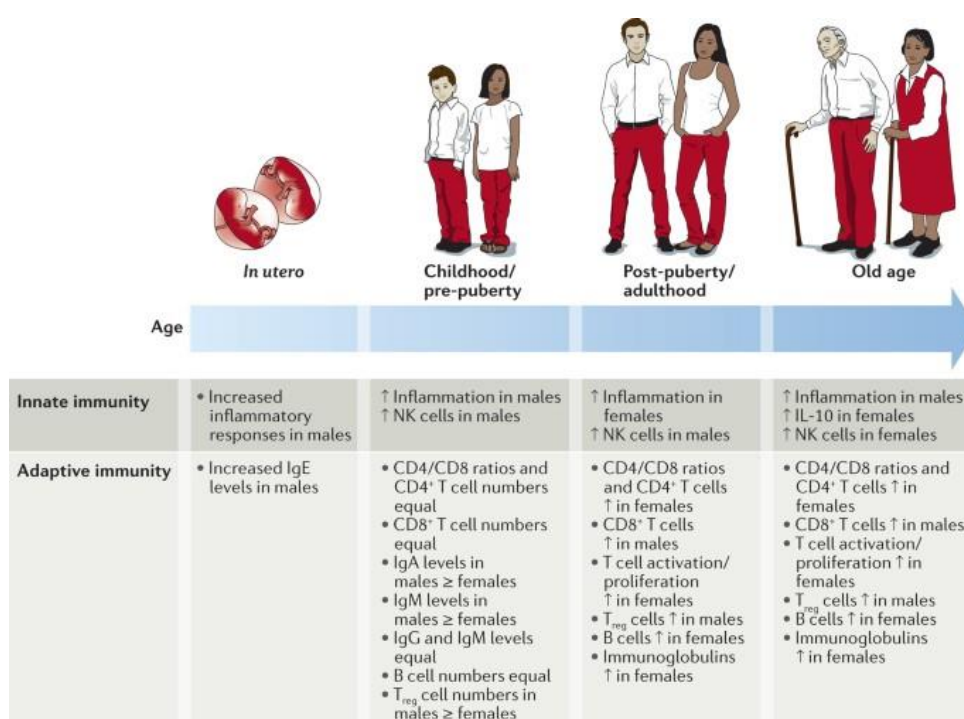


Figure 48l Sex-related hormones may lead to differences in human life stages. Some factors change in the life course such as pro-inflammatory responses. Others may not change during life such as elevation in female CD4⁺ T and CD4/CD8 T cell numbers [219].

It was reported that neutrophils isolated from adult males had elevated levels of immature neutrophil gene signature than in females. Thus, this reflects on activation, response to cytokines, and function which are less in males than females. Neutrophils, in females, upregulate type I INF-stimulated genes (ISGs). This could lead to an enhanced response to toll-like receptor stimulators. In contrast, neutrophils in males have increased levels of

mitochondrial metabolism more than in females [68, 220]. Neutrophils are affected by sex hormones like oestradiol, which increase the number of degranulation elastase. Furthermore, androgen can increase neutrophil numbers and decrease kinases, as well as leukotriene formation. Eosinophils increase in number by oestradiol and progesterone as well as decline in mobilization by oestradiol [219]. Factors such as sex, age, and even daytime due to the circadian rhythm of the neutrophils influence their capacity to respond to stimulation by PAMPs or DAMPs [222]. Further, Circadian rhythm regulates cell functions during 24 h and may affect cell fate. Further, it controls the time and duration of inflammatory cytokine products such as IL6 and TNF α . This includes transcription, translation, and post-translational modification. Research studies showed that the number and phenotype of neutrophils are related to circadian rhythm [223]. Thus, this may influence the results at which daytime the blood was isolated.

4.5.3 Geographical environment:

Geographic regions might have an impact on the immune system [224]. Heat, air pollution, and severe weather changes, for example, are factors related to the climate. The change in such factors influences the immune system and thus its function. These factors include a broad range of inducers such as heat stress, microbiota change, and other toxic compounds hyperstimulating innate and adaptive immune systems resulting in lacking an immune tolerance and leading to autoimmune diseases such as allergy and obesity [225]. Vaccination against malaria, for instance, protects approximately 100% and 20-50% in high- and low-income countries, respectively [224]. Differences in infection may originate from aridity gradient in tropical areas, like Africa's Sahara Desert to the Atlantic Ocean coast from west to south, affecting human immunity [226]. The increases in Universal Thermal Climate Index (UTCI), each 5-degree, raises key marker levels of immune cells during inflammation as the following 4.2%, 9.5%, 9.9%, and 7.0% in blood monocytes, eosinophils, natural killer cells, T-cells and tumor necrosis factor-alpha, respectively, and decrease in B cells for -6.8%. These parameters indicate that the temperature affects the function of the immune system and thus might elevate responsiveness to infection [227]. The basic exam explained that the immune system is affected by temperature in the heat shock response. This process is induced by some elements such as cold, heat, and others [222]. Environmental conditions may have an impact on the immune system. Working and living in hot environments increase monocytes and lymphocytes [228]. Other studies investigated human neutrophil activity at various temperature degrees. For instance, phagocytosis of heat-killed *S. aureus* increased at 38 and 39 °C compared to 37 but not 40 °C [229].

5 Conclusion:

In conclusion, neutrophils utilize pattern recognition receptors to detect microbial components, such as those from bacteria encapsulated in LTM, and respond through various mechanisms, including migration, phagocytosis, NET formation, and degranulation. Our findings highlight the enhanced migration of neutrophils in 3D cultures and their pronounced capacity for antibody-dependent tumor cell killing when stimulated with *E. coli* compared to *ClearColi*. Despite this, engineered *ClearColi* and *E. coli* BL21 exhibited comparable activation of neutrophil FPR and released similar levels of LPS, with the latter being modified in *ClearColi*. The addition of supernatants from *ClearColi* or *E. coli* to impedance assays further enhanced neutrophils' ability to kill IgA-opsonized tumor cells and further demonstrated the capacity of both strains to activate neutrophils.

The greater potency of the *E. coli* strain in promoting antibody-dependent cellular cytotoxicity (ADCC) and neutrophil migration, compared to *ClearColi*, likely correlates with differences in LPS structure. Additionally, *Lactobacillus plantarum* holds therapeutic potential but requires further investigation, particularly in long-term interactions with the immune system, including neutrophils. This study, along with research by Andrew O. Yam et al., 2020 [230], underscores the potential of using microorganisms as therapeutic agents or as enhancers of tumor therapy by converting neutrophils into effective anti-tumor agents. However, mutating LPS as in *ClearColi*, is just one step towards an LTM concept that stays under the radar of neutrophils, with the results shown clearly pointing to the requirement of further adjustments.

6 Abbreviations:

ADCC	Antibody-dependent cellular cytotoxicity
CI	Cell Index
cm	Centimeter
Conc.	Concentration
CO ₂	Carbon dioxide
°C	Celsius
CXCL8	Chemokine (C-X-C motif) ligand 8 = IL-8
DAMP	Damage-associated molecular pattern
Dest.	Distilled
DMEM	Dulbecco's Modified Eagle Medium
DMSO	Dimethyl sulfoxide
DNA	Deoxyribonucleic acid
dNTP	Deoxynucleotide triphosphate
dH ₂ O	Distilled water
e.g.	Exempli gratia
<i>E. coli</i>	<i>Escherichia coli</i>
EI	Electrical impedance
EGF	Epidermal growth factor
EGFR	Epidermal growth factor receptor
ELISA	Enzyme-linked Immunosorbent Assay
EMMPRIN	Extracellular Matrix Metalloproteinase Inducer (=CD147)
EtOH	Ethanol
EU	Endotoxin unite
FCS	Fetal calf serum
FcR	Fc- receptor
Fig.	Figure
FcαRI	Fc-alpha receptor I
FFPE	Formalin-fixed paraffin-embedded tissue
FPR	Formyle peptide receptor

G-CSF	Granulocyte colony-stimulating factor
GM-CSF	Granulocyte-macrophage colony-stimulating factor
h	Hour
HNSCC	Head and neck squamous cell carcinoma
HE	Hämatoxylin und Eosin
HPV	Human papillomavirus
HRP	Horseradish-peroxidase
Hu	Human
i.a.	Inter alia (among others)
IgA	Immunoglobulin A
IgG	Immunoglobulin G
IHC	Immunohistochemistry
IL	Interleukin
IL-8	Interleukin 8 = CXCL8
kb	Kilobase
KBM	Keratinocyte basal medium
kDa	Kilodalton
L	Liter
LB	Luria Bertani
LIF	Leukemia inhibitory factor
LPS	Lipopolysaccharide
mAbs	Mouse antibodies
mA	Milliampere
M	Molar
mg	Milligram
MIF	Macrophage migration inhibitory factor
min	Minute
ml	Milliliter
mM	Millimolar
MMP	Matrix Metallproteinase
MQ	Milli-Q water

n	Number
NaCl	Sodium chloride
nm	Nanometer
NK-cell	Natural killer cell
nCI	Normalized cell index
NFF	Normal foreskin fibroblasts
OC	Organotypic culture
OD	Optical density
PAMP	Pathogen-associated molecular pattern
PBS	Phosphate-buffered saline
PBST	PBS with Tween 20
PCR	Polymerase chain reaction
PeCa	Penile Cancer
PMNs	Polymorphonuclear cells /granulocytes
pH.	Potential of hydrogen
PFA	Paraformaldehyde
Ref.	Reference
RFI	Relative fluorescence intensity
RNA	Ribonucleic acid
ROI	Reactive oxygen intermediates
ROS	Reactive oxygen species
RTCA	Real-Time Cell Analyzer
rpm	Revolutions per minute
RT	Room temperature
s	Second
SCC	Squamous cell carcinoma
SDS	Sodium dodecyl sulfate
SD	Standard deviation
SEM	Standard deviation of the sampling distribution
STD	Standard
TBS	Tris-buffered saline

TE	Tris-EDTA
TLR	Toll-like receptor
TMB	3,3',5,5'-Tetramethylbenzidine
TNF- α	Tumor necrosis factor α
TNF- β	Tumor necrosis factor β
TRAIL	TNF-related apoptosis-inducing ligand
UV	Ultraviolet
V	Volt
VEGF	Vascular endothelial growth factor
α	Alpha
β	Beta
γ	Gamma
μm	Micrometer
μl	Microliter
μCs	Microcapsules
3-D	Three-dimensional
μg	Microgram
μl	Microliter

7 Literatures:

1. Grady NG, Petrof EO, Claud EC. Microbial therapeutic interventions. *Seminars in Fetal and Neonatal Medicine*. 2016;21(6):418-423. doi: <https://doi.org/10.1016/j.siny.2016.04.005>
2. Cao Y, Xia H, Tan X, et al. Intratumoural microbiota: a new frontier in cancer development and therapy. *Signal transduction and targeted therapy*. 2024;9(1). doi: <https://doi.org/10.1038/s41392-023-01693-0>
3. Piñero-Lambea C, Ruano-Gallego D, Fernández LÁ. Engineered bacteria as therapeutic agents. *Current Opinion in Biotechnology*. 2015;35(0):94-102. doi: <https://doi.org/10.1016/j.copbio.2015.05.004>
4. Cruz N, Abernathy GA, Dichosa AEK, Kumar A. The Age of Next-Generation Therapeutic-Microbe Discovery: Exploiting Microbe-Microbe and Host-Microbe Interactions for Disease Prevention. Ottemann KM, ed. *Infection and Immunity*. 2022;90(5). doi: <https://doi.org/10.1128/iai.00589-21>
5. J. Chitra, Rajendren S, Jeyaraman Jeyakanthan, et al. Microbes and their products as novel therapeutics in medical applications. *Elsevier eBooks*. 2022;0(0):203-221. doi: <https://doi.org/10.1016/b978-0-323-90958-7.00019-4>
6. Mills H, Acquah R, Tang N, et al. The Use of Bacteria in Cancer Treatment: A Review from the Perspective of Cellular Microbiology. *Emergency Medicine International*. 2022;2022(0):e8127137. doi: <https://doi.org/10.1155/2022/8127137>
7. Zhou M, Tang Y, Xu W, et al. Bacteria-based immunotherapy for cancer: a systematic review of preclinical studies. *Frontiers in Immunology*. 2023;14(0). doi: <https://doi.org/10.3389/fimmu.2023.1140463>
8. Charbonneau MR, Isabella VM, Li N, Kurtz CB. Developing a new class of engineered live bacterial therapeutics to treat human diseases. *Nature Communications*. 2020;11(0). doi: <https://doi.org/10.1038/s41467-020-15508-1>
9. Yadav M, Chauhan NS. Microbiome therapeutics: exploring the present scenario and challenges. *Gastroenterology Report*. 2021;0(0). doi: <https://doi.org/10.1093/gastro/goab046>
10. Demain AL, Sanchez S. Microbial drug discovery: 80 years of progress. *The Journal of Antibiotics*. 2009;62(1):5-16. doi: <https://doi.org/10.1038/ja.2008.16>
11. Weiman S. Cover of Harnessing the Power of Microbes as Therapeutics: Bugs as Drugs. Harnessing the Power of Microbes as Therapeutics: Bugs as Drugs. Fox J, ed. *Harnessing the Power of Microbes as Therapeutics: Bugs as Drugs*. 2014;0(0). doi: <https://doi.org/10.1128/aamcol.apr.2014>
12. Hornef MW, Wick MJ, Rhen M, Normark S. Bacterial strategies for overcoming host innate and adaptive immune responses. *Nature Immunology*. 2002;3(11):1033-1040. doi: <https://doi.org/10.1038/ni1102-1033>
13. Vestby LK, Grønseth T, Simm R, Nesse LL. Bacterial Biofilm and Its Role in the Pathogenesis of Disease. *Antibiotics*. 2020;9(2):59. doi: <https://doi.org/10.3390/antibiotics9020059>
14. Hahn J, Ding S, Im J, Harimoto T, Leong KW, Danino T. Bacterial therapies at the interface of synthetic biology and nanomedicine. *Nature Reviews Bioengineering*. 2023;0(0). doi: <https://doi.org/10.1038/s44222-023-00119-4>
15. Patyar S, Joshi R, Byrav DP, Prakash A, Medhi B, Das B. Bacteria in cancer therapy: a novel experimental strategy. *Journal of Biomedical Science*. 2010;17(1):21. doi: <https://doi.org/10.1186/1423-0127-17-21>
16. Mol S, Florianne M. J. Hafkamp, Varela L, et al. Efficient Neutrophil Activation Requires Two Simultaneous Activating Stimuli. *0*. 2021;22(18):10106-10106. doi: <https://doi.org/10.3390/ijms221810106>
17. Burn GL, Foti A, Marsman G, Patel DF, Zychlinsky A. The Neutrophil. *Immunity*. 2021;54(7):1377-1391. doi: <https://doi.org/10.1016/j.immuni.2021.06.006>

18. Han X, Alu A, Liu H, et al. Biomaterial-assisted biotherapy: A brief review of biomaterials used in drug delivery, vaccine development, gene therapy, and stem cell therapy. *Bioactive Materials*. 2022;0(0). doi: <https://doi.org/10.1016/j.bioactmat.2022.01.011>
19. Jiann Chong ET, Ng JW, Lee PC. Classification and Medical Applications of Biomaterials—A Mini Review. *BIO Integration*. 2022;0(0). doi: <https://doi.org/10.15212/bioi-2022-0009>
20. Muffly TM, Tizzano AP, Walters MD. The history and evolution of sutures in pelvic surgery. *Journal of the Royal Society of Medicine*. 2011;104(3):107-112. doi: <https://doi.org/10.1258/jrsm.2010.100243>
21. Todros S, Todesco M, Bagno A. Biomaterials and Their Biomedical Applications: From Replacement to Regeneration. *Processes*. 2021;9(11):1949. doi: <https://doi.org/10.3390/pr9111949>
22. Cambridge Dictionary. MATERIAL | meaning in the Cambridge English Dictionary. Cambridge.org. Published 2020. <https://dictionary.cambridge.org/dictionary/english/material>
23. Marschallek BE, Jacobsen T. Classification of material substances: Introducing a standards-based approach. *Materials & Design*. 2020;193(0):108784. doi: <https://doi.org/10.1016/j.matdes.2020.108784>
24. Linganis LZ. Fibre-reinforced laminates in aerospace engineering. *Advanced Composite Materials for Aerospace Engineering*. 2016;0(0):101-127.
25. Yu Y, Bu F, Zhou H, et al. Biosafety materials: an emerging new research direction of materials science from the COVID-19 outbreak. *Materials Chemistry Frontiers*. 2020;4(7):1930-1953. doi: <https://doi.org/10.1039/d0qm00255k>
26. Detsch R, Will J, Hum J, Roether JA, Boccaccini AR. Biomaterials. *Cell Culture Technology*. 2018;0(0):91-105. doi: https://doi.org/10.1007/978-3-319-74854-2_6
27. National Institute of Biomedical Imaging and Bioengineering. Biomaterials | National Institute of Biomedical Imaging and Bioengineering. Nih.gov. Published 2009. <https://www.nibib.nih.gov/science-education/science-topics/biomaterials>
28. Marin E, Boschetto F, Pezzotti G. Biomaterials and biocompatibility: An historical overview. *Journal of Biomedical Materials Research Part A*. 2020;108(8):1617-1633. doi: <https://doi.org/10.1002/jbm.a.36930>
29. Williams DF. On the nature of biomaterials. *Biomaterials*. 2009;30(30):5897-5909. doi: <https://doi.org/10.1016/j.biomaterials.2009.07.027>
30. Rodrigo-Navarro A, Sankaran S, Dalby MJ, del Campo A, Salmeron-Sanchez M. Engineered living biomaterials. *Nature Reviews Materials*. 2021;6(12):1175-1190. doi: <https://doi.org/10.1038/s41578-021-00350-8>
31. Franz S, Rammelt S, Scharnweber D, Simon JC. Immune responses to implants – A review of the implications for the design of immunomodulatory biomaterials. *Biomaterials*. 2011;32(28):6692-6709. doi: <https://doi.org/10.1016/j.biomaterials.2011.05.078>
32. Agrawal R, Kumar A, Mohammed MKA, Singh S. Biomaterial types, properties, medical applications, and other factors: a recent review. *Journal of Zhejiang University-SCIENCE A*. 2023;0(0). doi: <https://doi.org/10.1631/jzus.a2200403>
33. Pulikanti Guruprasad Reddy, Ravi Saklani, Manas Kumar Mandal, Domb AJ. Introduction to Biomaterials. *AAPS Introductions in the Pharmaceutical Sciences*. 2023;0(0):1-32. doi: https://doi.org/10.1007/978-3-031-36135-7_1
34. Ajmal S, Athar Hashmi F, Imran I. Recent progress in development and applications of biomaterials. *Materials Today: Proceedings*. 2022;0(0). doi: <https://doi.org/10.1016/j.matpr.2022.04.233>
35. Ige OO, Umoru LE, Aribio S. Natural Products: A Minefield of Biomaterials. *ISRN Materials Science*. 2012;2012(0):1-20. doi: <https://doi.org/10.5402/2012/983062>
36. Ozdemir T, Fedorec AJH, Danino T, Barnes CP. Synthetic Biology and Engineered Live Biotherapeutics: Toward Increasing System Complexity. *Cell Systems*. 2018;7(1):5-16. doi: <https://doi.org/10.1016/j.cels.2018.06.008>

37. Omer R, Mohsin MZ, Mohsin A, et al. Engineered Bacteria-Based Living Materials for Biotherapeutic Applications. *Frontiers in Bioengineering and Biotechnology*. 2022;10(0):870675. doi: <https://doi.org/10.3389/fbioe.2022.870675>
38. Liu AP, Appel EA, Ashby PD, et al. The living interface between synthetic biology and biomaterial design. 2022;21(4):390-397. doi: <https://doi.org/10.1038/s41563-022-01231-3>
39. Caro-Astorga J, Walker KT, Herrera N, Lee KY, Ellis T. Bacterial cellulose spheroids as building blocks for 3D and patterned living materials and for regeneration. *Nature Communications*. 2021;12(1):5027. doi: <https://doi.org/10.1038/s41467-021-25350-8>
40. Huang J, Liu S, Zhang C, et al. Programmable and printable *Bacillus subtilis* biofilms as engineered living materials. *Nature Chemical Biology*. 2018;15(1):34-41. doi: <https://doi.org/10.1038/s41589-018-0169-2>
41. Lathuilière A, Mach N, Schneider B. Encapsulated Cellular Implants for Recombinant Protein Delivery and Therapeutic Modulation of the Immune System. *International Journal of Molecular Sciences*. 2015;16(12):10578-10600. doi: <https://doi.org/10.3390/ijms160510578>
42. Singh N, Philippe Vayer, Shivalika Tanwar, Jean-Luc Poyet, Katya Tsaïoun, Villoutreix BO. Drug discovery and development: introduction to the general public and patient groups. *Frontiers in drug discovery*. 2023;3(0). doi: <https://doi.org/10.3389/fddsv.2023.1201419>
43. Chan CTY, Lee JW, Cameron DE, Bashor CJ, Collins JJ. “Deadman” and “Passcode” microbial kill switches for bacterial containment. *Nature Chemical Biology*. 2016;12(2):82-86. doi: <https://doi.org/10.1038/nchembio.1979>
44. Hughes J, Rees S, Kalindjian S, Philpott K. Principles of Early Drug Discovery. *British Journal of Pharmacology*. 2011;162(6):1239-1249. doi: <https://doi.org/10.1111/j.1476-5381.2010.01127.x>
45. James M McKim J. Building a Tiered Approach to In Vitro Predictive Toxicity Screening: A Focus on Assays with In Vivo Relevance. *Combinatorial Chemistry & High Throughput Screening*. 2010;13(2):188. doi: <https://doi.org/10.2174/138620710790596736>
46. Söhling N, Ondreka M, Konradowitz K, Reichel T, Marzi I, Henrich D. Early Immune Response in Foreign Body Reaction Is Implant/Material Specific. *Materials*. 2022;15(6):2195. doi: <https://doi.org/10.3390/ma15062195>
47. Kandárová H, Pôbiš P. The “Big Three” in biocompatibility testing of medical devices: implementation of alternatives to animal experimentation—are we there yet?. *Frontiers in toxicology*. 2024;5(0). doi: <https://doi.org/10.3389/ftox.2023.1337468>
48. Bruinink A, Luginbuehl R. Evaluation of Biocompatibility Using In Vitro Methods: Interpretation and Limitations. *Tissue Engineering III: Cell - Surface Interactions for Tissue Culture*. 2011;0(0):117-152. doi: https://doi.org/10.1007/10_2011_111
49. Lock A, Cornish J, Musson DS. The Role of In Vitro Immune Response Assessment for Biomaterials. *Journal of Functional Biomaterials*. 2019;10(3):31. doi: <https://doi.org/10.3390/jfb10030031>
50. Marshall JS, Warrington R, Watson W, Kim HL. An Introduction to Immunology and Immunopathology. *Allergy, Asthma & Clinical Immunology*. 2018;14(S2). doi: <https://doi.org/10.1186/s13223-018-0278-1>
51. Chaplin DD. Overview of the Immune Response. *Journal of Allergy and Clinical Immunology*. 2010;125(2):S3-S23. doi: <https://doi.org/10.1016/j.jaci.2009.12.980>
52. Forsman H, Wu Y, Mårtensson J, et al. AZ2158 is a more potent formyl peptide receptor 1 inhibitor than the commonly used peptide antagonists in abolishing neutrophil chemotaxis. *Biochemical pharmacology*. 2023;211:115529-115529. doi: <https://doi.org/10.1016/j.bcp.2023.115529>
53. Kraus RF, Gruber MA. Neutrophils—From Bone Marrow to First-Line Defense of the Innate Immune System. *Frontiers in Immunology*. 2021;12. doi: <https://doi.org/10.3389/fimmu.2021.767175>
54. Łukasiewicz K, Fol M. Microorganisms in the Treatment of Cancer: Advantages and

- Limitations. *Journal of Immunology Research*. 2018;2018(0):1-8. doi: <https://doi.org/10.1155/2018/2397808>
55. Netea MG, Joosten LAB, Latz E, et al. Trained immunity: A program of innate immune memory in health and disease. *Science*. 2016;352(6284):aaf1098-aaf1098. doi: <https://doi.org/10.1126/science.aaf1098>
56. Hajishengallis G, Chavakis T. Mechanisms and Therapeutic Modulation of Neutrophil-Mediated Inflammation. *Journal of Dental Research*. 2022;0(0):002203452211076. doi: <https://doi.org/10.1177/00220345221107602>
57. Behrens LM, van Egmond M, van den Berg TK. Neutrophils as immune effector cells in antibody therapy in cancer. *Immunological Reviews*. 2022;0(0). doi: <https://doi.org/10.1111/imr.13159>
58. Teng TS, Ji A, Ji XY, Li YZ. Neutrophils and Immunity: From Bactericidal Action to Being Conquered. *Journal of Immunology Research*. 2017;2017(0):1-14. doi: <https://doi.org/10.1155/2017/9671604>
59. Dahdah A, Johnson J, Gopalkrishna S, et al. Neutrophil Migratory Patterns: Implications for Cardiovascular Disease. *Frontiers in Cell and Developmental Biology*. 2022;10(0). doi: <https://doi.org/10.3389/fcell.2022.795784>
60. Rosales C. Neutrophil: a Cell with Many Roles in Inflammation or Several Cell Types? *Frontiers in Physiology*. 2018;9(113). doi: <https://doi.org/10.3389/fphys.2018.00113>
61. Liew PX, Kubes P. The Neutrophil's Role During Health and Disease. *Physiological Reviews*. 2019;99(2):1223-1248. doi: <https://doi.org/10.1152/physrev.00012.2018>
62. Silvestre-Roig C, Brandau S. Controversies associated with the identification of the true origins of human neutrophils. *Journal of Leukocyte Biology*. 2024;115(5):797-800. doi: <https://doi.org/10.1093/jleuko/qiae036>
63. Qu J, Jin J, Zhang M, Ng LG. Neutrophil diversity and plasticity: Implications for organ transplantation. *Cellular & Molecular Immunology*. 2023;20(9):993-1001. doi: <https://doi.org/10.1038/s41423-023-01058-1>
64. Tecchio C, Micheletti A, Cassatella MA. Neutrophil-Derived Cytokines: Facts Beyond Expression. *Frontiers in Immunology*. 2014;5(0). doi: <https://doi.org/10.3389/fimmu.2014.00508>
65. Silvestre-Roig C, Fridlender ZG, Glogauer M, Scapini P. Neutrophil Diversity in Health and Disease. *Trends in Immunology*. 2019;40(7):565-583. doi: <https://doi.org/10.1016/j.it.2019.04.012>
66. Johansson C, Kirsebom FCM. Neutrophils in respiratory viral infections. *Mucosal Immunology*. 2021;14(4):815-827. doi: <https://doi.org/10.1038/s41385-021-00397-4>
67. Tsioumpekou M, Krijgsman D, Leusen JHW, Olofsen PA. The Role of Cytokines in Neutrophil Development, Tissue Homing, Function and Plasticity in Health and Disease. *Cells*. 2023;12(15):1981. doi: <https://doi.org/10.3390/cells12151981>
68. Burn GL, Foti A, Marsman G, Patel DF, Zychlinsky A. The Neutrophil. *Immunity*. 2021;54(7):1377-1391. doi: <https://doi.org/10.1016/j.immuni.2021.06.006>
69. Li D, Wu M. Pattern Recognition Receptors in Health and Diseases. *Signal Transduction and Targeted Therapy*. 2021;6(1):1-24. doi: <https://doi.org/10.1038/s41392-021-00687-0>
70. de Oliveira S, Rosowski EE, Huttenlocher A. Neutrophil migration in infection and wound repair: going forward in reverse. *Nature Reviews Immunology*. 2016;16(6):378-391. doi: <https://doi.org/10.1038/nri.2016.49>
71. Zivkovic S, Ayazi M, Hammel G, Ren Y. For Better or for Worse: A Look Into Neutrophils in Traumatic Spinal Cord Injury. *Frontiers in Cellular Neuroscience*. 2021;15(0):648076. doi: <https://doi.org/10.3389/fncel.2021.648076>
72. Lawrence SM, Corriden R, Nizet V. Age-Appropriate Functions and Dysfunctions of the Neonatal Neutrophil. *Frontiers in Pediatrics*. 2017;5. doi: <https://doi.org/10.3389/fped.2017.00023>

73. Zarbock A, Ley K. Neutrophil Adhesion and Activation under Flow. *Microcirculation*. 2009;16(1):31-42. doi:<https://doi.org/10.1080/10739680802350104>
74. Castro-Ferreira R, Neves JS, Ladeiras-Lopes R, et al. Revisiting the slow force response: The role of the PKG signaling pathway in the normal and the ischemic heart. *Revista Portuguesa de Cardiologia*. 2014;33(9):493-499. doi:<https://doi.org/10.1016/j.repc.2014.03.006>
75. Fitzgerald KA, Malhotra M, Curtin CM, O' Brien FJ, O' Driscoll CM. Life in 3D is never flat: 3D models to optimise drug delivery. *Journal of Controlled Release*. 2015;215(0):39-54. doi:<https://doi.org/10.1016/j.jconrel.2015.07.020>
76. Aroca-Crevillén A, Tommaso Vicanolo, Ovadia S, Hidalgo A. Neutrophils in Physiology and Pathology. *Annual Review of Pathology-mechanisms of Disease*. 2024;19(1):227-259. doi:<https://doi.org/10.1146/annurev-pathmechdis-051222-015009>
77. Zhu Y, Huang Y, Ji Q, et al. Interplay between Extracellular Matrix and Neutrophils in Diseases. *Journal of Immunology Research*. 2021;2021:8243378. doi:<https://doi.org/10.1155/2021/8243378>
78. Kolaczowska E, Kubes P. Neutrophil recruitment and function in health and inflammation. *Nature reviews Immunology*. 2013;13(3):159-175. doi:<https://doi.org/10.1038/nri3399>
79. Padmanabhan J, Gonzalez AL. The effects of extracellular matrix proteins on neutrophil-endothelial interaction--a roadway to multiple therapeutic opportunities. *The Yale journal of biology and medicine*. 2012;85(2):167-185. Accessed August 26, 2024. <https://www.ncbi.nlm.nih.gov/pmc/articles/PMC3375712/>
80. Hind LE, Huttenlocher A. Neutrophil Reverse Migration and a Chemokinetic Resolution. *Developmental Cell*. 2018;47(4):404-405. doi:<https://doi.org/10.1016/j.devcel.2018.11.004>
81. Kirsebom FCM, Kausar F, Nuriev R, Makris S, Johansson C. Neutrophil recruitment and activation are differentially dependent on MyD88/TRIF and MAVS signaling during RSV infection. *Mucosal Immunology*. 2019;12(5):1244-1255. doi:<https://doi.org/10.1038/s41385-019-0190-0>
82. Rizo-Téllez SA, Filep JG. Beyond host defense and tissue injury: the emerging role of neutrophils in tissue repair. *AJP Cell Physiology*. 2024;326(3):C661-C683. doi:<https://doi.org/10.1152/ajpcell.00652.2023>
83. Kirsebom FCM, Kausar F, Nuriev R, Makris S, Johansson C. Neutrophil recruitment and activation are differentially dependent on MyD88/TRIF and MAVS signaling during RSV infection. *Mucosal Immunology*. 2019;12(5):1244-1255. doi:<https://doi.org/10.1038/s41385-019-0190-0>
84. Sollberger G, Brenes AJ, Warner J, Arthur SC, Andrew. Quantitative proteomics reveals tissue-specific, infection-induced and species-specific neutrophil protein signatures. *Scientific Reports*. 2024;14(1). doi:<https://doi.org/10.1038/s41598-024-56163-6>
85. Thomas CJ, Schroder K. Pattern recognition receptor function in neutrophils. *Trends in Immunology*. 2013;34(7):317-328. doi:<https://doi.org/10.1016/j.it.2013.02.008>
86. Tsai YF, Yang SC, Hwang TL. Formyl peptide receptor modulators: a patent review and potential applications for inflammatory diseases (2012-2015). *Expert Opinion on Therapeutic Patents*. 2016;26(10):1139-1156. doi:<https://doi.org/10.1080/13543776.2016.1216546>
87. Molfino N, van der Merwe. Challenge models to assess new therapies in chronic obstructive pulmonary disease. *International Journal of Chronic Obstructive Pulmonary Disease*. 2012;(0):597. doi:<https://doi.org/10.2147/copd.s30664>
88. Bell E. TLR4 signalling. *Nature Reviews Immunology*. 2008;8(4):241-241. doi:<https://doi.org/10.1038/nri2301>
89. Kobayashi Scott D, Malachowa N, DeLeo Frank R. Neutrophils and Bacterial Immune Evasion. *Journal of Innate Immunity*. 2018;10(5-6):432-441. doi:<https://doi.org/10.1159/000487756>
90. Kath Baines KJ. Leukocyte Activation - an overview | ScienceDirect Topics.

www.sciencedirect.com. Published 2014. <https://www.sciencedirect.com/topics/medicine-and-dentistry/leukocyte-activation>

91. Adriana Laura López-Lobato, Lorena M, Gabriel H, Clara Luz Sampieri, Hugo V. Quantification of the presence of enzymes in gelatin zymography using the Gini index. 2022;20(06). doi:<https://doi.org/10.1142/s0219720022500251>
92. Ren Z, Chen J, Khalil RA. Zymography as a Research Tool in the Study of Matrix Metalloproteinase Inhibitors. *Methods in molecular biology (Clifton, NJ)*. 2017;1626:79-102. doi:https://doi.org/10.1007/978-1-4939-7111-4_8
93. Bormann T, Maus R, Stolper J, et al. Role of matrix metalloprotease-2 and MMP-9 in experimental lung fibrosis in mice. *Respiratory Research*. 2022;23(1). doi:<https://doi.org/10.1186/s12931-022-02105-7>
94. Leber TM, Balkwill FR. Zymography: A Single-Step Staining Method for Quantitation of Proteolytic Activity on Substrate Gels. *Analytical Biochemistry*. 1997;249(1):24-28. doi:<https://doi.org/10.1006/abio.1997.2170>
95. Li K, Li D, Hafez B, et al. Identifying and validating MMP family members (MMP2, MMP9, MMP12, and MMP16) as therapeutic targets and biomarkers in kidney renal clear cell carcinoma (KIRC). *Oncology Research Featuring Preclinical and Clinical Cancer Therapeutics*. 2024;32(4):737-752. doi:<https://doi.org/10.32604/or.2023.042925>
96. Darbousset R, Mezouar S, Dignat-George F, Panicot-Dubois L, Dubois C. Involvement of neutrophils in thrombus formation in living mice. *Pathologie Biologie*. 2014;62(1):1-9. doi:<https://doi.org/10.1016/j.patbio.2013.11.002>
97. Ardi VC, Kupriyanova TA, Deryugina EI, Quigley JP. Human neutrophils uniquely release TIMP-free MMP-9 to provide a potent catalytic stimulator of angiogenesis. *Proceedings of the National Academy of Sciences*. 2007;104(51):20262-20267. doi:<https://doi.org/10.1073/pnas.0706438104>
98. Olson MW, Bernardo MMargarida, Pietila M, et al. Characterization of the Monomeric and Dimeric Forms of Latent and Active Matrix Metalloproteinase-9. *Journal of Biological Chemistry*. 2000;275(4):2661-2668. doi:<https://doi.org/10.1074/jbc.275.4.2661>
99. Stefanidakis M, Terhi Ruohtula, Niels Borregaard, Gahmberg CG, Erkki Koivunen. Intracellular and Cell Surface Localization of a Complex between α M β 2 Integrin and Promatrix Metalloproteinase-9 Progelatinase in Neutrophils. *The Journal of Immunology*. 2004;172(11):7060-7068. doi:<https://doi.org/10.4049/jimmunol.172.11.7060>
100. Nikolov A, Popovski N. Role of Gelatinases MMP-2 and MMP-9 in Healthy and Complicated Pregnancy and Their Future Potential as Preeclampsia Biomarkers. *Diagnostics*. 2021;11(3):480. doi:<https://doi.org/10.3390/diagnostics11030480>
101. Grillet B, Yu K, Estefania Ugarte-Berzal, et al. Proteoform Analysis of Matrix Metalloproteinase-9/Gelatinase B and Discovery of Its Citrullination in Rheumatoid Arthritis Synovial Fluids. *Frontiers in immunology*. 2021;12. doi:<https://doi.org/10.3389/fimmu.2021.763832>
102. Nuti E, Rossello A, Cuffaro D, et al. Bivalent Inhibitor with Selectivity for Trimeric MMP-9 Amplifies Neutrophil Chemotaxis and Enables Functional Studies on MMP-9 Proteoforms. *Cells*. 2020;9(7):1634-1634. doi:<https://doi.org/10.3390/cells9071634>
103. Song J, Wu C, Zhang X, Sorokin LM. In Vivo Processing of CXCL5 (LIX) by Matrix Metalloproteinase (MMP)-2 and MMP-9 Promotes Early Neutrophil Recruitment in IL-1 β -Induced Peritonitis. *The Journal of immunology*. 2013;190(1):401-410. doi:<https://doi.org/10.4049/jimmunol.1202286>
104. Liu MF, Hu YY, Jin T, et al. Matrix Metalloproteinase-9/Neutrophil Gelatinase-Associated Lipocalin Complex Activity in Human Glioma Samples Predicts Tumor Presence and Clinical Prognosis. *Disease Markers*. 2015;2015:1-7. doi:<https://doi.org/10.1155/2015/138974>

105. Candido S, Maestro R, Polesel J, et al. Roles of neutrophil gelatinase-associated lipocalin (NGAL) in human cancer. *Oncotarget*. 2014;5(6). doi:<https://doi.org/10.18632/oncotarget.1738>
106. Bradley LM, Douglass MF, Chatterjee D, Akira S, Baaten BJG. Matrix Metalloprotease 9 Mediates Neutrophil Migration into the Airways in Response to Influenza Virus-Induced Toll-Like Receptor Signaling. Kawaoka Y, ed. *PLoS Pathogens*. 2012;8(4):e1002641. doi:<https://doi.org/10.1371/journal.ppat.1002641>
107. Li T, Li X, Liu X, Yang J, Ma C. The elevated expression of TLR4 and MMP9 in human abdominal aortic aneurysm tissues and its implication. *BMC Cardiovascular Disorders*. 2021;21:378. doi:<https://doi.org/10.1186/s12872-021-02193-1>
108. Chang M. Matrix metalloproteinase profiling and their roles in disease. *RSC Advances*. 2023;13(9):6304-6316. doi:<https://doi.org/10.1039/d2ra07005g>
109. Han Sol Lee, Woo Joo Kim. The Role of Matrix Metalloproteinase in Inflammation with a Focus on Infectious Diseases. *International Journal of Molecular Sciences*. 2022;23(18):10546-10546. doi:<https://doi.org/10.3390/ijms231810546>
110. Tamassia N, Bianchetto-Aguilera FM, Fabio Arruda-Silva, et al. Cytokine production by human neutrophils: Revisiting the “dark side of the moon.” *European Journal of Clinical Investigation*. 2018;48(S2). doi:<https://doi.org/10.1111/eci.12952>
111. National Library of Medicine ND. Datasets. NCBI. Accessed July 31, 2024. <https://www.ncbi.nlm.nih.gov/datasets>
112. Xiong X, Liao X, Qiu S, et al. CXCL8 in Tumor Biology and Its Implications for Clinical Translation. *Frontiers in Molecular Biosciences*. 2022;9(0). doi:<https://doi.org/10.3389/fmolb.2022.723846>
113. Ushigoe K, Irahara M, Fukumochi M, Kamada M, Aono T. Production and Regulation of Cytokine-Induced Neutrophil Chemoattractant in Rat Ovulation. *Biology of Reproduction*. 2000;63(1):121-126. doi:<https://doi.org/10.1095/biolreprod63.1.121>
114. Priyanka Dhakane, Varun Sai Tadimarri, Sankaran S. Light-Regulated Pro-Angiogenic Engineered Living Materials. *Advanced Functional Materials*. 2023;33(31). doi:<https://doi.org/10.1002/adfm.202212695>
115. Grünewald FS, Prota AE, Giese A, Ballmer-Hofer K. Structure–function analysis of VEGF receptor activation and the role of coreceptors in angiogenic signaling. *Biochimica et Biophysica Acta (BBA) - Proteins and Proteomics*. 2010;1804(3):567-580. doi:<https://doi.org/10.1016/j.bbapap.2009.09.002>
116. Holmes DI, Zachary I. The vascular endothelial growth factor (VEGF) family: angiogenic factors in health and disease. *Genome Biology*. 2005;6(2):209. doi:<https://doi.org/10.1186/gb-2005-6-2-209>
117. Metzemaekers M, Gouwy M, Proost P. Neutrophil chemoattractant receptors in health and disease: double-edged swords. *Cellular & Molecular Immunology*. 2020;17(5):433-450. doi:<https://doi.org/10.1038/s41423-020-0412-0>
118. Christoffersson G, Vågesjö E, Vandooren J, et al. VEGF-A recruits a proangiogenic MMP-9–delivering neutrophil subset that induces angiogenesis in transplanted hypoxic tissue. *Blood*. 2012;120(23):4653-4662. doi:<https://doi.org/10.1182/blood-2012-04-421040>
119. Ning Y, Yang H, Weng P, Wu Z. Zymogram Analysis and Identification of the Extracellular Proteases from *Bacillus velezensis* SW5. *Applied Biochemistry and Microbiology*. 2021;57(S1):S27-S37. doi:
- There are no sources in the current document.**
120. Velnar T, Bunc G, Klobucar R, Gradisnik L. Biomaterials and host versus graft response: a short review. *Bosnian Journal of Basic Medical Sciences*. 2016;0(0). doi:<https://doi.org/10.17305/bjbms.2016.525>
121. Nilsson B, Kristina Nilsson Ekdahl, Tom Eirik Mollnes, Lambris JD. The role of complement in biomaterial-induced inflammation. *Molecular Immunology*. 2007;44(1-3):82-

94. doi:<https://doi.org/10.1016/j.molimm.2006.06.020>
122. Salthouse D, Novakovic K, Hilkins CMU, Ferreira AM. Interplay between biomaterials and the immune system: challenges and opportunities in regenerative medicine. *Acta Biomaterialia*. 2022;0(0). doi:<https://doi.org/10.1016/j.actbio.2022.11.003>
123. Kämmerling L, Fisher LE, Antmen E, et al. Mitigating the foreign body response through “immune-instructive” biomaterials. *Journal of Immunology and Regenerative Medicine*. 2021;12:100040. doi:<https://doi.org/10.1016/j.jregen.2021.100040>
124. Wei F, Liu S, Chen M, et al. Host Response to Biomaterials for Cartilage Tissue Engineering: Key to Remodeling. *Frontiers in Bioengineering and Biotechnology*. 2021;9(0). doi:<https://doi.org/10.3389/fbioe.2021.664592>
125. Mayadas TN, Cullere X, Lowell CA. The Multifaceted Functions of Neutrophils. *Annual Review of Pathology: Mechanisms of Disease*. 2014;9(1):181-218. doi:<https://doi.org/10.1146/annurev-pathol-020712-164023>
126. Whitaker R, Hernaez-Estrada B, Hernandez RM, Santos-Vizcaino E, Spiller KL. Immunomodulatory Biomaterials for Tissue Repair. *Chemical Reviews*. 2021;121(18):11305-11335. doi:<https://doi.org/10.1021/acs.chemrev.0c00895>
127. Hanks CT, Wataha JC, Sun Z. In vitro models of biocompatibility: A review. *Dental Materials*. 1996;12(3):186-193. doi:[https://doi.org/10.1016/s0109-5641\(96\)80020-0](https://doi.org/10.1016/s0109-5641(96)80020-0)
128. Young L, Sung J, Stacey G, Masters JR. Detection of Mycoplasma in cell cultures. *Nature Protocols*. 2010;5(5):929-934. doi:<https://doi.org/10.1038/nprot.2010.43>
129. Nikfarjam L, Farzaneh P. Prevention and detection of Mycoplasma contamination in cell culture. *Cell journal*. 2012;13(4):203-212.
130. Junhua J, Wu S, Xie Yuanhong, Liu H, Gao Xiuzhi, Zhang HX. Live and heat-killed cells of *Lactobacillus plantarum* Zhang-LL ease symptoms of chronic ulcerative colitis induced by
131. Blanter M, Gouwy M, Struyf S. Studying Neutrophil Function in vitro: Cell Models and Environmental Factors. *Journal of Inflammation Research*. 2021;Volume 14(0):141-162. doi:<https://doi.org/10.2147/jir.s284941>
132. Marfa Blanter, Cambier S, Mirre De Bondt, et al. Method Matters: Effect of Purification Technology on Neutrophil Phenotype and Function. *Frontiers in Immunology*. 2022;13(0). doi:<https://doi.org/10.3389/fimmu.2022.820058>
133. Krabbe J, Beilmann V, Alamzad-Krabbe H, et al. Blood collection technique, anticoagulants and storing temperature have minor effects on the isolation of polymorphonuclear neutrophils. *Scientific Reports*. 2020;10(1). doi:<https://doi.org/10.1038/s41598-020-71500-1>
134. Sankaran S, Becker J, Wittmann C, del Campo A. Optoregulated Drug Release from an Engineered Living Material: Self-Replenishing Drug Depots for Long-Term, Light-Regulated Delivery. *Small*. 2018;15(5):1804717. doi:<https://doi.org/10.1002/smll.201804717>
135. Hayrapetyan H, Tran T, Tellez-Corrales E, Madiraju C. Enzyme-Linked Immunosorbent Assay: Types and Applications. *Methods in Molecular Biology*. 2023;2612(0):1-17. doi:https://doi.org/10.1007/978-1-0716-2903-1_1
136. Alhajj M, Farhana A, Zubair M. Enzyme Linked Immunosorbent Assay (ELISA). PubMed. Published April 23, 2023. <https://www.ncbi.nlm.nih.gov/books/NBK555922/>
137. Peper JK, Schuster H, Löffler MW, Schmid-Horch B, Rammensee HG, Stevanović S. An impedance-based cytotoxicity assay for real-time and label-free assessment of T-cell-mediated killing of adherent cells. *Journal of Immunological Methods*. 2014;405:192-198. doi:<https://doi.org/10.1016/j.jim.2014.01.012>
138. Zwick A, Muriel Charlotte Bernhard, Arne Knoerck, et al. Monitoring kinetics reveals critical parameters of IgA-dependent granulocyte-mediated anti-tumor cell cytotoxicity. 2019;473:112644-112644. doi:<https://doi.org/10.1016/j.jim.2019.112644>
139. Kho D, MacDonald C, Johnson R, et al. Application of xCELLigence RTCA Biosensor Technology for Revealing the Profile and Window of Drug Responsiveness in Real Time.

- Biosensors*. 2015;5(2):199-222. doi:<https://doi.org/10.3390/bios5020199>
140. xCELLigence. *RTCA Software Manual Software Version 1.2 Version.*; 2009. Accessed August 5, 2024. <http://www.cytometrie-imagerie-saint-antoine.org/media/4140/RTCA>
141. Candini O, Grisendi G, Foppiani EM, et al. A Novel 3D In Vitro Platform for Pre-Clinical Investigations in Drug Testing, Gene Therapy, and Immuno-oncology. *Scientific Reports*. 2019;9(1). doi:<https://doi.org/10.1038/s41598-019-43613-9>
142. Ravi M, Paramesh V, Kaviya SR, Anuradha E, Solomon FDP. 3D Cell Culture Systems: Advantages and Applications. *Journal of Cellular Physiology*. 2014;230(1):16-26. doi:<https://doi.org/10.1002/jcp.24683>
143. Geckil H, Xu F, Zhang X, Moon S, Demirci U. Engineering hydrogels as extracellular matrix mimics. *Nanomedicine*. 2010;5(3):469-484. doi:<https://doi.org/10.2217/nnm.10.12>
144. Iwanaga S. Biochemical principle of Limulus test for detecting bacterial endotoxins. *Proceedings of the Japan Academy Series B, Physical and Biological Sciences*. 2007;83(4):110-119. Accessed July 31, 2024. <https://www.ncbi.nlm.nih.gov/pmc/articles/PMC3756735/>
145. Justus CR, Marie MA, Sanderlin EJ, Yang LV. Transwell In Vitro Cell Migration and Invasion Assays. 2023;(0):349-359. doi:https://doi.org/10.1007/978-1-0716-3052-5_22
146. Pham HTT, Magez S, Choi B, Baatar B, Jung J, Radwanska M. Neutrophil metalloproteinase driven spleen damage hampers infection control of trypanosomiasis. *Nature Communications*. 2023;14(1):5418. doi:<https://doi.org/10.1038/s41467-023-41089-w>
147. Cambier S, Gouwy M, Proost P. The chemokines CXCL8 and CXCL12: molecular and functional properties, role in disease and efforts towards pharmacological intervention. *Cellular & Molecular Immunology*. 2023;20(3):217-251. doi:<https://doi.org/10.1038/s41423-023-00974-6>
148. Taktak-BenAmar A, Morjen M, Ben Mabrouk H, et al. Expression, purification and functionality of bioactive recombinant human vascular endothelial growth factor VEGF165 in *E. coli*. *AMB Express*. 2017;7(1). doi:<https://doi.org/10.1186/s13568-016-0300-2>
149. Nima Beheshtizadeh, Maliheh Gharibshahian, Bayati M, et al. Vascular endothelial growth factor (VEGF) delivery approaches in regenerative medicine. *Biomedicine & Pharmacotherapy*. 2023;166:115301-115301. doi:<https://doi.org/10.1016/j.biopha.2023.115301>
150. Yanamandra AK, Shardul Bhusari, Aránzazu del Campo, Sankaran S, Qu B. In vitro evaluation of immune responses to bacterial hydrogels for the development of living therapeutic materials. *Biomaterials advances*. 2023;153:213554-213554. doi:<https://doi.org/10.1016/j.bioadv.2023.213554>
151. Santulli G, Ciccarelli M, Palumbo G, et al. In vivo properties of the proangiogenic peptide QK. 2009;7(1). doi:<https://doi.org/10.1186/1479-5876-7-41>
152. Bonilla MC, Fingerhut L, Alfonso-Castro A, et al. How Long Does a Neutrophil Live?—The Effect of 24 h Whole Blood Storage on Neutrophil Functions in Pigs. *Biomedicine*. 2020;8(8):278. doi:<https://doi.org/10.3390/biomedicines8080278>
153. Saalbach A, Arnhold J, Leßig J, Simon J, Anderegg U. Human Thy-1 induces secretion of matrix metalloproteinase-9 and CXCL8 from human neutrophils. *European Journal of Immunology*. 2008;38(5):1391-1403. doi:<https://doi.org/10.1002/eji.200737901>
154. Mitsuo W, Jéssica Andrade-Silva, Joice, Julieta Helena Scialfa, José Cipolla-Neto. Neutrophil activation causes tumor regression in Walker 256 tumor-bearing rats. *Scientific Reports*. 2019;9(1). doi:<https://doi.org/10.1038/s41598-019-52956-2>
155. Cao Y, Chen J, Liu F, et al. Formyl peptide receptor 2 activation by mitochondrial formyl peptides stimulates the neutrophil proinflammatory response via the ERK pathway and exacerbates ischemia–reperfusion injury. *Cellular & Molecular Biology Letters*. 2023;28(1). doi:<https://doi.org/10.1186/s11658-023-00416-1>
156. Wenceslau CF, McCarthy CG, Webb RC. Formyl Peptide Receptor Activation Elicits

- Endothelial Cell Contraction and Vascular Leakage. *Frontiers in Immunology*. 2016;7. doi:<https://doi.org/10.3389/fimmu.2016.00297>
157. Zhou Y, Bian X, Le Y, et al. Formylpeptide Receptor FPR and the Rapid Growth of Malignant Human Gliomas. *JNCI: Journal of the National Cancer Institute*. 2005;97(11):823-835. doi:<https://doi.org/10.1093/jnci/dji142>
158. Zhang M, Gao J, Chen K, et al. A Critical Role of Formyl Peptide Receptors in Host Defense against *Escherichia coli*. *Journal of Immunology*. 2020;204(9):2464-2473. doi:<https://doi.org/10.4049/jimmunol.1900430>
159. Bufe B, Schumann T, Reinhard Kappl, et al. Recognition of Bacterial Signal Peptides by Mammalian Formyl Peptide Receptors. *Journal of Biological Chemistry*. 2015;290(12):7369-7387. doi:<https://doi.org/10.1074/jbc.m114.626747>
160. Babatunde KA, Wang X, Hopke A, Lannes N, Mantel PY, Irimia D. Chemotaxis and swarming in differentiated HL-60 neutrophil-like cells. *Scientific Reports*. 2021;11(1):778. doi:<https://doi.org/10.1038/s41598-020-78854-6>
161. Atwood BK, Lopez J, Wager-Miller J, Mackie K, Straiker A. Expression of G protein-coupled receptors and related proteins in HEK293, AtT20, BV2, and N18 cell lines as revealed by microarray analysis. *BMC Genomics*. 2011;12(1). doi:<https://doi.org/10.1186/1471-2164-12-14>
162. Bufe B, Zufall F. The sensing of bacteria: emerging principles for the detection of signal sequences by formyl peptide receptors. *Biomolecular Concepts*. 2016;7(3):205-214. doi:<https://doi.org/10.1515/bmc-2016-0013>
163. Weiß EH, Hanzelmann D, Fehlhaber B, et al. Formyl-peptide receptor 2 governs leukocyte influx in local *Staphylococcus aureus* infections. *The FASEB Journal*. 2017;32(1):26-36. doi:<https://doi.org/10.1096/fj.201700441r>
164. Mamat U, Woodard RW, Wilke K, et al. Endotoxin-free protein production—ClearColi™ technology. *Nature Methods*. 2013;10(9):916-916. doi:<https://doi.org/10.1038/nmeth.f.367>
165. Cardoso VM, Paredes SAH, Campani G, Gonçalves VM, Zangirolami TC. ClearColi as a platform for untagged pneumococcal surface protein A production: cultivation strategy, bioreactor culture, and purification. *Applied Microbiology and Biotechnology*. 2022;106(3):1011-1029. doi:<https://doi.org/10.1007/s00253-022-11758-9>
167. Ravi M, Paramesh V, Kaviya SR, Anuradha E, Solomon FDP. 3D Cell Culture Systems: Advantages and Applications. *Journal of Cellular Physiology*. 2014;230(1):16-26. doi:<https://doi.org/10.1002/jcp.24683>
168. Dempsey E, Corr SC. Lactobacillus spp. for Gastrointestinal Health: Current and Future Perspectives. *Frontiers in Immunology*. 2022;13:840245. doi:<https://doi.org/10.3389/fimmu.2022.840245>
169. Dey S, Blanch-Asensio M, Balaji Kuttas S, Sankaran S. Novel genetic modules encoding high-level antibiotic-free protein expression in probiotic lactobacilli. *Microbial Biotechnology*. 2023;0(0). doi:<https://doi.org/10.1111/1751-7915.14228>
170. Schuermann LE, Bergmann CB, Goetzman H, Caldwell CC, Satish L. Heat-killed probiotic Lactobacillus plantarum affects the function of neutrophils but does not improve survival in murine burn injury. *Burns*. Published online June 2022. doi:<https://doi.org/10.1016/j.burns.2022.06.015>
171. van, Saskia van Hemert, Claassen E, Willem. *Lactobacillus plantarum* WCFS 1 and its host interaction: a dozen years after the genome. *Microbial biotechnology*. 2016;9(4):452-465. doi:<https://doi.org/10.1111/1751-7915.12368>
172. Mitja N. P. Remus-Emsermann, Richard van Kranenburg, Iris, et al. Impact of 4 Lactobacillus plantarum capsular polysaccharide clusters on surface glycan composition and host cell signaling. *O*. 2012;11(1). doi:<https://doi.org/10.1186/1475-2859-11-149>
173. Murphy EJ, Fehrenbach GW, Abidin IZ, et al. Polysaccharides—Naturally Occurring Immune Modulators. *Polymers*. 2023;15(10):2373.

doi:<https://doi.org/10.3390/polym15102373>

174. Wai Ting Chan, M. Pilar Garcillán-Barcia, Chew Chieng Yeo, Espinosa M. Type II bacterial toxin-antitoxins: hypotheses, facts, and the newfound plethora of the PezAT system. *Fems Microbiology Reviews*. 2023;47(5). doi:<https://doi.org/10.1093/femsre/fuad052>
175. van Zyl WF, Deane SM, Dicks LMT. Use of the mCherry Fluorescent Protein To Study Intestinal Colonization by *Enterococcus mundtii* ST4SA and *Lactobacillus plantarum* 423 in Mice. *Applied and Environmental Microbiology*. 2015;81(17):5993-6002. doi:<https://doi.org/10.1128/AEM.01247-15>
176. Xiao C, Li L, Lao L, et al. Application of the red fluorescent protein mCherry in mycelial labeling and organelle tracing in the dermatophyte *Trichophyton mentagrophytes*. *Fems Microbiology Letters*. 2018;365(6). doi:<https://doi.org/10.1093/femsle/fny006>
177. Yao Y, Gui L, Gao B, et al. An I6P7peptide modified fluorescent probe for bio-imaging. *New Journal of Chemistry*. Published online January 1, 2019. doi:<https://doi.org/10.1039/c8nj04255a>
178. Wang S, Reinhard S, Li C, et al. Antitumoral Cascade-Targeting Ligand for IL-6 Receptor-Mediated Gene Delivery to Glioma. *Molecular Therapy*. 2017;25(7):1556-1566. doi:<https://doi.org/10.1016/j.ymthe.2017.04.023>
179. Jiang SJ, Tsai PI, Peng SY, et al. A potential peptide derived from cytokine receptors can bind proinflammatory cytokines as a therapeutic strategy for anti-inflammation. *Scientific Reports*. 2019;9(1). doi:<https://doi.org/10.1038/s41598-018-36492-z>
180. MagriA, Diego La Mendola, Enrico Rizzarelli. Nerve Growth Factor Peptides Bind Copper(II) with High Affinity: A Thermodynamic Approach to Unveil Overlooked Neurotrophin Roles. *International Journal of Molecular Sciences*. 2021;22(10):5085-5085. doi:<https://doi.org/10.3390/ijms22105085>
181. Andres RY, Bradshaw RA. NERVE GROWTH FACTOR. ScienceDirect. Published January 1, 1980. Accessed November 30, 2023. <https://www.sciencedirect.com/science/article/abs/pii/B9780080213453500241?via%3Dihub>
182. Zhang L, Reha-Krantz LJ. Nuclease. ScienceDirect. Published January 1, 2013. Accessed November 30, 2023. <https://www.sciencedirect.com/science/article/abs/pii/B978012374984001069X?via%3Dihub>
183. Nishino T, Morikawa K. Structure and function of nucleases in DNA repair: shape, grip and blade of the DNA scissors. *Oncogene*. 2002;21(58):9022-9032. doi:<https://doi.org/10.1038/sj.onc.1206135>
184. Gibson B, Wilson DJ, Feil E, Eyre-Walker A. The distribution of bacterial doubling times in the wild. *Proceedings of the Royal Society B: Biological Sciences*. 2018;285(1880):20180789. doi:<https://doi.org/10.1098/rspb.2018.0789>
185. Richardson IM, Calo CJ, Ginter EL, Niehaus E, Pacheco KA, Hind LE. Diverse bacteria elicit distinct neutrophil responses in a physiologically relevant model of infection. *iScience*. 2024;27(1):108627-108627. doi:<https://doi.org/10.1016/j.isci.2023.108627>
186. A.M. Soler-Rodriguez, Zhang H, Lichenstein H, et al. Neutrophil Activation by Bacterial Lipoprotein Versus Lipopolysaccharide: Differential Requirements for Serum and CD14. 2000;164(5):2674-2683. doi:<https://doi.org/10.4049/jimmunol.164.5.2674>
187. Fux AC, Cristiane Casonato Melo, Michelini S, et al. Heterogeneity of Lipopolysaccharide as Source of Variability in Bioassays and LPS-Binding Proteins as Remedy. *International Journal of Molecular Sciences*. 2023;24(9):8395-8395. doi:<https://doi.org/10.3390/ijms24098395>
188. Witko-Sarsat V, Rieu P, Descamps-Latscha B, Lesavre P, Halbwachs-Mecarelli L. Neutrophils: Molecules, Functions and Pathophysiological Aspects. *Laboratory Investigation*. 2000;80(5):617-653. doi:<https://doi.org/10.1038/labinvest.3780067>
189. Lin M, Jackson P, Tester AM, et al. Matrix Metalloproteinase-8 Facilitates Neutrophil Migration through the Corneal Stromal Matrix by Collagen Degradation and Production of the

- Chemotactic Peptide Pro-Gly-Pro. *The American Journal of Pathology*. 2008;173(1):144-153. doi:<https://doi.org/10.2353/ajpath.2008.080081>
190. de Oliveira S, Reyes-Aldasoro CC, Candel S, Renshaw SA, Mulero V, Calado A. Cxcl8 (IL-8) mediates neutrophil recruitment and behavior in the zebrafish inflammatory response. *Journal of Immunology (Baltimore, Md: 1950)*. 2013;190(8):4349-4359. doi:<https://doi.org/10.4049/jimmunol.1203266>
191. Caronia JM, Sorensen DW, Leslie HM, Berlo van, Azarin SM. Adhesive thermosensitive gels for local delivery of viral vectors. *Biotechnology and Bioengineering*. 2019;116(9):2353-2363. doi:<https://doi.org/10.1002/bit.27007>
192. Pramanik T;Thapa M;Saikia TC. Effect of temperature on phagocytic activity of neutrophils. *Nepal Medical College journal : NMCJ*. 2020;6(1). Accessed August 15, 2024. <https://pubmed.ncbi.nlm.nih.gov/15449652/#:~:text=Temperature%20higher%20than%2039%20degrees>
193. Lupu A, Luiza Madalina Gradinaru, Rusu D, Bercea M. Self-Healing of Pluronic® F127 Hydrogels in the Presence of Various Polysaccharides. *Gels*. 2023;9(9):719-719. doi:<https://doi.org/10.3390/gels9090719>
194. Shardul Bhusari, Hoffmann MJ, Herbeck-Engel P, Sankaran S, Wilhelm M, Aránzazu del Campo. Rheological behavior of Pluronic/Pluronic diacrylate hydrogels used for bacteria encapsulation in living materials. *bioRxiv (Cold Spring Harbor Laboratory)*. Published online 195.
195. Federica Finetti, Basile A, Capasso D, et al. Functional and pharmacological characterization of a VEGF mimetic peptide on reparative angiogenesis. *Biochemical Pharmacology*. 2012;84(3):303-311. doi:<https://doi.org/10.1016/j.bcp.2012.04.011>
196. de Vos P, Mujagic Z, de Haan BJ, et al. Lactobacillus plantarum Strains Can Enhance Human Mucosal and Systemic Immunity and Prevent Non-steroidal Anti-inflammatory Drug Induced Reduction in T Regulatory Cells. *Frontiers in Immunology*. 2017;8:1000. doi:<https://doi.org/10.3389/fimmu.2017.01000>
197. Warshakoon HJ, Burns MR, David SA. Structure-Activity Relationships of Antimicrobial and Lipoteichoic Acid-Sequestering Properties in Polyamine Sulfonamides. *Antimicrobial agents and chemotherapy*. 2009;53(1):57-62. doi:<https://doi.org/10.1128/aac.00812-08>
198. Pribadi N, Rahayu RP, Ismiyatin K, Putri CR, Surboyo MDC. The Effect of Lipoteichoic Acid from Lactobacillus plantarum on Dental Pulp Inflammation. *European Journal of Dentistry*. 2021;15(04):682-686. doi:<https://doi.org/10.1055/s-0041-1728238>
199. Lee I-Chiao, van Swam II, Boeren S, et al. Lipoproteins Contribute to the Anti-inflammatory Capacity of Lactobacillus plantarum WCFS1. *Frontiers in Microbiology*. 2020;11. doi:<https://doi.org/10.3389/fmicb.2020.01822>
200. Nowak B, Śróttek M, Ciszek-Lenda M, et al. Exopolysaccharide from Lactobacillus rhamnosus KL37 Inhibits T Cell-dependent Immune Response in Mice. *Archivum Immunologiae et Therapiae Experimentalis*. 2020;68(3). doi:<https://doi.org/10.1007/s00005-020-00581-7>
201. Walch-Rückheim B, Mavrova R, Henning M, et al. Stromal Fibroblasts Induce CCL20 through IL6/C/EBP β to Support the Recruitment of Th17 Cells during Cervical Cancer Progression. *Cancer Research*. 2015;75(24):5248-5259. doi:<https://doi.org/10.1158/0008-5472.can-15-0732>
202. Walch-Rückheim B, Russalina Ströder, Theobald L, et al. Cervical Cancer–Instructed Stromal Fibroblasts Enhance IL23 Expression in Dendritic Cells to Support Expansion of Th17 Cells. *Cancer research (Chicago, Ill)*. 2019;79(7):1573-1586. doi:<https://doi.org/10.1158/0008-5472.can-18-1913>
203. Bohmwald K, Gálvez NMS, Canedo-Marroquín G, et al. Contribution of Cytokines to Tissue Damage During Human Respiratory Syncytial Virus Infection. *Frontiers in Immunology*. 2019;10. doi:<https://doi.org/10.3389/fimmu.2019.00452>
204. Chang CC, Peng SY, Tsao HH, et al. A Multitarget Therapeutic Peptide Derived From

- Cytokine Receptors Based on in Silico Analysis Alleviates Cytokine-Stimulated Inflammation. *Frontiers in Pharmacology*. 2022;13. doi:<https://doi.org/10.3389/fphar.2022.853818>
205. Hashizume M, Higuchi Y, Uchiyama Y, Mihara M. IL-6 plays an essential role in neutrophilia under inflammation. *Cytokine*. 2011;54(1):92-99. doi:<https://doi.org/10.1016/j.cyto.2011.01.007>
206. Terracina S, Giampiero Ferraguti, Tarani L, et al. Nerve Growth Factor and Autoimmune Diseases. *Current Issues in Molecular Biology*. 2023;45(11):8950-8973. doi:<https://doi.org/10.3390/cimb45110562>
207. Liao C, Mao F, Qian M, Wang X. Pathogen-Derived Nucleases: An Effective Weapon for Escaping Extracellular Traps. *Frontiers in Immunology*. 2022;13. doi:<https://doi.org/10.3389/fimmu.2022.899890>
208. Berends ETM, Horswill AR, Haste NM, Monestier M, Nizet V, von Köckritz-Blickwede M. Nuclease Expression by Staphylococcus aureus Facilitates Escape from Neutrophil Extracellular Traps. *Journal of Innate Immunity*. 2010;2(6):576-586. doi:<https://doi.org/10.1159/000319909>
209. Wilson AS, Randall KL, Pettitt JA, et al. Neutrophil extracellular traps and their histones promote Th17 cell differentiation directly via TLR2. *Nature Communications*. 2022;13:528. doi:<https://doi.org/10.1038/s41467-022-28172-4>
210. Hsieh I-Ni, Deluna X, White MR, Hartshorn KL. Histone H4 directly stimulates neutrophil activation through membrane permeabilization. *Journal of Leukocyte Biology*. 2020;109(4):763-775. doi:<https://doi.org/10.1002/jlb.3a0620-342r>
211. KISHIMOTO M, NOMOTO R, MIZUNO M, OSAWA R. An *in vitro* investigation of immunomodulatory properties of *Lactobacillus plantarum* and *L. delbrueckii* cells and their extracellular polysaccharides. *Bioscience of Microbiota Food and Health*. 2017;36(3):101-110. doi:<https://doi.org/10.12938/bmfh.17-001>
212. Javid H, Mahsa Akbari Oryani, Akbari S, et al. *L. plantarum* and *L. lactis* as a promising agent in treatment of inflammatory bowel disease and colorectal cancer. *Future Microbiology*. 2023;18(16):1197-1209. doi:<https://doi.org/10.2217/fmb-2023-0076>
213. Ana Isabel Beltrán-Velasco, Reiriz M, Uceda S, Víctor Echeverry-Alzate. Lactiplantibacillus (Lactobacillus) plantarum as a Complementary Treatment to Improve Symptomatology in Neurodegenerative Disease: A Systematic Review of Open Access Literature. *International journal of molecular sciences*. 2024;25(5):3010-3010. doi:<https://doi.org/10.3390/ijms25053010>
214. Ni F, Luo X, Zhu Z, et al. Enhancing viability of *Lactobacillus plantarum* encapsulated by alginate-gelatin hydrogel beads during gastrointestinal digestion, storage and in the mimic beverage systems. *International Journal of Biological Macromolecules*. 2023;224:94-104. doi:<https://doi.org/10.1016/j.ijbiomac.2022.10.106>
215. Agnes Dahlstrand Rudin, Firoozeh Amirbeagi, Davidsson L, et al. The neutrophil subset defined by CD177 expression is preferentially recruited to gingival crevicular fluid in periodontitis. *Journal of Leukocyte Biology*. 2020;109(2):349-362. doi:<https://doi.org/10.1002/jlb.3a0520-081rr>
216. Wang E. Human Leukocyte Antigen and Human Neutrophil Antigen Systems. <https://www.sciencedirect.com/topics/immunology-and-microbiology/cd177>.
217. Zhou G, Peng K, Song Y, et al. CD177+ neutrophils suppress epithelial cell tumourigenesis in colitis-associated cancer and predict good prognosis in colorectal cancer. *Carcinogenesis*. 2017;39(2):272-282. doi:<https://doi.org/10.1093/carcin/bgx142>
218. Duarte M, Maskarinec SA, Khandelwal S, Arepally GM, Lee GM. Variation in Neutrophil Function Among Healthy Subjects Influences Response to Bacteria. *Blood*. 2020;136(Supplement 1):34-34. doi:<https://doi.org/10.1182/blood-2020-141674>
219. Klein SL, Flanagan KL. Sex differences in immune responses. *Nature Reviews Immunology*. 2016;16(10):626-638. doi:<https://doi.org/10.1038/nri.2016.90>
-

220. Gupta S, Nakabo S, Blanco LP, et al. Sex differences in neutrophil biology modulate response to type I interferons and immunometabolism. *Proceedings of the National Academy of Sciences*. 2020;117(28):16481-16491. doi:<https://doi.org/10.1073/pnas.2003603117>
221. Liston A, Humblet-Baron S, Duffy D, Goris A. Human immune diversity: from evolution to modernity. *Nature Immunology*. 2021;22(12):1479-1489. doi:<https://doi.org/10.1038/s41590-021-01058-1>
222. Maloney E, Duffy D. Deciphering the relationship between temperature and immunity. *Discovery immunology*. Published online January 30, 2024. doi:<https://doi.org/10.1093/discim/kyae001>
223. Held J, Sivaraman K, Wrenger S, et al. Ex vivo study on the human blood neutrophil circadian features and effects of alpha1-antitrypsin and lipopolysaccharide. *Vascular Pharmacology*. 2024;156:107396. doi:<https://doi.org/10.1016/j.vph.2024.107396>
224. van Dorst MMAR, Pyuza JJ, Nkurunungi G, et al. Immunological factors linked to geographical variation in vaccine responses. *Nature Reviews Immunology*. 2023;0(9):1-14. doi:<https://doi.org/10.1038/s41577-023-00941-2>
225. Skevaki C, Nadeau KC, Rothenberg ME, et al. Impact of climate change on immune responses and barrier defense. *Journal of Allergy and Clinical Immunology*. 2024;0. doi:<https://doi.org/10.1016/j.jaci.2024.01.016>
226. Nwaogu CJ, Cresswell W, B. Irene Tieleman. Geographic variation in baseline innate immune function does not follow variation in aridity along a tropical environmental gradient. *Scientific reports*. 2020;10(1). doi:<https://doi.org/10.1038/s41598-020-62806-1>
227. ScienceDaily AHA. Heat exposure may increase inflammation and impair the immune system. ScienceDaily. Published June 7, 2024. <https://www.sciencedaily.com/releases/2024/03/240320122607.htm>
228. KNEZ W, GIRARD O, RACINAIS S, WALSH A, GAOUA N, GRANTHAM J. Does Living and Working in a Hot Environment Induce Clinically Relevant Changes in Immune Function and Voluntary Force Production Capacity? *Industrial Health*. 2014;52(3):235-239. doi:<https://doi.org/10.2486/indhealth.2012-0032>
229. Kant V, Gopal A, Kumar D, et al. Topical pluronic F-127 gel application enhances cutaneous wound healing in rats. *Acta Histochemica*. 2014;116(1):5-13. doi:<https://doi.org/10.1016/j.acthis.2013.04.010>
230. Yam AO, Bailey J, Lin F, et al. Microbial activation converts neutrophils into anti-tumor effectors. *bioRxiv (Cold Spring Harbor Laboratory)*. Published online August 23, 2020. doi:<https://doi.org/10.1101/2020.08.21.259051>
231. Bischoff S, Dahinden C. Effect of nerve growth factor on the release of inflammatory mediators by mature human basophils. *Blood*. 1992;79(10):2662-2669. doi:<https://doi.org/10.1182/blood.v79.10.2662.2662>
232. Lentini G, De Gaetano GV, Famà A, et al. Neutrophils discriminate live from dead bacteria by integrating signals initiated by Fprs and TLRs. *The EMBO journal*. 2022;41(5):e109386. doi:<https://doi.org/10.15252/emboj.2021109386>
233. Kuijpers T. Leukocyte adhesion deficiency-type 1 (LAD-1)/variant: A novel immunodeficiency syndrome characterized by dysfunctional β_2 integrins. *Immunology Letters*. 1997;56(1-3):44. doi:[https://doi.org/10.1016/s0165-2478\(97\)87006-x](https://doi.org/10.1016/s0165-2478(97)87006-x)
234. O. Abaricia J, H. Shah A, M. Musselman R, Olivares-Navarrete R. Hydrophilic titanium surfaces reduce neutrophil inflammatory response and NETosis. *Biomaterials Science*. 2020;8(8):2289-2299. doi:<https://doi.org/10.1039/C9BM01474H>
235. Matlung HL, Babes L, Zhao XW, et al. Neutrophils Kill Antibody-Opsonized Cancer Cells by Trogoptosis. *Cell Reports*. 2018;23(13):3946-3959.e6. doi:<https://doi.org/10.1016/j.celrep.2018.05.082>
236. J.M. Adrover, J.A. Nicolas-Avila, A. Hidalgo. Aging: A Temporal Dimension for Neutrophils. *Trends Immunol.* (2016) 37. 334-345. <https://doi.org/10.1016/j.it.2016.03.005>.

237. J.M. McCracken, L.A. Allen. Regulation of human neutrophil apoptosis and lifespan in health and disease. *J Cell Death*. (2014) 7. 15-23. <https://doi.org/10.4137/JCD.S11038>.
238. S.D. Kobayashi, N. Malachowa, F.R. DeLeo. Influence of Microbes on Neutrophil Life and Death. *Front Cell Infect Microbiol*. (2017) 7. 159. <https://doi.org/10.3389/fcimb.2017.00159>.
239. J. Lahoz-Beneytez, M. Elemans, Y. Zhang, R. Ahmed, A. Salam, M. Block, et al. Human neutrophil kinetics: modeling of stable isotope labeling data supports short blood neutrophil half-lives. *Blood*. (2016) 127. 3431-3438. <https://doi.org/10.1182/blood-2016-03-700336>.
240. G. Le'Negrato, P. Rostagno, P. Auberger, B. Rossi, P. Hofman. Downregulation of caspases and Fas ligand expression, and increased lifespan of neutrophils after transmigration across intestinal epithelium. *Cell Death Differ*. (2003) 10. 153-162. <https://doi.org/10.1038/sj.cdd.4401110>.
241. Malengier-Devlies B, Metzemaekers M, Wouters C, Proost P, Matthys P. Neutrophil Homeostasis and Emergency Granulopoiesis: The Example of Systemic Juvenile Idiopathic Arthritis. *Frontiers in Immunology*. 2021;12:766620. doi: <https://doi.org/10.3389/fimmu.2021.766620>
242. Wu M, Ma M, Tan Z, Zheng H, Liu X. Neutrophil: A New Player in Metastatic Cancers. *Front Immunology*. 2020;11. doi: <https://doi.org/10.3389/fimmu.2020.565165>
243. Weiß E, Kretschmer D. Formyl-Peptide Receptors in Infection, Inflammation, and Cancer. *Trends in Immunology*. 2018;39(10):815-829. doi: <https://doi.org/10.1016/j.it.2018.08.005>
244. Lena, Mercier E, Wintermeyer W, Rodnina MV. Kinetic control of nascent protein biogenesis by peptide deformylase. *Scientific Reports*. 2021;11(1). doi: <https://doi.org/10.1038/s41598-021-03969-3>
245. Kineret Serebrinsky-Duek, Barra M, Danino T, Garrido D. Engineered Bacteria for Short-Chain-Fatty-Acid-Repressed Expression of Biotherapeutic Molecules. *Microbiology Spectrum*. 2023;11(2). doi: <https://doi.org/10.1128/spectrum.00049-23>
246. Rangan P, Mondino A. Microbial short-chain fatty acids: a strategy to tune adoptive T cell therapy. *Journal for ImmunoTherapy of Cancer*. 2022;10(7):e004147. doi: <https://doi.org/10.1136/jitc-2021-004147>
247. Wolf AJ. Peptidoglycan-induced modulation of metabolic and inflammatory responses. *Immunometabolism*. 2023;5(2):e00024. doi: <https://doi.org/10.1097/in9.0000000000000024>
248. Davis KM, Weiser JN. Modifications to the Peptidoglycan Backbone Help Bacteria To Establish Infection. Maurelli AT, ed. *Infection and Immunity*. 2010;79(2):562-570. doi: <https://doi.org/10.1128/iai.00651-10>
249. Liu XF, Shao JH, Liao YT, et al. Regulation of short-chain fatty acids in the immune system. *Frontiers in immunology*. 2023;14. doi: <https://doi.org/10.3389/fimmu.2023.1186892>
250. Wartha F, Beiter K, Albiger B, et al. Capsule and d-alanylated lipoteichoic acids protect *Streptococcus pneumoniae* against neutrophil extracellular traps. *Cellular Microbiology*. 2007;9(5):1162-1171. doi: <https://doi.org/10.1111/j.1462-5822.2006.00857.x>
251. Bassler K, Schulte-Schrepping J, Warnat-Herresthal S, Aschenbrenner AC, Schultze JL. The Myeloid Cell Compartment-Cell by Cell. *Annual Review of Immunology*. 2019;37:269-293. doi: <https://doi.org/10.1146/annurev-immunol-042718-041728>
252. Augusto Bleve, Motta F, Durante B, Pandolfo C, Selmi C, Sica A. Immunosenescence, Inflammaging, and Frailty: Role of Myeloid Cells in Age-Related Diseases. *Clinical Reviews in Allergy & Immunology*. 2022;64(2):123-144. doi: <https://doi.org/10.1007/s12016-021-08909-7>
253. Pang WW, Price EA, Sahoo D, et al. Human bone marrow hematopoietic stem cells are increased in frequency and myeloid-biased with age. *Proceedings of the National Academy of Sciences*. 2011;108(50):20012-20017. doi: <https://doi.org/10.1073/pnas.1116110108>

8 Publication/ Conference:

-Banerjee, Kuheli, Yanzhu Lin, Johannes Gahn, Julio Cordero, Purnima Gupta, **Islam Mohamed**, Mariona Graupera, Gergana Dobрева, Martin A Schwartz, and Roxana Ola. “*SMAD4 Maintains the Fluid Shear Stress Set Point to Protect against Arterial-Venous Malformations.*” *Journal of Clinical Investigation* 133, no. 18 (July 25, 2023). <https://doi.org/10.1172/jci168352>.

-Heiko Heilmann, Lukas Busch, Celine Buchmann, **Islam Mohamed**, Adrian Theiß, Stefan Lohse, and Bernd Bufe. “*Fragments of Viral Envelope Proteins Can Modulate Innate Immune Responses via Formyl Peptide Receptors.*” [Submitted to iScience].

-**Islam Mohamed**, Stefan Lohse “*The Transkingdom Cancer Effects on Neutrophil Survival and Lifespan.*” [Review, Submitted to Nature Reviews Cancer].

-**Islam Mohamed**, Stefan Lohse “*Adaptation of the Living Therapeutic Materials Concept to the Immune Sensing of Neutrophil Granulocytes.*” [Review, Journal of Leukocyte Biology in preparation].

-**Islam Mohamed**, Heiko Heilmann, Joelle A. Mekontso Ngaffo, Varun Tai Tadimarri, Shrikrishnan Sankaran, Sara Trujillo, Bernd Bufe, Stefan Lohse “*Keeping Living Therapeutic Materials under the Radar of Neutrophils*” [Advanced Materials, in preparation].

Conferences:

-Living Therapeutic Materials [03/07/2023 – 05/07/2023]

LSC Summer School, Europäische Akademie Otzenhausen, Germany.

The role of endotoxin in the activation of neutrophils by the engineered E. coli strain ClearColi

-Living Therapeutic Materials [12/02/2020 – 14/02/2020]

INM, Saarbrücken, Germany

Keeping living therapeutic materials (LTM) under the radar of neutrophils

-6th International Influenza Meeting [02/09/2019 – 04/09/2019]

Institute of Virology, Münster, Germany.

P112: PD0184264, an active metabolite of the MEK-inhibitor CI-1040 shows superior pharmacokinetics and antiviral activity against influenza virus

9 Acknowledgement:

I would like to express my heartfelt gratitude to everyone who helped me during my doctoral journey through blood donation, guidance, or any other support.

I extend special thanks to Dr. Stefan Lohse, whose exceptional scientific guidance made this doctorate possible and who was there for me at every step. I would also like to thank Prof. Dr. Klaus Römer for his prompt preparation of the initial report. Additionally, I am grateful to Prof. Dr. Sigrun Smola for granting me the opportunity to pursue my doctorate at the Institute of Virology.

Also, I would like to thank all my colleagues from AG Smola: Luca, Markus, Katharina, Julia, Anna, and Anabel for their support and for creating a good working environment. Many thanks to the technicians, Barbara and Katrin, as well as everyone in the diagnostic department and the other working groups at the institute for their good cooperation.

Finally, I would like to thank my family, including my father who passed away, and special thanks to my brother Soliman, for his encouragement and support during stressful situations

10 Curriculum Vitae

“For data protection reasons, the CV will not be published in the electronic version of the dissertation.”